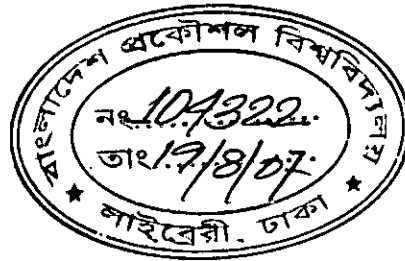


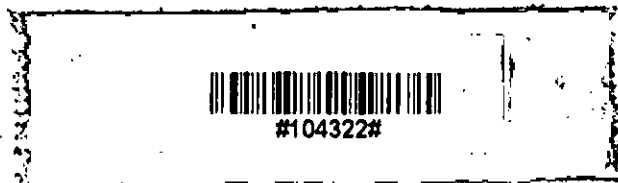
**ANALYSIS OF ELASTIC FIELD IN STRUCTURAL ELEMENTS OF
LAMINATED COMPOSITES BY DISPLACEMENT POTENTIAL
APPROACH**

by

Nayeem Md. Lutful Huq
B. Sc. Engineering (Mech.)



A THESIS SUBMITTED TO THE DEPARTMENT OF MECHANICAL
ENGINEERING IN PARTIAL FULFILLMENT OF THE REQUIREMENT FOR
THE DEGREE OF MASTER OF SCIENCE IN MECHANICAL ENGINEERING




BANGLADESH UNIVERSITY OF ENGINEERING AND TECHNOLOGY,
DHAKA, 2007

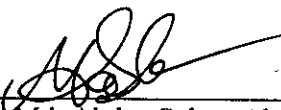
RECOMMENDATION OF THE BOARD OF EXAMINERS

The thesis titled, "Analysis of elastic field in structural elements of laminated composites by displacement potential approach", submitted by Naycem Md. Lutful Huq, Roll no: 040410042P, session: April 2004, has been accepted as satisfactory in partial fulfillment of the requirements for the degree of MASTER OF SCIENCE IN MECHANICAL ENGINEERING on 05 June, 2007.

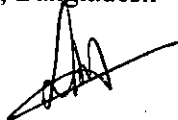
BOARD OF EXAMINERS




Dr. Md. Afsar Ali (Supervisor) Chairman
Associate Professor
Department of Mechanical Engineering, BUET
Dhaka, Bangladesh



Dr. Md. Abdus Salam Akanda Member
Associate Professor
Department of Mechanical Engineering, BUET
Dhaka, Bangladesh



Dr. Khan Mahmud Amanat Member
Professor (External)
Department of Civil Engineering, BUET
Dhaka, Bangladesh



Dr. Md. Maksud Helali Member
Professor and Head (Ex-Officio)
Department of Mechanical Engineering, BUET
Dhaka, Bangladesh

ACKNOWLEDGEMENT

The author would like to avow the Almighty's continual mercy and help without which no work would have been possible to accomplish the goal. The author would also like to express his heartiest gratitude to his supervisor Dr. Md. Afsar Ali, Associate Professor, Department of Mechanical Engineering, Bangladesh University of Engineering and Technology (BUET), Dhaka 1000, for his continuous, outstanding and untiring support, guidance, constructive comments, and encouragement towards the successful completion of this thesis. He is also grateful to Dr. S. K. Deb Nath, Ex-Ph. D. student, BUET, Bangladesh, for his support and intuitive suggestions in this work. Finally, the author would like to take the opportunity to thank the members of examination committee, for their comments and constructive criticism.

Dedicated To
My Parents and My Wife

CANDIDATE'S DECLARATION

No portion of the work contained in this thesis has been submitted in support of an application for another degree or qualification of this or any other University or Institution of learning.



Nayeem Md. Lutful Huq

June, 2007

List of Symbols

Notation	Definition
E_1	Elastic modulus of the material in direction 1
E_2	Elastic modulus of the material in direction 2
ν_{12}	Major Poisson's ratio
ν_{21}	Minor Poisson's ratio
G_{12}	In-plane shear modulus in the 1-2 plane
θ	Fiber orientation of the composites
$ A $	Stiffness matrix for composite laminate
u_x, u_y	Displacement components in the x - and y -direction
σ_x, σ_y	Normal stress components in the x - and y -direction
σ_{xy}	Shearing stress component in the xy plane
ψ	Displacement potential function
a, b	Width and length or height respectively
u_n	Normal displacement component
u_t	Tangential displacement component
σ_n	Normal stress component
σ_t	Tangential stress component
σ_x^0	Maximum applied stress in x direction
σ_y^0	Maximum applied stress in y direction
σ_{xy}^0	Maximum applied shear stress in xy -plane
n	No. of plies
h	Thickness of a laminate
b/a	Aspect ratio

Table of Contents

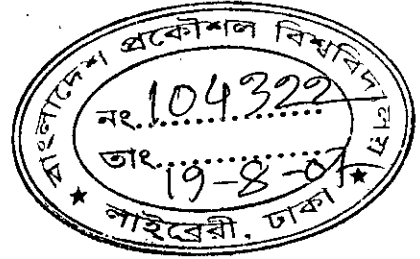
Item	Page
Title Page	i
Board of Examiners	ii
Acknowledgement	iii
Dedication	iv
Candidate's Declaration	v
List of symbols	vi
Table of Contents	vii
Abstract	1
Chapter 1 Introduction	2
1.1 Background	2
1.2 Literature review	3
1.3 Objectives	5
Chapter 2 Theoretical Formulation	7
2.1 Introduction	7
2.2 Plane stress condition	8
2.3 Definition of displacement potential function	11
2.4 General consideration of the boundary conditions	13
Chapter 3 Some Sample Problems of Laminated Composite Structures	15
3.1 A rectangular panel of cross-ply laminated composite under uniform tensile loading	15
3.2 A rectangular panel of cross-ply laminated composite under parabolic tensile loading	19
3.3 A rectangular panel of cross-ply laminated composite under parabolic shear loading	21
3.4 A rectangular panel of cross-ply laminated composite under linearly varying tensile loading	25
3.5 Angle-ply laminated composite panel	29
Chapter 4 Results and Discussion	30
4.1 Results of the problem of article 3.1	30

4.2 Results of the problem of article 3.2	34
4.3 Results of the problem of article 3.3	39
4.4 Results of the problem of article 3.4	43
4.5 Verification of equilibrium of forces	46
Chapter 5 Conclusions and Recommendations	48
5.1 Conclusions	48
7.2 Recommendation for future works	49
References	132

Abstract

Composite materials drew attention of researchers from all over the world due to their outstanding advantages over conventional materials. They are being increasingly used as structural elements in almost all engineering applications. To take full advantage and ensure reliable performance of these materials in an application, it is indispensable to analyze various aspects of these materials. However, these are anisotropic and microscopically nonhomogeneous materials due to the presence of two phases in them. This makes the analytical investigation quite complicated due to mathematical difficulties. Therefore, only numerical and experimental approaches are extensively used in the field of composites, especially in the case of mixed boundary conditions. A reliable analytical method of analysis of these materials under mixed boundary conditions still seems to be lacking.

In this study, an analytical method is developed to analyze the elastic field in structural elements of laminated composite materials under mixed boundary conditions. The two displacement components of the two-dimensional elasticity problem are expressed in terms of a single displacement potential function, which satisfies one of the equilibrium equations automatically. The other equilibrium equation is transformed into a fourth order partial differential equation of unknown displacement potential function. Thus, the two dimensional mixed boundary value elasticity problem is reduced to the solution of a single fourth order partial differential equation. The solution of the fourth order partial differential equation is obtained in the form of Fourier series. To demonstrate the method, it is applied to a rectangular panel consisting of (i) cross-ply laminated composite and (ii) angle-ply laminated composite. Analytical solutions of different components of stress and displacement are presented in the form of graphs. Further, the effects of laminate thickness, fiber orientation, and panel aspect ratio on the components of stress and displacement have been discussed in details. The results conform to the intuitively expected characteristics of the structures which verify that the method developed in the study can be applied reliably to structural elements of laminated composites under mixed boundary conditions to analyze elastic field.



CHAPTER-1 INTRODUCTION

1.1 Background

In cases of engineering problems, the elementary methods of strength of materials are just not enough to provide sufficient and accurate information of elastic field in a body. So, some more powerful methods are needed in the study of elastic field. Further the elementary methods are insufficient to give information regarding local stresses near the loads and near the supports of bars. Again for the cases where the stress distribution in bodies, with all the dimensions of same order, has to be investigated, these methods are incapable of furnishing satisfactory information. For example, the stress in rollers and in balls of bearings can be found only by using the methods of the theory of elasticity [1]. So, to obtain satisfactory and reliable information of elastic fields in engineering structures of practical applications, it is mandatory to adopt the theory of elasticity.

To solve any elasticity problem, it is mandatory to satisfy all the boundary conditions imposed on the boundaries along with the equilibrium and compatibility relations. All the elasticity problems can be categorized as any of the following three fundamental boundary value problems:

1. Determination of elastic field in an elastic body, that is in equilibrium, under prescribed forces on the boundary.
2. Determination of elastic field in an elastic body, that is in equilibrium, with a prescribed displacement of the surface.
3. Determination of elastic field in an elastic body, that is in equilibrium, under prescribed forces on the boundary and with a prescribed displacement of the surface, where these two parameters denote the bounding surface of the body. These categories of problems are called mixed mode boundary value problems.

The problems, which are very simple in terms of geometry and boundary conditions, can be solved analytically. But the fact is that these problems are of almost no application in the field of engineering and technology. On the other hand the

approximate methods have received considerable attention in the field of elasticity. These include boundary-element method, finite element method, and finite difference method among others. There are some experimental methods of stress analysis which are employed for bodies with intricate shapes. But these methods are expensive. Therefore, despite availability of good numerical and experimental methods, analytical solution of any elastic field problem is always desirable.

1.2 Literature Review:

In the field of elasticity the stress analysis has now become a classical subject. At present the stress function approach [2-16] and the displacement formulation [17] are noticeable among the existing mathematical models. Although the theories of elasticity had long been established, the solutions of practical problems started mainly after the introduction of a stress function by Airy [2]. The Airy stress function is governed by a fourth order partial differential equation and the stress components are related to it through its various second order derivatives. Solutions were initially sought through various polynomial expressions of the stress function [3,4], but the success of this approach was very limited. Using these polynomial expressions, an elementary derivation of the effect of the shearing force on the curvature of the deflection curve of beams were made by Rankine[5] in England and Grashof [6] in Germany. The problem of stress in masonry dams is of great practical interest and has been attempted by various authors [7,8] using polynomial expressions for the stress functions. But it should be noted that the solutions thus obtained do not satisfy the conditions at the bottom of the beam where it is connected with the foundation and would predict reasonable values of stress in the region far away from the foundation on account of Saint-Venant's principle [9]. The first application of trigonometric series in the solution of elastic problems using stress function method was given by Ribiere [10] in his thesis. Further progress in the application of these solutions was made by Filon [11]. Several particular examples were worked by Bleich [12]. Using Fourier series, Beyer [13] solved the problem of a continuous beam on equidistant supports under gravity loading. Stress function technique has also been used by Ribiere [14] for analyzing the stresses around a circular hole in a plate, Sadowsky [15] for stresses around a slender hole, Flamant [16] for stresses

around a concentrated load on a straight boundary and Stokes [18] for stresses around a concentrated load on a beam. But somehow these stress analysis problems are still suffering from a lot of shortcomings and thus are being constantly looked into [19-25].

Although elasticity problems were formulated long before, exact solutions of practical problems are hardly available because of the inability of managing the physical conditions imposed on them. Actually, management of boundary conditions is one of the major obstacles to the reliable solution of practical problems. The famous Saint – Venant’s principle is still applied and its merit is evaluated in solving problems of solid mechanics [20-21] in which full boundary effects could not be taken into account satisfactorily in the process of solution. For complex shapes of boundary, the difficulties of obtaining analytical solutions become formidable. These difficulties were partially avoided by resorting to experimental methods, such as extensometers, strain gages or the photoelastic method. Using photoelasticity, Hetengi [26] investigated the stresses in the threads of a bolt and nut fastening. Most of the experimental investigations of elastic problems are reported in the “Handbook of Experimental Stress Analysis” [27] and by Frocht [28] in “Photoelasticity”. Even now, photoelastic studies are being carried out for classical problems like uniformly loaded beams on two supports [29] mainly because the boundary effects could not be taken into account fully in their analytical method of solutions.

Successful application of the stress function formulation in conjunction with finite-difference technique has been reported for the solution of plane elastic problems where all the conditions on the boundary are prescribed in terms of stresses only [19,30]. Further, Conway and Ithaca [31] extended the stress function formulation in the form of Fourier integrals to the case where the material is orthotropic and obtained analytical solutions for a number of ideal problems. The difficulties involved in trying to solve practical stress problems using the existing models are clearly pointed out by Durelli and Ranganayakamma [29] and others [32-47].

An investigation was undertaken to develop a rigorous mathematical solution of

stress and strain for a composite pole consisting of a reinforced plastic jacket laminated on a solid wood core [48], which was also a numerical procedure. Adams and Doner [49] worked on a double periodic rectangular array of elastic filaments contained in an elastic matrix material, which has been formulated using a theory of elasticity. Principal elastic moduli of unidirectional composites with anisotropic filaments had been predicted using the available elasticity solutions of multiple-inclusion problems by Whitney [50] where the measured data was obtained from previous experimental research. Pagano developed some equations to evaluate flexure experiments on bi-directional composites [51]. Using the limit analysis method, Shu and Rosen [52] analyzed in-plane shear strength and the transverse strength in shear and in tension of composites in terms of yield strength and volume fraction. A recent work has been carried out by Tsai and Wu [53]. They developed, operationally, a simple criterion for anisotropic materials. Most recent work has been carried out on strength of composites, which is a numerical estimation of compressive strength [54]. Two works on laminated composite has been carried out using the displacement potential function. Here mixed mode boundary value problems are handled analytically [55-56].

From above discussions, it is found that various elasticity problems of different materials, including isotropic, anisotropic, homogeneous, and non-homogeneous materials, have been solved. However, a reliable and effective analytical method seems to be still lacking for the solution of elastic problems of practical applications, which are subject to mixed mode of boundary conditions. Recently Shankar [57] and Shankar *et. al.* [58-60] carried out some works for solving the mixed mode boundary value problem which are quite useful but only for a single lamina.

1.3 Objectives

As discussed above, most of the methods for analytical solution of elasticity problems are only available either in the form of stress function formulations or of displacement formulations. However, neither is suitable for solving problems of mixed-boundary conditions. Furthermore, these formulations cannot be directly applied to the case of anisotropic and non-homogeneous composite materials, which

are being increasingly used to meet the requirements of current applications. The objectives of the present study are

- I. to develop a simple, effective, and reliable analytical method for the analysis of elastic field in structural elements of a laminated composite using displacement potential function. The method will be applicable to problems of any boundary conditions, whether they are specified in terms of either stresses or displacements or any combination of both.
- II. to demonstrate the methods by solving some problems under different boundary conditions.

CHAPTER-2 THEORITICAL FORMULATION

2.1 Introduction

The most engineering materials possess, to a certain extent, the properties of elasticity. Unless the external forces exceed a certain limit, a material returns to its original shape after withdrawal of the forces from it. This limit is called the elastic limit. This study is concerned with the analysis of elastic field of composite materials within the elastic limit. The elastic field comprises stress field, strain field, and displacement field. In order to provide a complete information on an elastic field of a body, nine components of stress ($\sigma_x, \sigma_y, \sigma_z, \sigma_{xy}, \sigma_{yx}, \sigma_{yz}, \sigma_{zy}, \sigma_{zx},$ and σ_{xz}), six components of strains ($\epsilon_x, \epsilon_y, \epsilon_z, \gamma_{xy}, \gamma_{yz}, \gamma_{zx}$), and three components of displacements (u_x, u_y, u_z) have to be determined. However, the components of strains can be readily obtained from displacement components through some simple relations. Further, the components of strains and displacements provide the same informations. Therefore, in the analysis of elastic field, only stress and displacement components will be dealt with. The convention of nine stress components acting at a point of a body is illustrated in Fig. 2.1. All the stress components shown in the figure are positive. The directions of stresses other than those indicated in the figure are considered negative.

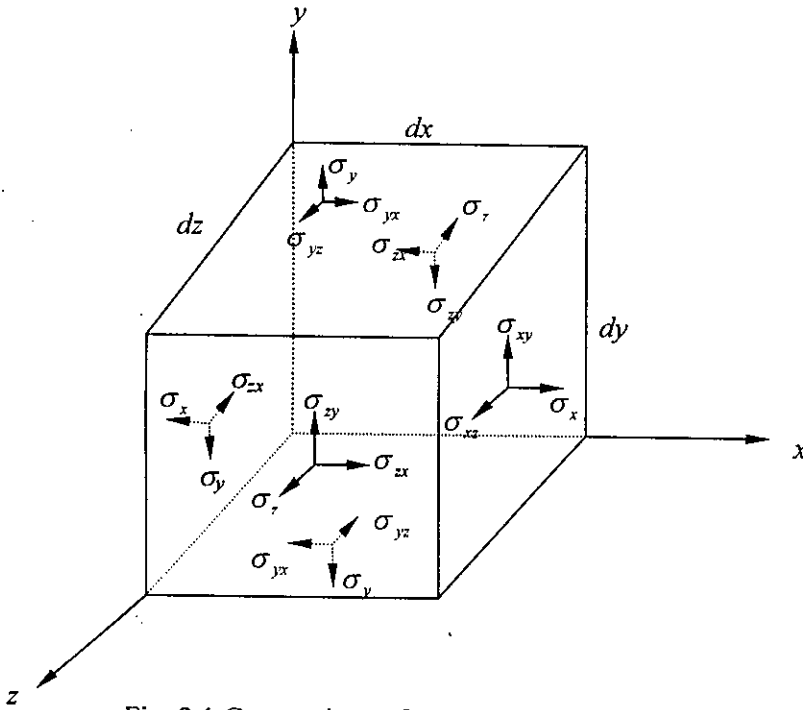


Fig. 2.1 Conventions of stress components.

By considering moment of forces at the center of the cubic element of Fig. 2.1, it can be shown that $\sigma_{xy} = \sigma_{yx}$, $\sigma_{yz} = \sigma_{zy}$, $\sigma_{zx} = \sigma_{xz}$. Thus, the nine stress components reduce to six in number. Furthermore, the condition of static equilibrium of forces acting on the body gives:

$$\begin{aligned}\frac{\partial \sigma_x}{\partial x} + \frac{\partial \sigma_{xy}}{\partial y} + \frac{\partial \sigma_{xz}}{\partial z} + F_x &= 0 \\ \frac{\partial \sigma_y}{\partial y} + \frac{\partial \sigma_{xy}}{\partial x} + \frac{\partial \sigma_{yz}}{\partial z} + F_y &= 0 \\ \frac{\partial \sigma_z}{\partial z} + \frac{\partial \sigma_{xz}}{\partial x} + \frac{\partial \sigma_{yz}}{\partial y} + F_z &= 0\end{aligned}\quad (2.1)$$

These equations are known as the equations of equilibrium. The parameters F_x , F_y , and F_z are the components of body force in x , y , and z directions, respectively. Again the relations between strain and displacement components are given by

$$\epsilon_x = \frac{\partial u_x}{\partial x}, \epsilon_y = \frac{\partial u_y}{\partial y}, \epsilon_z = \frac{\partial u_z}{\partial z}, \gamma_{xy} = \frac{\partial u_x}{\partial y} + \frac{\partial u_y}{\partial x}, \gamma_{yz} = \frac{\partial u_y}{\partial z} + \frac{\partial u_z}{\partial y}, \gamma_{zx} = \frac{\partial u_x}{\partial z} + \frac{\partial u_z}{\partial x}\quad (2.2)$$

Now from Eq. 2.2, one obtains the following relations by simple manipulation.

$$\begin{aligned}\frac{\partial^2 \epsilon_x}{\partial y^2} + \frac{\partial^2 \epsilon_y}{\partial x^2} &= \frac{\partial^2 \gamma_{xy}}{\partial x \partial y}; & 2 \frac{\partial^2 \epsilon_x}{\partial y \partial z} &= \left(-\frac{\partial \gamma_{yz}}{\partial x} + \frac{\partial \gamma_{zx}}{\partial y} + \frac{\partial \gamma_{xy}}{\partial z} \right) \\ \frac{\partial^2 \epsilon_y}{\partial z^2} + \frac{\partial^2 \epsilon_z}{\partial y^2} &= \frac{\partial^2 \gamma_{yz}}{\partial y \partial z}; & 2 \frac{\partial^2 \epsilon_y}{\partial x \partial z} &= \left(\frac{\partial \gamma_{yz}}{\partial x} - \frac{\partial \gamma_{zx}}{\partial y} + \frac{\partial \gamma_{xy}}{\partial z} \right) \\ \frac{\partial^2 \epsilon_z}{\partial x^2} + \frac{\partial^2 \epsilon_x}{\partial z^2} &= \frac{\partial^2 \gamma_{zx}}{\partial z \partial x}; & 2 \frac{\partial^2 \epsilon_z}{\partial x \partial y} &= \left(\frac{\partial \gamma_{yz}}{\partial x} + \frac{\partial \gamma_{zx}}{\partial y} - \frac{\partial \gamma_{xy}}{\partial z} \right)\end{aligned}\quad (2.3)$$

These differential equations are known as the conditions of compatibility. The solution of elasticity problems must satisfy the equilibrium equations and the compatibility conditions along with the specific boundary conditions.

2.2 Plane stress condition

The thickness of a single lamina or a laminate is small in comparison with its other dimensions. Thus, the analysis of a lamina or a laminate predominantly falls under the plane stress condition. For plane stress condition

$$\sigma_z = 0; \sigma_{zx} = 0; \sigma_{yz} = 0\quad (2.4)$$

Therefore, for plane stress, the equilibrium Eq. (2.1) having no body force reduces to

$$\begin{aligned}\frac{\partial \sigma_x}{\partial x} + \frac{\partial \sigma_{xy}}{\partial y} &= 0 \\ \frac{\partial \sigma_y}{\partial y} + \frac{\partial \sigma_{xy}}{\partial x} &= 0\end{aligned}\quad (2.5)$$

The strain-displacement relations Eq. (2.2) and the compatibility conditions given by Eq. (2.3), respectively, reduce to

$$\varepsilon_x = \frac{\partial u_x}{\partial x}, \varepsilon_y = \frac{\partial u_y}{\partial y}, \gamma_{xy} = \frac{\partial u_x}{\partial y} + \frac{\partial u_y}{\partial x} \quad (2.6)$$

$$\text{and } \frac{\partial^2 \varepsilon_x}{\partial y^2} + \frac{\partial^2 \varepsilon_y}{\partial x^2} = \frac{\partial^2 \gamma_{xy}}{\partial x \partial y} \quad (2.7)$$

A symmetric laminate is one in which the material, fiber angle, and thickness of the plies are same above and below the mid plane. For a symmetric laminated composite, there is no curvature of the laminate under inplane loading. For this case, the mid-plane strains are equal to the global strains and the stress-strain relations are given by [61]

$$\begin{bmatrix} \sigma_x \\ \sigma_y \\ \sigma_{xy} \end{bmatrix} = \frac{1}{ah} \begin{bmatrix} A_{11} & A_{12} & 0 \\ A_{12} & A_{22} & 0 \\ 0 & 0 & A_{66} \end{bmatrix} \begin{bmatrix} \varepsilon_x \\ \varepsilon_y \\ \gamma_{xy} \end{bmatrix} \quad (2.8)$$

Here, the elements of stiffness matrix are given by [57]

$$A_{11} = \sum_{k=1}^n [Q_{11}c^4 + Q_{22}s^4 + 2(Q_{12} + 2Q_{66})s^2c^2]_k (h_k - h_{k-1}) \quad (2.9)$$

$$A_{12} = \sum_{k=1}^n [(Q_{11} + Q_{22} - 4Q_{66})s^2c^2 + Q_{12}(c^4 + s^4)]_k (h_k - h_{k-1}) \quad (2.10)$$

$$A_{22} = \sum_{k=1}^n [Q_{11}s^4 + Q_{22}c^4 + 2(Q_{12} + 2Q_{66})s^2c^2]_k (h_k - h_{k-1}) \quad (2.11)$$

$$A_{66} = \sum_{k=1}^n [(Q_{11} + Q_{22} - 2Q_{12} - 2Q_{66})s^2c^2 + Q_{66}(s^4 + c^4)]_k (h_k - h_{k-1}) \quad (2.12)$$

where $Q_{11} = \frac{E_1}{1 - \nu_{21}\nu_{12}}$, $Q_{12} = \frac{\nu_{12}E_2}{1 - \nu_{21}\nu_{12}}$, $Q_{22} = \frac{E_2}{1 - \nu_{21}\nu_{12}}$, $Q_{66} = G_{12}$, $c = \cos \theta$,

$s = \sin \theta$; $h_k - h_{k-1}$ is the thickness of the k -th ply, h is the total thickness of the laminate, E_1 and E_2 are the young's moduli in longitudinal and transverse direction

of each ply, respectively; ν_{12} and ν_{21} are the major and minor Poisson's ratios, respectively; G_{12} is the in-plane shear modulus, n is the total number of plies. Further, the reciprocal relation between the poisson's ratios and the elastic moduli is given by [61]

$$\frac{\nu_{12}}{E_1} = \frac{\nu_{21}}{E_2}$$

Equations (2.5) and (2.7) form a complete set of equations for the two dimensional plane stress elasticity problem. Equation (2.7) can be expressed in terms of three stress components by using Eq. (2.8). Thus, this set of equations includes three unknown stress components, which should be solved satisfying the associated boundary conditions. However, instead of solving three unknown quantities (three stress components) from three equations simultaneously, it would be convenient if the number of unknown quantities and the number of unknown equations could be reduced. One approach to achieve this goal is to express all the equation in terms of displacement components. First, Eq. (2.8) is expressed in terms displacement components by making use of Eq. (2.6) as

$$\sigma_x = \frac{1}{ah} \left[A_{11} \frac{\partial u_x}{\partial x} + A_{12} \frac{\partial u_y}{\partial y} \right] \quad (2.13)$$

$$\sigma_y = \frac{1}{ah} \left[A_{21} \frac{\partial u_x}{\partial x} + A_{22} \frac{\partial u_y}{\partial y} \right] \quad (2.14)$$

$$\sigma_{xy} = \frac{1}{ah} A_{66} \left[\frac{\partial u_x}{\partial y} + \frac{\partial u_y}{\partial x} \right] \quad (2.15)$$

Substitution of Eqs. (2.13) - (2.15) into equilibrium Eqs. (2.5) yields

$$A_{11} \frac{\partial^2 u_x}{\partial x^2} + (A_{12} + A_{66}) \frac{\partial^2 u_y}{\partial x \partial y} + A_{66} \frac{\partial^2 u_x}{\partial y^2} = 0 \quad (2.16)$$

$$A_{22} \frac{\partial^2 u_y}{\partial y^2} + (A_{12} + A_{66}) \frac{\partial^2 u_x}{\partial x \partial y} + A_{66} \frac{\partial^2 u_y}{\partial x^2} = 0 \quad (2.17)$$

Now, it is seen that there are only two equilibrium equations (Eqs. (2.16) and (2.17)) of two unknown quantities i.e. two unknown displacement components. The third equation i.e. the compatibility Eq. (2.7) becomes irrelevant in this case.

2.3 Definition of displacement potential function

In this article, it is aimed at defining a function, called displacement potential function, so as to further reduce the governing differential equations (Eqs. (2.16) and (2.17)). With this view, the displacement potential function ψ is defined as a function of displacement components as follows:

$$\begin{aligned} u_x &= \alpha_1 \frac{\partial^2 \psi}{\partial x^2} + \alpha_2 \frac{\partial^2 \psi}{\partial x \partial y} + \alpha_3 \frac{\partial^2 \psi}{\partial y^2} \\ u_y &= \alpha_4 \frac{\partial^2 \psi}{\partial x^2} + \alpha_5 \frac{\partial^2 \psi}{\partial x \partial y} + \alpha_6 \frac{\partial^2 \psi}{\partial y^2} \end{aligned} \quad (2.18)$$

Here, α 's are unknown material constants.

Combining Eqs. (2.13) - (2.15) and (2.18), one can arrive at

$$\begin{aligned} \sigma_x &= \alpha_1 A_{11} \frac{\partial^3 \psi}{\partial x^3} + (\alpha_2 A_{11} + \alpha_4 A_{12}) \frac{\partial^3 \psi}{\partial x^2 \partial y} + (\alpha_3 A_{11} + \alpha_5 A_{12}) \frac{\partial^3 \psi}{\partial x \partial y^2} + \alpha_6 A_{12} \frac{\partial^3 \psi}{\partial y^3} \\ \sigma_y &= \alpha_1 A_{12} \frac{\partial^3 \psi}{\partial x^3} + (\alpha_2 A_{12} + \alpha_4 A_{22}) \frac{\partial^3 \psi}{\partial x^2 \partial y} + (\alpha_3 A_{12} + \alpha_5 A_{22}) \frac{\partial^3 \psi}{\partial x \partial y^2} + \alpha_6 A_{22} \frac{\partial^3 \psi}{\partial y^3} \\ \sigma_{xy} &= \alpha_4 A_{66} \frac{\partial^3 \psi}{\partial x^3} + (\alpha_1 A_{66} + \alpha_5 A_{66}) \frac{\partial^3 \psi}{\partial x^2 \partial y} + (\alpha_2 A_{66} + \alpha_6 A_{66}) \frac{\partial^3 \psi}{\partial x \partial y^2} + \alpha_3 A_{66} \frac{\partial^3 \psi}{\partial y^3} \end{aligned} \quad (2.19)$$

Applying Eq. (2.19) into Eqs. (2.16) and (2.17), one obtains the equilibrium equations in terms of the function $\psi(x, y)$, which are given as

$$\begin{aligned} \alpha_1 A_{11} \frac{\partial^4 \psi}{\partial x^4} + (\alpha_2 A_{11} + \alpha_4 A_{12} + \alpha_4 A_{66}) \frac{\partial^4 \psi}{\partial x^3 \partial y} + (\alpha_3 A_{11} + \alpha_1 A_{66} + \alpha_5 A_{12} + \alpha_5 A_{66}) \frac{\partial^4 \psi}{\partial x^2 \partial y^2} + \\ (\alpha_2 A_{66} + \alpha_6 A_{12} + \alpha_5 A_{12} + \alpha_6 A_{66}) \frac{\partial^4 \psi}{\partial x \partial y^3} + \alpha_3 A_{66} \frac{\partial^4 \psi}{\partial y^4} = 0 \\ \alpha_4 A_{66} \frac{\partial^4 \psi}{\partial x^4} + (\alpha_1 A_{12} + \alpha_1 A_{66} + \alpha_5 A_{66}) \frac{\partial^4 \psi}{\partial x^3 \partial y} + (\alpha_2 A_{12} + \alpha_2 A_{66} + \alpha_6 A_{66} + \alpha_4 A_{22}) \frac{\partial^4 \psi}{\partial x^2 \partial y^2} + \\ (\alpha_3 A_{12} + \alpha_3 A_{66} + \alpha_5 A_{22}) \frac{\partial^4 \psi}{\partial x \partial y^3} + \alpha_6 A_{22} \frac{\partial^4 \psi}{\partial y^4} = 0 \end{aligned} \quad (2.20)$$

This gives two equilibrium equations in terms of a single function ψ . The constants α 's are chosen in such a way that the first equation of Eqs. (2.20) is automatically satisfied under all circumstances. This will happen when coefficients of all the derivatives of the first equation of Eqs. (2.20) are individually zero. That is, when

$$\begin{aligned}
\alpha_1 A_{11} &= 0 \\
\alpha_2 A_{11} + \alpha_4 A_{12} + \alpha_6 A_{66} &= 0 \\
\alpha_3 A_{11} + \alpha_1 A_{66} + \alpha_5 A_{12} + \alpha_5 A_{66} &= 0 \\
\alpha_2 A_{66} + \alpha_6 A_{12} + \alpha_5 A_{12} + \alpha_6 A_{66} &= 0 \\
\alpha_3 A_{66} &= 0
\end{aligned} \tag{2.21}$$

From these relations, it is found that

$$\begin{aligned}
\alpha_1 &= 0 \\
\alpha_3 &= 0 \\
\alpha_5 &= 0
\end{aligned}$$

The remaining three constants have the following relations:

$$\begin{aligned}
\alpha_4 &= -\frac{\alpha_2 A_{11}}{A_{12} + A_{66}} \\
\alpha_6 &= -\frac{\alpha_2 A_{66}}{A_{12} + A_{66}}
\end{aligned} \tag{2.22}$$

Thus for ψ to be a solution of the stress problem, it has to satisfy the second equilibrium equation of Eqs. (2.20) only. However, the values of α 's must be known in advance. Here, we have basically two equations Eq. (2.22) for determining three unknown α 's. An arbitrary value is thus assigned to any one of these three unknowns and the remaining α 's are solved from Eq. (2.22). Assuming $\alpha_2 = 1$, the values of α_4 and α_6 are obtained as

$$\begin{aligned}
\alpha_4 &= -\frac{A_{11}}{A_{12} + A_{66}} \\
\alpha_6 &= -\frac{A_{66}}{A_{12} + A_{66}}
\end{aligned} \tag{2.23}$$

When the above values of α 's are substituted in the second equation of Eq. (2.20), the governing differential equation for the solution of two dimensional laminated composite structures becomes

$$\frac{\partial^4 \psi}{\partial x^4} + \left[\frac{A_{22}}{A_{66}} - \frac{A_{12}^2}{A_{11} A_{66}} - \frac{2A_{12}}{A_{11}} \right] \frac{\partial^4 \psi}{\partial x^2 \partial y^2} + \frac{A_{22}}{A_{11}} \frac{\partial^4 \psi}{\partial y^4} = 0 \tag{2.24}$$

By making use of the above values of α 's in Eqs. (2.18) and (2.19), one obtains the components of displacement and stress as follows:

$$u_x = \frac{\partial^2 \psi}{\partial x \partial y}$$

$$u_y = -\frac{A_{11}}{A_{12} + A_{66}} \frac{\partial^2 \psi}{\partial x^2} - \frac{A_{66}}{A_{12} + A_{66}} \frac{\partial^2 \psi}{\partial y^2} \quad (2.25)$$

$$\sigma_x = \frac{A_{66}}{ah(A_{12} + A_{66})} \left[A_{11} \frac{\partial^3 \psi}{\partial x^2 \partial y} - A_{12} \frac{\partial^3 \psi}{\partial y^3} \right]$$

$$\sigma_y = \frac{1}{ah(A_{12} + A_{66})} \left[(A_{12}^2 + A_{12}A_{66} - A_{11}A_{22}) \frac{\partial^3 \psi}{\partial x^2 \partial y} - A_{22}A_{66} \frac{\partial^3 \psi}{\partial y^3} \right] \quad (2.26)$$

$$\sigma_{xy} = \frac{A_{66}}{ah(A_{12} + A_{66})} \left[A_{12} \frac{\partial^3 \psi}{\partial x \partial y^2} - A_{11} \frac{\partial^3 \psi}{\partial x^3} \right]$$

Now, it is found that there is only one governing differential equation Eq. (2.24) for the solution of the displacement potential function ψ . Once the displacement potential function ψ is known, the components of displacement and stress can be readily found from Eqs. (2.25) and (2.26).

2.4 General consideration of the boundary conditions

Equation (2.24) is solved for the displacement potential function ψ , which is further used to determine the components of displacement and stress from Eqs. (2.25) and (2.26). The components of stress and displacement vary over the volume of the body. At the boundary, they must be such as to satisfy the boundary conditions. The practical situations, which may exist along the edge or boundary of a structure, are visualized in two different ways, namely

- a) Displacements and
- b) Loading or stress

Both the displacements and the stresses are defined by their respective components.

These components are

1. Normal displacement
2. Tangential displacement
3. Normal stress
4. Tangential stress

At any point on the boundary, out of these four quantities, two are known at a time. Therefore, the four quantities, taking two at a time, may provide six different boundary conditions. These six boundary conditions are given by

- a) Normal displacement, tangential displacement
- b) Normal displacement, tangential stress
- c) Tangential displacement, normal stress
- d) Normal stress, tangential stress
- e) Normal displacement, normal stress
- f) Tangential displacement, tangential stress

Out of these six possible combinations, the last two combinations, namely (e) and (f), do not generally exist in physical problems. Therefore, at any point on the boundary, the first four possible boundary conditions are concerned with. If the shape of the boundary considered is rectangular, the structure may be oriented so that its edges are parallel to the co-ordinate axes. In that case, the normal and the tangential components of stress and displacement at the boundary are the co-ordinate components of stress and displacement inside the structure. When the first four boundary conditions are stated mathematically in terms of the functions to be determined, one obtains

1. $u_n = \psi_1(x, y), u_t = \psi_2(x, y)$
2. $u_n = \psi_3(x, y), \sigma_t = \psi_4(x, y)$
3. $u_t = \psi_5(x, y), \sigma_n = \psi_6(x, y)$
4. $\sigma_n = \psi_7(x, y), \sigma_t = \psi_8(x, y)$

(2.27)

From the above expressions of boundary conditions, it is revealed that, there is no technical difficulty in satisfying all the modes of boundary conditions appropriately. Moreover, compared to the approach of solving the problem in terms of displacement components, the displacement potential function approach has the advantage that only one function ψ is required to be evaluated instead of solving for two variables u_x and u_y simultaneously.

CHAPTER-3 SOME SAMPLE PROBLEMS OF LAMINATED COMPOSITE STRUCTURES

In this chapter, some sample problems of laminated composite structures are solved to demonstrate the method developed in the preceding chapters. Two different types of laminate will be considered: (i) cross-ply laminate and (ii) angle-ply laminate. For each of the laminates, different conditions will be imposed on the boundary.

3.1 A rectangular panel of cross-ply laminated composite under uniform tensile loading:

A symmetric cross-ply laminated composite panel consisting of n number of plies is shown in Fig. 3.1. A cross-ply laminate is a laminate in which the fibers are oriented only at 0° and 90° . The thickness of the panel is h . A cross-ply laminate (also called laminates with especially orthotropic layers) is one in which fiber angles are only 0° and 90° . The left end of the panel is rigidly fixed while the two longitudinal ends are stiffened. The other end is subjected to a uniform tensile load σ_x^0 . The length of the panel is b and the width is a . The conditions on the stiffeners are mathematically formulated by the fact that there is no displacement along the length of the stiffened edges under the action of load and the stress in the direction perpendicular to the

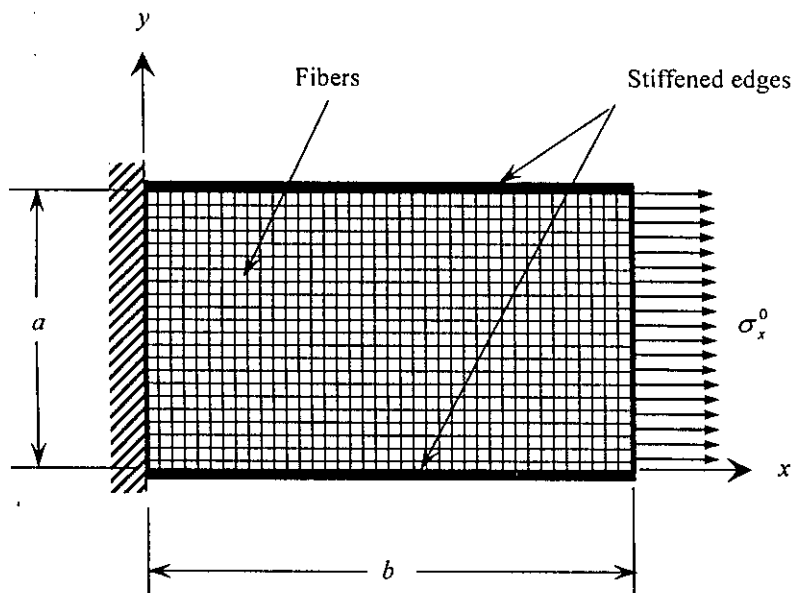


Fig. 3.1 A rectangular panel of cross-ply laminated composite under uniform tensile loading.

stiffener is zero. Thus, the boundary conditions of the problem are given by

- (1) $u_x(x, 0) = u_x(x, a) = 0; 0 \leq x \leq b$
- (2) $\sigma_y(x, 0) = \sigma_y(x, a) = 0; 0 \leq x \leq b$
- (3) $u_x(0, y) = u_y(0, y) = 0; 0 \leq y \leq a$
- (4) $\sigma_x(b, y) = \sigma_x^0, \sigma_{xy}(b, y) = 0; 0 \leq y \leq a$

Under these boundary conditions the elastic field in the panel has to be determined. To accomplish this, Eq. (2.24) has to be solved for the unknown displacement potential function ψ from which the components of stress and displacement can be found using Eqs. (2.25) and (2.26). For a unique solution, ψ has to satisfy Eq. (2.24) as well as the boundary conditions described above.

For the present problem, the displacement potential function is assumed to be

$$\psi = \sum_{m=1}^{\infty} X_m \cos \alpha y \quad (3.1)$$

where X_m is a function of x only and $\alpha = \frac{m\pi}{a}$.

Now substitution of Eq. (3.1) into Eq. (2.24) yields

$$X_m'''' - BX_m''\alpha^2 + CX_m\alpha^4 = 0 \quad (3.2)$$

where (') indicates differentiation with respect to x and

$$B = \frac{A_{22}}{A_{66}} - \frac{A_{12}^2}{A_{11}A_{66}} - \frac{2A_{12}}{A_{11}}, \quad C = \frac{A_{22}}{A_{11}}$$

The general solution of Eq. (3.2) can be given by

$$X_m = A_m e^{n_1 x} + B_m e^{n_2 x} + C_m e^{n_3 x} + D_m e^{n_4 x} \quad (3.3)$$

where

$$n_1, n_2 = \alpha \sqrt{\frac{B \pm \sqrt{B^2 - 4C}}{2}} \quad (3.4)$$

$$n_3, n_4 = -\alpha \sqrt{\frac{B \pm \sqrt{B^2 - 4C}}{2}}$$

and A_m, B_m, C_m and D_m are arbitrary constants.

Substituting Eq. (3.1) into Eqs. (2.25) and (2.26), the expressions of displacement and stress components are obtained as

$$u_x(x, y) = -\sum_{m=1}^{\infty} \alpha X'_m \sin \alpha y \quad (3.5a)$$

$$u_y(x, y) = \frac{1}{A_{12} + A_{66}} \sum_{m=1}^{\infty} [A_{66} X_m \alpha^2 - A_{11} X_m''] \cos \alpha y \quad (3.5b)$$

$$\sigma_x(x, y) = -\frac{A_{66}}{ah(A_{12} + A_{66})} \sum_{m=1}^{\infty} [A_{12} X_m \alpha^3 + A_{11} X_m'''] \sin \alpha y \quad (3.5c)$$

$$\sigma_y(x, y) = -\frac{1}{ah(A_{12} + A_{66})} \sum_{m=1}^{\infty} [A_{22} A_{66} X_m \alpha^3 + (A_{12}^2 + A_{12} A_{66} - A_{11} A_{22}) X_m'''] \sin \alpha y \quad (3.5d)$$

$$\sigma_{xy}(x, y) = -\frac{A_{66}}{ah(A_{12} + A_{66})} \sum_{m=1}^{\infty} [A_{12} X_m' \alpha^2 + A_{11} X_m'''] \cos \alpha y \quad (3.5e)$$

Substituting different derivatives of X_m in the expressions of the stress and displacement components (Eqs. (3.5a) – (3.5e)), one can obtain

$$u_x(x, y) = \sum_{m=1}^{\infty} \left[-(n_1 A_m e^{n_1 x} + n_2 B_m e^{n_2 x} + n_3 C_m e^{n_3 x} + n_4 D_m e^{n_4 x}) \alpha \sin \alpha y \right] \quad (3.6a)$$

$$u_y(x, y) = \frac{1}{A_{12} + A_{66}} \sum_{m=1}^{\infty} \left[A_{66} (A_m e^{n_1 x} + B_m e^{n_2 x} + C_m e^{n_3 x} + D_m e^{n_4 x}) \alpha^2 \right. \\ \left. - A_{11} (n_1^2 A_m e^{n_1 x} + n_2^2 B_m e^{n_2 x} + n_3^2 C_m e^{n_3 x} + n_4^2 D_m e^{n_4 x}) \right] \cos \alpha y \quad (3.6b)$$

$$\sigma_x(x, y) = -\frac{A_{66}}{ah(A_{12} + A_{66})} \sum_{m=1}^{\infty} \left[A_{12} (A_m e^{n_1 x} + B_m e^{n_2 x} + C_m e^{n_3 x} + D_m e^{n_4 x}) \alpha^3 + \right. \\ \left. A_{11} (n_1^2 A_m e^{n_1 x} + n_2^2 B_m e^{n_2 x} + n_3^2 C_m e^{n_3 x} + n_4^2 D_m e^{n_4 x}) \alpha \right] \sin \alpha y \quad (3.6c)$$

$$\sigma_y(x, y) = -\frac{1}{ah(A_{12} + A_{66})} \sum_{m=1}^{\infty} \left[A_{22} A_{66} (A_m e^{n_1 x} + B_m e^{n_2 x} + C_m e^{n_3 x} + D_m e^{n_4 x}) \alpha^3 + \right. \\ \left. (A_{12}^2 + A_{12} A_{66} - A_{11} A_{22}) \right. \\ \left. (n_1^2 A_m e^{n_1 x} + n_2^2 B_m e^{n_2 x} + n_3^2 C_m e^{n_3 x} + n_4^2 D_m e^{n_4 x}) \alpha \right] \sin \alpha y \quad (3.6d)$$

$$\sigma_{xy}(x, y) = -\frac{A_{66}}{ah(A_{12} + A_{66})} \sum_{m=1}^{\infty} \left[A_{12} (n_1 A_m e^{n_1 x} + n_2 B_m e^{n_2 x} + n_3 C_m e^{n_3 x} + n_4 D_m e^{n_4 x}) \alpha^2 + \right. \\ \left. A_{11} (n_1^3 A_m e^{n_1 x} + n_2^3 B_m e^{n_2 x} + n_3^3 C_m e^{n_3 x} + n_4^3 D_m e^{n_4 x}) \right] \cos \alpha y \quad (3.6e)$$

For the present problem, it is seen from Eqs. (3.6a) and (3.6d) that the boundary conditions (1) and (2) are satisfied automatically. Therefore, only the boundary conditions (3), and (4) are remaining to be satisfied. The uniform tensile load σ_x^0 applied at the edge $x = b$ can be expressed in Fourier series as

$$\sigma_x(b, y) = \sigma_x^0 = \sum_{m=1}^{\infty} E_m \sin \alpha y \quad (3.7)$$

$$\text{where } E_m = \frac{2}{a} \int_0^a \sigma_x^0 \sin \alpha y dy = -\frac{4\sigma_x^0}{m\pi} \quad \text{for } m = 1, 3, 5, \dots, \infty \quad (3.8)$$

Now, by applying the boundary conditions (3) and (4) in Eqs. (3.6a) - (3.6c) and (3.6e) and making use of relation (3.7), the following four algebraic equations can be obtained for the four unknown coefficients A_m , B_m , C_m , and D_m .

$$n_1 A_m + n_2 B_m + n_3 C_m + n_4 D_m = 0 \quad (3.9a)$$

$$(A_{11} n_1^2 - A_{66} \alpha^2) A_m + (A_{11} n_2^2 - A_{66} \alpha^2) B_m + (A_{11} n_3^2 - A_{66} \alpha^2) C_m + (A_{11} n_4^2 - A_{66} \alpha^2) D_m = 0 \quad (3.9b)$$

$$(A_{11} n_1^2 \alpha + A_{12} \alpha^3) A_m e^{n_1 b} + (A_{11} n_2^2 \alpha + A_{12} \alpha^3) B_m e^{n_2 b} + (A_{11} n_3^2 \alpha + A_{12} \alpha^3) C_m e^{n_3 b} + (A_{11} n_4^2 \alpha + A_{12} \alpha^3) D_m e^{n_4 b} = \bar{E}_m \quad (3.9c)$$

$$(A_{11} n_1^3 + A_{12} n_1 \alpha^2) A_m e^{n_1 b} + (A_{11} n_2^3 + A_{12} n_2 \alpha^2) B_m e^{n_2 b} + (A_{11} n_3^3 + A_{12} n_3 \alpha^2) C_m e^{n_3 b} + (A_{11} n_4^3 + A_{12} n_4 \alpha^2) D_m e^{n_4 b} = 0 \quad (3.9d)$$

$$\text{where } \bar{E}_m = -\frac{E_m a h (A_{12} + A_{66})}{A_{66}}$$

The above equations can be written in a simplified form for the solution of the unknowns as follows:

$$\begin{bmatrix} n_1 & n_2 & n_3 & n_4 \\ P_1 & P_2 & P_3 & P_4 \\ Q_1 & Q_2 & Q_3 & Q_4 \\ R_1 & R_2 & R_3 & R_4 \end{bmatrix} \begin{bmatrix} A_m \\ B_m \\ C_m \\ D_m \end{bmatrix} = \begin{bmatrix} 0 \\ 0 \\ \bar{E}_m \\ 0 \end{bmatrix} \quad (3.10)$$

where

$$\begin{aligned} P_i &= A_{11} n_i^2 - A_{66} \alpha^2 \\ Q_i &= (A_{11} n_i^2 \alpha + A_{12} \alpha^3) e^{n_i b} \\ R_i &= (A_{11} n_i^3 + A_{12} n_i \alpha^2) e^{n_i b} \end{aligned} \quad i = 1, 2, 3, \text{ and } 4.$$

The solution of the above algebraic Eq. (3.10) yields the unknown constants A_m , B_m , C_m , and D_m . Once the values of the unknowns are determined, they are directly substituted into Eqs. (3.6a) - (3.6e) to obtain the explicit expressions for the different parameters of interest, namely, the two displacement and the three stress components, which are valid for the entire region of the stiffened edge panel of

laminated composite. It is noted that Eq. (3.10) is derived by satisfying the remaining boundary conditions (3) and (4). Thus, the solution of Eq. (3.10) ensures that all the boundary conditions are satisfied identically.

3.2 A rectangular panel of cross-ply laminated composite under parabolic tensile loading:

A symmetric cross-ply laminated composite panel consisting of n number of plies is shown in Fig. 3.2. The thickness of the panel is h . The left end of the panel is rigidly fixed while the two longitudinal ends are stiffened. The other end is subjected to a parabolic tensile load, as shown in the figure. The length of the panel is b and the width is a , the boundary conditions of the problem are given by

- (1) $u_x(x, 0) = u_x(x, a) = 0; 0 \leq x \leq b$
- (2) $\sigma_y(x, 0) = \sigma_y(x, a) = 0; 0 \leq x \leq b$
- (3) $u_x(0, y) = u_y(0, y) = 0; 0 \leq y \leq a$
- (4) $\sigma_x(b, y) = \sigma_x^0 = \frac{4P}{a^2}(ay - y^2), \sigma_{xy}(b, y) = 0; 0 \leq y \leq a$

where P is the maximum value of the tensile load, for this case it is at $y = a/2$.

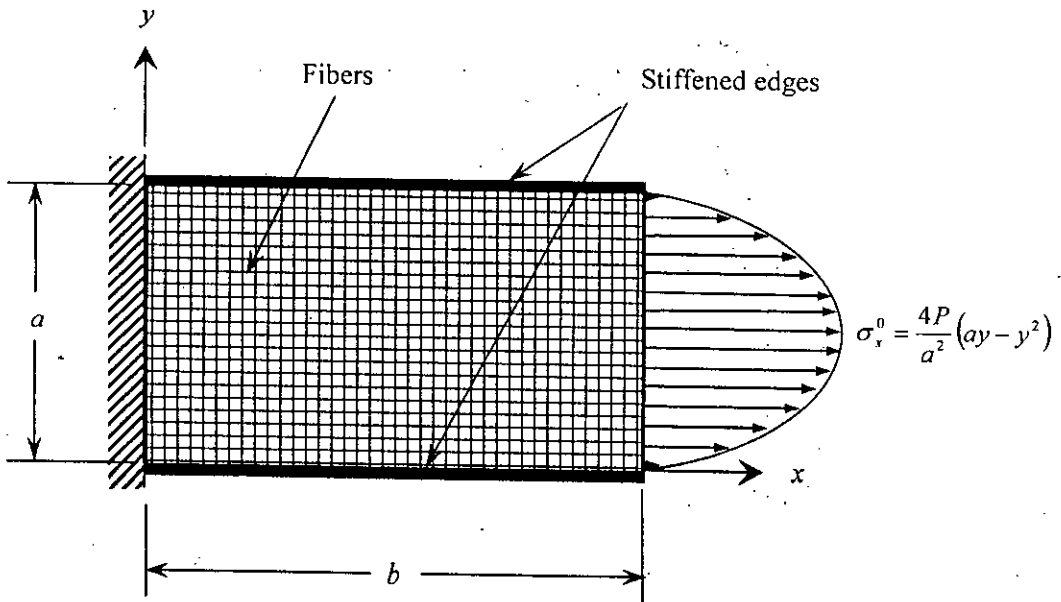


Fig. 3.2 A rectangular panel of cross-ply laminated composite under parabolic tensile loading.

For this problem, the displacement potential function is assumed to be same as given by Eq. (3.1). Further Eqs. (3.2) to (3.6e) also apply to the present problem. The boundary conditions (1) and (2), as before, are satisfied automatically. Therefore, only the boundary conditions (3) and (4) are remaining to be satisfied. The parabolic tensile load applied at the edge $x = b$ can be expressed in Fourier series as

$$\sigma_x(h, y) = \sigma_x^0 = \sum_{m=1}^{\infty} E_m \sin \alpha y \quad (3.11)$$

$$\text{where } E_m = \frac{8P}{\alpha^3} \int_0^a (ay - y^2) \sin \alpha y dy = \frac{32P}{m^3 \pi^3} \quad \text{for } m = 1, 3, 5, \dots \infty \quad (3.12)$$

applying the remaining boundary conditions (3) and (4) in Eqs. (3.6a) - (3.6c) and (3.6e) and making use of relation (3.11), the following four algebraic equations can be obtained for four unknown coefficients $A_m, B_m, C_m,$ and D_m .

$$n_1 A_m + n_2 B_m + n_3 C_m + n_4 D_m = 0 \quad (3.13a)$$

$$(A_{11} n_1^2 - A_{66} \alpha^2) A_m + (A_{11} n_2^2 - A_{66} \alpha^2) B_m + (A_{11} n_3^2 - A_{66} \alpha^2) C_m + (A_{11} n_4^2 - A_{66} \alpha^2) D_m = 0 \quad (3.13b)$$

$$(A_{11} n_1^2 \alpha + A_{12} \alpha^3) A_m e^{n_1 h} + (A_{11} n_2^2 \alpha + A_{12} \alpha^3) B_m e^{n_2 h} + (A_{11} n_3^2 \alpha + A_{12} \alpha^3) C_m e^{n_3 h} + (A_{11} n_4^2 \alpha + A_{12} \alpha^3) D_m e^{n_4 h} = \bar{E}_m \quad (3.13c)$$

$$(A_{11} n_1^3 + A_{12} n_1 \alpha^2) A_m e^{n_1 h} + (A_{11} n_2^3 + A_{12} n_2 \alpha^2) B_m e^{n_2 h} + (A_{11} n_3^3 + A_{12} n_3 \alpha^2) C_m e^{n_3 h} + (A_{11} n_4^3 + A_{12} n_4 \alpha^2) D_m e^{n_4 h} = 0 \quad (3.13d)$$

$$\text{where } \bar{E}_m = -\frac{E_m a h (A_{12} + A_{66})}{A_{66}}$$

The above equations can be written in a simplified form for the solution of the unknowns as follows:

$$\begin{bmatrix} n_1 & n_2 & n_3 & n_4 \\ P_1 & P_2 & P_3 & P_4 \\ Q_1 & Q_2 & Q_3 & Q_4 \\ R_1 & R_2 & R_3 & R_4 \end{bmatrix} \begin{bmatrix} A_m \\ B_m \\ C_m \\ D_m \end{bmatrix} = \begin{bmatrix} 0 \\ 0 \\ \bar{E}_m \\ 0 \end{bmatrix} \quad (3.14)$$

where

$$\begin{aligned} P_i &= A_{11} n_i^2 - A_{66} \alpha^2 \\ Q_i &= (A_{11} n_i^2 \alpha + A_{12} \alpha^3) e^{n_i h} \\ R_i &= (A_{11} n_i^3 + A_{12} n_i \alpha^2) e^{n_i h} \end{aligned} \quad i = 1, 2, 3, \text{ and } 4.$$

The solution of the above algebraic Eq. (3.14) yields the unknown constants A_m , B_m , C_m , and D_m . Once the values of the unknowns are determined, they are directly substituted into Eq. (3.6) to obtain the explicit expressions for the different parameters of interest, namely, the two displacement and the three stress components, which are valid for the entire region of the stiffened edge panel of laminated composite.

3.3 A rectangular panel of cross-ply laminated composite under parabolic shear loading:

A symmetric cross-ply laminated composite panel consisting of n number of plies is shown in Fig. 3.3. The thickness of the panel is h . The left end of the panel is rigidly fixed while the two longitudinal edges are stiffened. The other end is subjected to a parabolic shear load $\sigma_{xy}^0 = \frac{4P}{a^2}(y^2 - ay)$. The length of the panel is b and the width is

a . The boundary conditions of the problem are given by

$$(1) u_x(x, 0) = u_x(x, a) = 0; 0 \leq x \leq b$$

$$(2) \sigma_y(x, 0) = \sigma_y(x, a) = 0; 0 \leq x \leq b$$

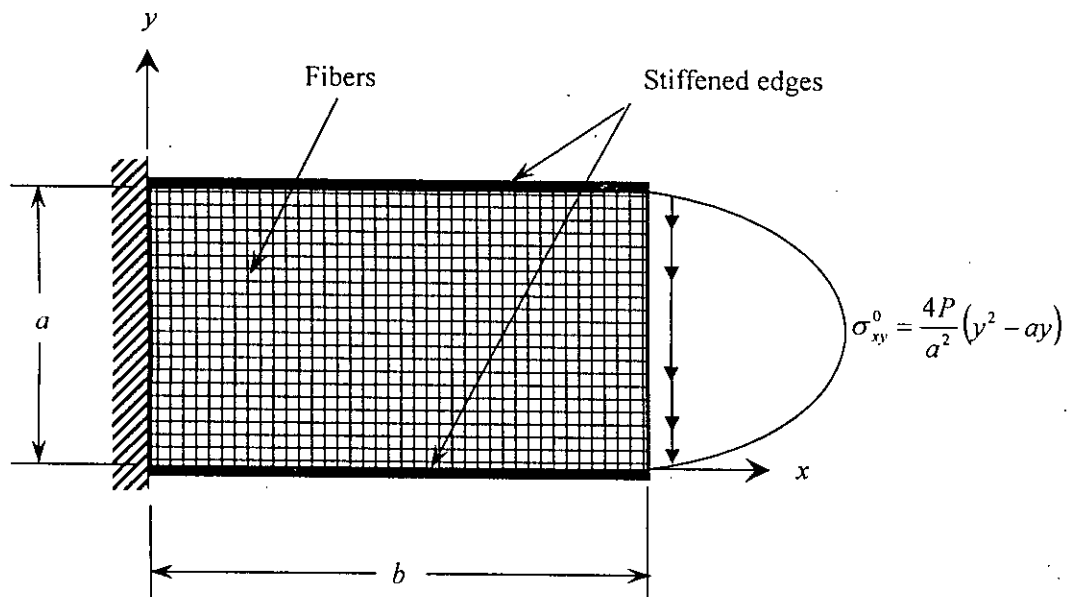


Fig. 3.3 A rectangular panel of cross-ply laminated composite under parabolic shear loading.

$$(3) u_x(0, y) = u_y(0, y) = 0; 0 \leq y \leq a$$

$$(4) \sigma_x(b, y) = 0, \sigma_{xy}(b, y) = \sigma_{xy}^0 = \frac{4P}{a^2}(y^2 - ay); 0 \leq y \leq a$$

For the present problem, the displacement potential function is assumed to be

$$\psi = \sum_{m=1}^{\infty} X_m \cos \alpha y + Mx^3 \quad (3.15)$$

where X_m is a function of x only and $\alpha = \frac{m\pi}{a}$.

Now substitution of Eq. (3.15) into Eq. (2.24) yields

$$X_m'''' - BX_m''\alpha^2 + CX_m\alpha^4 = 0 \quad (3.16)$$

$$B = \frac{A_{22}}{A_{66}} - \frac{A_{12}^2}{A_{11}A_{66}} - \frac{2A_{12}}{A_{11}} \text{ and } C = \frac{A_{22}}{A_{11}}$$

The general solution of Eq. (3.16) is given by

$$X_m = A_m e^{n_1 x} + B_m e^{n_2 x} + C_m e^{n_3 x} + D_m e^{n_4 x} \quad (3.17)$$

where

$$n_1, n_2 = \alpha \sqrt{\frac{B \pm \sqrt{B^2 - 4C}}{2}} \quad (3.18)$$

$$n_3, n_4 = -\alpha \sqrt{\frac{B \pm \sqrt{B^2 - 4C}}{2}}$$

and $A_m, B_m, C_m,$ and D_m are arbitrary constants.

Now substituting Eq. (3.21) into Eqs. (2.25) and (2.26), the expressions of displacement and stress components are obtained as

$$u_x(x, y) = -\sum_{m=1}^{\infty} \alpha X_m' \sin \alpha y \quad (3.19a)$$

$$u_y(x, y) = \frac{1}{A_{12} + A_{66}} \sum_{m=1}^{\infty} [(A_{66} X_m \alpha^2 - A_{11} X_m'') \cos \alpha y + 6Mx A_{11}] \quad (3.19b)$$

$$\sigma_x(x, y) = -\frac{A_{66}}{ah(A_{12} + A_{66})} \sum_{m=1}^{\infty} [A_{12} X_m \alpha^3 + A_{11} X_m'' \alpha] \sin \alpha y \quad (3.19c)$$

$$\sigma_y(x, y) = -\frac{1}{ah(A_{12} + A_{66})} \sum_{m=1}^{\infty} [A_{22} A_{66} X_m \alpha^3 + (A_{12}^2 + A_{12} A_{66} - A_{11} A_{22}) X_m'' \alpha] \sin \alpha y \quad (3.19d)$$

$$\sigma_{xy}(x, y) = -\frac{A_{66}}{ah(A_{12} + A_{66})} \sum_{m=1}^{\infty} [A_{12} X'_m \alpha^2 + A_{11} X''_m] \cos \alpha y + \frac{6MA_{11}A_{66}}{ah(A_{12} + A_{66})} \quad (3.19c)$$

Substituting different derivatives of X_m in the expressions of the stress and displacement components (Eqs. (3.19a) – (3.19e)), one can obtain

$$u_x(x, y) = \sum_{m=1}^{\infty} \left[-(n_1 A_m e^{n_1 x} + n_2 B_m e^{n_2 x} + n_3 C_m e^{n_3 x} + n_4 D_m e^{n_4 x}) \alpha \sin \alpha y \right] \quad (3.20a)$$

$$u_y(x, y) = \frac{1}{A_{12} + A_{66}} \sum_{m=1}^{\infty} \left\{ \begin{aligned} & A_{66} (A_m e^{n_1 x} + B_m e^{n_2 x} + C_m e^{n_3 x} + D_m e^{n_4 x}) \alpha^2 \\ & - A_{11} (n_1^2 A_m e^{n_1 x} + n_2^2 B_m e^{n_2 x} + n_3^2 C_m e^{n_3 x} + n_4^2 D_m e^{n_4 x}) \\ & + 6Mx A_{11} \end{aligned} \right\} \cos \alpha y \quad (3.20b)$$

$$\sigma_x(x, y) = -\frac{A_{66}}{ah(A_{12} + A_{66})} \sum_{m=1}^{\infty} \left[A_{12} (A_m e^{n_1 x} + B_m e^{n_2 x} + C_m e^{n_3 x} + D_m e^{n_4 x}) \alpha^3 + \right. \\ \left. A_{11} (n_1^2 A_m e^{n_1 x} + n_2^2 B_m e^{n_2 x} + n_3^2 C_m e^{n_3 x} + n_4^2 D_m e^{n_4 x}) \alpha \right] \sin \alpha y \quad (3.20c)$$

$$\sigma_y(x, y) = -\frac{1}{ah(A_{12} + A_{66})} \sum_{m=1}^{\infty} \left[\begin{aligned} & A_{22} A_{66} (A_m e^{n_1 x} + B_m e^{n_2 x} + C_m e^{n_3 x} + D_m e^{n_4 x}) \alpha^3 + \\ & (A_{12}^2 + A_{12} A_{66} - A_{11} A_{22}) \\ & (n_1^2 A_m e^{n_1 x} + n_2^2 B_m e^{n_2 x} + n_3^2 C_m e^{n_3 x} + n_4^2 D_m e^{n_4 x}) \alpha \end{aligned} \right] \sin \alpha y \quad (3.20d)$$

$$\sigma_{xy}(x, y) = -\frac{A_{66}}{ah(A_{12} + A_{66})} \sum_{m=1}^{\infty} \left[\begin{aligned} & A_{12} (n_1 A_m e^{n_1 x} + n_2 B_m e^{n_2 x} + n_3 C_m e^{n_3 x} + n_4 D_m e^{n_4 x}) \alpha^2 + \\ & A_{11} (n_1^3 A_m e^{n_1 x} + n_2^3 B_m e^{n_2 x} + n_3^3 C_m e^{n_3 x} + n_4^3 D_m e^{n_4 x}) \end{aligned} \right] \cos \alpha y \\ + \frac{6MA_{11}A_{66}}{ah(A_{12} + A_{66})} \quad (3.20e)$$

With these expressions of displacement and stress components, the boundary conditions (1) and (2) are satisfied automatically. Therefore, only the boundary conditions (3) and (4) are remaining to be satisfied. The parabolic shear load applied at the edge $x = b$ can be expressed in Fourier series as

$$\sigma_{xy}(b, y) = \sigma_{xy}^0 = E_0 + \sum_{m=1}^{\infty} E_m \cos \alpha y \quad (3.21)$$

where

$$E_0 = \frac{4P}{a^3} \int_0^a (ay - y^2) dy = -\frac{2P}{3} \\ E_m = \frac{8P}{a^3} \int_0^a (ay - y^2) \cos \alpha y dy = \frac{16P}{m^2 \pi^2} \quad \text{for } m = 2, 4, 6, \dots, \infty \quad (3.22)$$

Using Eqs. (3.20e) - (3.22) the value of M can be obtained as

$$M = \frac{ahP(A_{12} + A_{66})}{9A_{11}A_{66}}$$

Now, by applying the boundary conditions (3) and (4) in Eqs. (3.20a) - (3.20c) and (3.20e) and making use of relation (3.21), the following four algebraic equations can be obtained for four unknown coefficients A_m , B_m , C_m , and D_m .

$$n_1 A_m + n_2 B_m + n_3 C_m + n_4 D_m = 0 \quad (3.23a)$$

$$(A_{11}n_1^2 - A_{66}\alpha^2)A_m + (A_{11}n_2^2 - A_{66}\alpha^2)B_m + (A_{11}n_3^2 - A_{66}\alpha^2)C_m + (A_{11}n_4^2 - A_{66}\alpha^2)D_m = 0 \quad (3.23b)$$

$$(A_{11}n_1^2\alpha + A_{12}\alpha^3)A_m e^{n_1 b} + (A_{11}n_2^2\alpha + A_{12}\alpha^3)B_m e^{n_2 b} + (A_{11}n_3^2\alpha + A_{12}\alpha^3)C_m e^{n_3 b} + (A_{11}n_4^2\alpha + A_{12}\alpha^3)D_m e^{n_4 b} = 0 \quad (3.23c)$$

$$(A_{11}n_1^3 + A_{12}n_1\alpha^2)A_m e^{n_1 b} + (A_{11}n_2^3 + A_{12}n_2\alpha^2)B_m e^{n_2 b} + (A_{11}n_3^3 + A_{12}n_3\alpha^2)C_m e^{n_3 b} + (A_{11}n_4^3 + A_{12}n_4\alpha^2)D_m e^{n_4 b} = \bar{E}_m \quad (3.23d)$$

where

$$\bar{E}_m = -\frac{E_m ah(A_{12} + A_{66})}{A_{66}}$$

The above equations can be written in a simplified form for the solution of the unknowns as follows:

$$\begin{bmatrix} n_1 & n_2 & n_3 & n_4 \\ P_1 & P_2 & P_3 & P_4 \\ Q_1 & Q_2 & Q_3 & Q_4 \\ R_1 & R_2 & R_3 & R_4 \end{bmatrix} \begin{bmatrix} A_m \\ B_m \\ C_m \\ D_m \end{bmatrix} = \begin{bmatrix} 0 \\ 0 \\ 0 \\ \bar{E}_m \end{bmatrix} \quad (3.24)$$

where

$$\begin{aligned} P_i &= A_{11}n_i^2 - A_{66}\alpha^2 \\ Q_i &= (A_{11}n_i^2\alpha + A_{12}\alpha^3)e^{n_i b} \\ R_i &= (A_{11}n_i^3 + A_{12}n_i\alpha^2)e^{n_i b} \end{aligned} \quad i = 1, 2, 3, \text{ and } 4.$$

The solution of the above algebraic Eq. (3.24) yields the unknown constants, A_m , B_m , C_m , and D_m . Once the values of the unknowns are determined, they are directly substituted into Eq. (3.20) to obtain the explicit expressions for the different parameters of interest, namely, the two displacement and the three stress components, which are valid for the entire region of the stiffened edge panel of laminated composite.

3.4 A rectangular panel of cross-ply laminated composite under linearly varying tensile loading:

A symmetric cross-ply laminated composite panel consisting of n number of plies is shown in Fig. 3.4. The thickness of the panel is h . The left end of the panel is rigidly fixed while the two longitudinal edges are roller supported. The other end is subjected to a linearly varying eccentric tensile load, varying from the maximum value of P at $y = 0$ to zero at $y = a/2$. The length and width of the panel are denoted by b and a respectively. The conditions on the rollers are mathematically formulated by the fact that there is no displacement in the direction perpendicular to the roller edges and no shear stresses along the edges under the action of load. Thus, the boundary conditions of the problem can be formulated as

- (1) $u_y(x, 0) = u_y(x, a) = 0; 0 \leq x \leq b$
- (2) $\sigma_{xy}(x, 0) = \sigma_{xy}(x, a) = 0; 0 \leq x \leq b$
- (3) $u_x(0, y) = u_y(0, y) = 0; 0 \leq y \leq a$
- (4) $\sigma_x(b, y) = \sigma_x^0 = \left(P - \frac{2Py}{a}\right); 0 \leq y \leq a/2, \quad \sigma_{xy}(b, y) = 0; 0 \leq y \leq a$

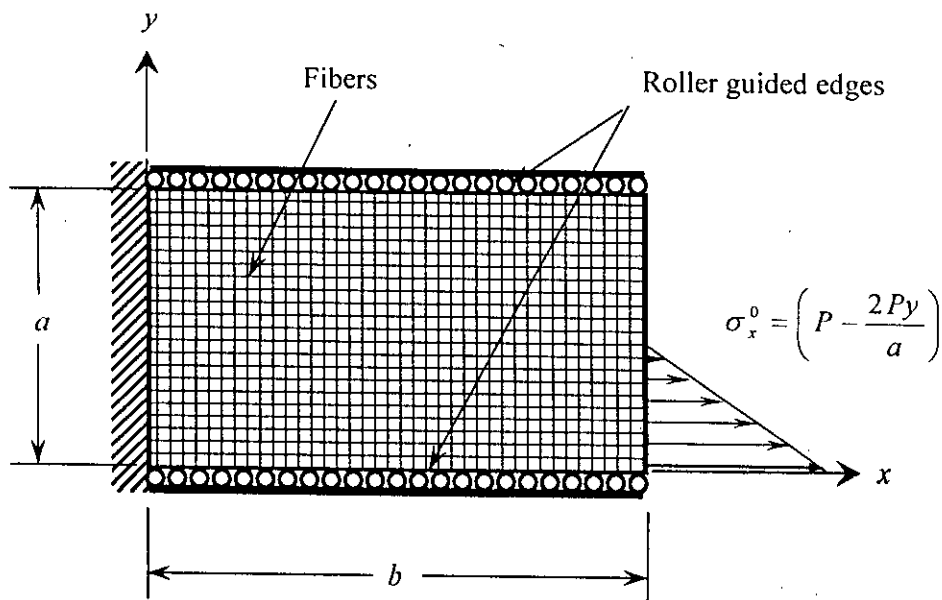


Fig. 3.4 A rectangular panel of cross-ply laminated composite under linearly varying tensile loading.

For the problem, the displacement potential function is assumed to be

$$\psi = \sum_{m=1}^{\infty} X_m \sin \alpha y + Mx^2 y + Ny^3 \quad (3.25)$$

where X_m is a function of x only and $\alpha = \frac{m\pi}{a}$.

Now substitution of Eq. (3.25) into Eq. (2.24) yields

$$X_m'''' - BX_m''\alpha^2 + CX_m\alpha^4 = 0 \quad (3.26)$$

$$\text{where } B = \frac{A_{22}}{A_{66}} - \frac{A_{12}^2}{A_{11}A_{66}} - \frac{2A_{12}}{A_{11}}, \quad C = \frac{A_{22}}{A_{11}}.$$

The general solution of Eq. (3.26) can be given by

$$X_m = A_m e^{n_1 x} + B_m e^{n_2 x} + C_m e^{n_3 x} + D_m e^{n_4 x} \quad (3.27)$$

where

$$n_1, n_2 = \alpha \sqrt{\frac{B \pm \sqrt{B^2 - 4C}}{2}} \quad (3.28)$$

$$n_3, n_4 = -\alpha \sqrt{\frac{B \pm \sqrt{B^2 - 4C}}{2}}$$

and $A_m, B_m, C_m,$ and D_m are arbitrary constants.

Now substituting Eq. (3.25) into Eqs. (2.25) and (2.26), the expressions of displacement and stress components are obtained as

$$u_x(x, y) = \sum_{m=1}^{\infty} \alpha X_m' \cos \alpha y + 2Mx \quad (3.29a)$$

$$u_y(x, y) = \frac{1}{A_{12} + A_{66}} \sum_{m=1}^{\infty} \left[(A_{66} X_m \alpha^2 - A_{11} X_m'') \sin \alpha y - 2y(A_{11}M + 3A_{66}N) \right] \quad (3.29b)$$

$$\sigma_x(x, y) = \frac{A_{66}}{ah(A_{12} + A_{66})} \sum_{m=1}^{\infty} \left[(A_{12} X_m \alpha^3 + A_{11} X_m'' \alpha) \cos \alpha y + 2(M + 3N) \right] \quad (3.29c)$$

$$\sigma_y(x, y) = \frac{1}{ah(A_{12} + A_{66})} \sum_{m=1}^{\infty} \left[\left\{ A_{22} A_{66} X_m \alpha^3 + (A_{12}^2 + A_{12} A_{66} - A_{11} A_{22}) X_m'' \alpha \right\} \cos \alpha y \right. \\ \left. + 2(A_{12}^2 + A_{12} A_{66} - A_{11} A_{22}) M + 6A_{22} A_{66} N \right] \quad (3.29d)$$

$$\sigma_{xy}(x, y) = -\frac{A_{66}}{ah(A_{12} + A_{66})} \sum_{m=1}^{\infty} \left[A_{12} X_m' \alpha^2 + A_{11} X_m''' \right] \sin \alpha y \quad (3.29e)$$

Now substituting different derivatives of X_m in the expressions of the stress and displacement components (Eqs. (3.29a) – (3.29e)), one can obtain

$$u_x(x, y) = \sum_{m=1}^{\infty} (n_1 A_m e^{n_1 x} + n_2 B_m e^{n_2 x} + n_3 C_m e^{n_3 x} + n_4 D_m e^{n_4 x}) \alpha \cos \alpha y + 2Mx \quad (3.30a)$$

$$u_y(x, y) = \frac{1}{A_{12} + A_{66}} \sum_{m=1}^{\infty} \left[\begin{array}{l} \left\{ A_{66} (A_m e^{n_1 x} + B_m e^{n_2 x} + C_m e^{n_3 x} + D_m e^{n_4 x}) \alpha^2 \right. \\ \left. - A_{11} (n_1^2 A_m e^{n_1 x} + n_2^2 B_m e^{n_2 x} + n_3^2 C_m e^{n_3 x} + n_4^2 D_m e^{n_4 x}) \right\} \sin \alpha y \\ \left. - 2y (A_{11} M + 3A_{66} N) \right] \quad (3.30b)$$

$$\sigma_x(x, y) = \frac{A_{66}}{ah(A_{12} + A_{66})} \sum_{m=1}^{\infty} \left[\begin{array}{l} \left\{ A_{12} (A_m e^{n_1 x} + B_m e^{n_2 x} + C_m e^{n_3 x} + D_m e^{n_4 x}) \alpha^3 + \right. \\ \left. A_{11} (n_1^2 A_m e^{n_1 x} + n_2^2 B_m e^{n_2 x} + n_3^2 C_m e^{n_3 x} + n_4^2 D_m e^{n_4 x}) \alpha \right\} \cos \alpha y \\ \left. + 2(M + 3N) \right] \quad (3.30c)$$

$$\sigma_y(x, y) = \frac{1}{ah(A_{12} + A_{66})} \sum_{m=1}^{\infty} \left[\begin{array}{l} \left\{ A_{22} A_{66} (A_m e^{n_1 x} + B_m e^{n_2 x} + C_m e^{n_3 x} + D_m e^{n_4 x}) \alpha^3 \right. \\ \left. + (A_{12}^2 + A_{12} A_{66} - A_{11} A_{22}) \right. \\ \left. (n_1^2 A_m e^{n_1 x} + n_2^2 B_m e^{n_2 x} + n_3^2 C_m e^{n_3 x} + n_4^2 D_m e^{n_4 x}) \alpha \right\} \cos \alpha y \\ \left. + 2(A_{12}^2 + A_{12} A_{66} - A_{11} A_{22}) M + 6A_{22} A_{66} N \right] \quad (3.30d)$$

$$\sigma_{xy}(x, y) = -\frac{A_{66}}{ah(A_{12} + A_{66})} \sum_{m=1}^{\infty} \left[\begin{array}{l} \left[A_{12} (n_1 A_m e^{n_1 x} + n_2 B_m e^{n_2 x} + n_3 C_m e^{n_3 x} + n_4 D_m e^{n_4 x}) \alpha^2 + \right. \\ \left. A_{11} (n_1^3 A_m e^{n_1 x} + n_2^3 B_m e^{n_2 x} + n_3^3 C_m e^{n_3 x} + n_4^3 D_m e^{n_4 x}) \right] \sin \alpha y \end{array} \right] \quad (3.30e)$$

As before, the boundary conditions (1) and (2) are satisfied automatically. Therefore, only the boundary conditions (3) and (4) are remaining to be satisfied. The linearly varying tensile load $\sigma_x^0 = \left(P - \frac{2Py}{a} \right)$ applied at the edge $x = b$ can be expressed in

Fourier series as

$$\sigma_x(b, y) = E_0 + \sum_{m=1}^{\infty} E_m \cos \alpha y \quad (3.31)$$

where

$$E_0 = \frac{P}{a} \int_0^a \left(1 - \frac{2y}{a}\right) dy = \frac{P}{4}$$

$$E_m = \frac{2P}{a} \int_0^a \left(1 - \frac{2y}{a}\right) \cos \alpha y dy = \frac{4P}{m^2 \pi^2} \left(1 - \cos \frac{m\pi}{2}\right) \quad \text{for } m = 1, 2, 3, \dots, \infty \quad (3.32)$$

By making use of Eqs. (3.30b) – (3.30c), (3.31) – (3.32), and satisfying the boundary condition (1), the value of M and N can be obtained as

$$M = \frac{ahP(A_{12} + A_{66})}{8(A_{66} - A_{11})}$$

$$N = -\frac{ahPA_{11}(A_{12} + A_{66})}{24A_{66}(A_{66} - A_{11})}$$

By applying the boundary conditions (3) and (4) in Eqs. (3.30a) - (3.30c) and (3.30e) and making use of relation (3.31), the following four algebraic equations can be obtained for four unknown coefficients A_m , B_m , C_m , and D_m .

$$n_1 A_m + n_2 B_m + n_3 C_m + n_4 D_m = 0 \quad (3.33a)$$

$$(A_{11}n_1^2 - A_{66}\alpha^2)A_m + (A_{11}n_2^2 - A_{66}\alpha^2)B_m + (A_{11}n_3^2 - A_{66}\alpha^2)C_m + (A_{11}n_4^2 - A_{66}\alpha^2)D_m = 0 \quad (3.33b)$$

$$(A_{11}n_1^2\alpha + A_{12}\alpha^3)A_m e^{n_1 b} + (A_{11}n_2^2\alpha + A_{12}\alpha^3)B_m e^{n_2 b} + (A_{11}n_3^2\alpha + A_{12}\alpha^3)C_m e^{n_3 b} + (A_{11}n_4^2\alpha + A_{12}\alpha^3)D_m e^{n_4 b} = \bar{E}_m \quad (3.33c)$$

$$(A_{11}n_1^3 + A_{12}n_1\alpha^2)A_m e^{n_1 b} + (A_{11}n_2^3 + A_{12}n_2\alpha^2)B_m e^{n_2 b} + (A_{11}n_3^3 + A_{12}n_3\alpha^2)C_m e^{n_3 b} + (A_{11}n_4^3 + A_{12}n_4\alpha^2)D_m e^{n_4 b} = 0 \quad (3.33d)$$

where

$$\bar{E}_m = \frac{E_m ah(A_{12} + A_{66})}{A_{66}}$$

The above equations can be written in a simplified form for the solution of the unknowns as follows:

$$\begin{bmatrix} n_1 & n_2 & n_3 & n_4 \\ P_1 & P_2 & P_3 & P_4 \\ Q_1 & Q_2 & Q_3 & Q_4 \\ R_1 & R_2 & R_3 & R_4 \end{bmatrix} \begin{Bmatrix} A_m \\ B_m \\ C_m \\ D_m \end{Bmatrix} = \begin{Bmatrix} 0 \\ 0 \\ \bar{E}_m \\ 0 \end{Bmatrix} \quad (3.34)$$

where

$$\begin{aligned} P_i &= A_{11}n_i^2 - A_{66}\alpha^2 \\ Q_i &= (A_{11}n_i^2\alpha + A_{12}\alpha^3)e^{n_i b} \\ R_i &= (A_{11}n_i^3 + A_{12}n_i\alpha^2)e^{n_i b} \end{aligned} \quad i = 1, 2, 3, \text{ and } 4.$$

The solution of the above algebraic Eq. (3.34) yields the unknown constants A_m , B_m , C_m , and D_m . Once the values of the unknowns are determined, they are directly substituted into Eq. (3.30) to obtain the explicit expressions for the different parameters of interest, namely, the two displacement and the three stress components, which are valid for the entire region of the stiffened edge panel of laminated composite.

3.5 Angle-ply laminated composite panel

A laminate is called an angle-ply laminate if it has plies of same material and thickness, and only oriented at $+\theta$ and $-\theta$ directions. All the four different types of boundary conditions discussed for cross-ply laminates are also considered for angle-ply laminates. The corresponding angle-ply laminate has the same formulations as for the cross-ply laminate. The only difference lies in the components of the stiffness matrix given by Eqs. (2.9) – (2.12). Here the values of s and c should be calculated from the prescribed values of θ .

CHAPTER-4 RESULTS AND DISCUSSION

In this chapter, some numerical results are presented for the problems discussed in the preceding chapter. All the results are obtained with reference to a glass epoxy composite. Although the formulations can be applied to any composite, the glass/epoxy composite is chosen merely as an example. The mechanical properties of the ingredient materials and their composites are shown in Table 4.1 and 4.2. In order to make the results non-dimensional, the displacements are expressed as the ratio of actual displacement to the actual dimension of the panel, and the stresses are expressed as the ratio of the actual stress to the applied loading parameter.

Table 4.1 Properties of fiber and matrix material:

Material	Property	
Fiber (Glass)	$E_f (\times 10^3 \text{ MPa})$	85.0
	ν_f	0.20
(Epoxy)	$E_m (\times 10^3 \text{ MPa})$	3.40
	ν_m	0.30

Table 4.2 Properties of glass/epoxy composite:

Material	Property	
Composite	$E_1 (\times 10^3 \text{ MPa})$	38.6
	$E_2 (\times 10^3 \text{ MPa})$	8.27
	$G_{12} (\times 10^3 \text{ MPa})$	41.4
	ν_{12}	0.26
	ν_{21}	0.055

4.1 Results of the problem of article 3.1

The problem at article 3.1 refers to a rectangular panel of symmetric cross-ply laminated composite. The panel is subjected to a uniform tensile load σ_x^0 at one lateral end while the other lateral end is fixed. The two longitudinal edges of the

panel are stiffened. The geometry and the type of the loading of the problem are shown in Fig. 3.1.

The result shown in Fig. 4.1 is the normalized longitudinal displacement component u_x/b as a function of normalized position y/a at different sections of the panel. The distribution of the longitudinal displacement is parabolic and symmetric with respect to the line $y/a = 0.5$. The magnitude of the longitudinal displacement increases with the increase of x/b . It is zero at the fixed end ($x/b = 0$) and two stiffened edges ($y/a = 0$, and 1.0), which satisfies the physical boundary conditions of the problem. The result correspond to the number of plies $n = 3$ and the aspect ratio $b/a = 3.0$.

Figures 4.2 and 4.3 illustrate the variation of normalized lateral displacement component u_y/a at different sections of the panel for $n = 3$ and $b/a = 3.0$. The lateral displacement varies anti-symmetrically with respect to the line $y/a = 0.5$. For any particular value of x/b , the lateral displacement is the maximum at the two stiffened edges ($y/a = 0$ and 1) and zero at the mid plane ($y/a = 0.5$). The lateral displacement is also zero at the section $x/b = 0$, i.e. at the left lateral boundary. This conforms to the physical phenomenon of the problem. The characteristics of lateral displacement are similar for all the sections apart from the right lateral end $x/b = 1$, i.e. the displacement varies from a positive value at the bottom surface $y/a = 0$ to negative value at the top surface $y/a = 1$. The reverse characteristics are obtained at the section $x/b = 1$ and its few adjoining section. The magnitude of the lateral displacement is much higher at section $x/b = 1$ than those of the other sections ($x/b < 1$). Therefore, the detail characteristics of variation of the displacement at the sections of $x/b < 1$ can not be obtained from Fig. 4.2. To observe detail characteristics, the results of these sections ($x/b < 1$) only are plotted in Fig. 4.3

Figure 4.4 shows the original and the deformed shape of the panel, which is obtained, from Fig. 4.1, and Fig. 4.2. It represents the combined effect of deformations in both the x -and y -directions. The lateral displacement component u_y/a , which expresses expansion or contraction in y -direction, shows the intuitively expected behavior. Tensile loading in axial direction should have normally led to contraction in the y -

direction due to the effect of Poisson's ratio, which is found to be true over the range of $0 < x/b < 0.9$. But, for the small region, $x/b \geq 0.9$, the bar is observed to be expanding in the y -direction and the explanation is that, it may be attributed to the applied conditions of the stiffened boundary under tension. The solutions for both the displacement components u_x and u_y are found to be zero at the fixed support, which is also expected for the physical characteristic of the problem.

Figure 4.5 illustrates the distribution of normalized longitudinal stress component σ_x/σ_x^0 at different sections of the panel for $n = 3$ and $b/a = 3.0$. The stress distribution is symmetric with respect to the mid longitudinal section $y/a = 0.5$. The magnitude of the stress increases as the right lateral end approaches, i.e. as the value of x/b increases. At $x/b = 1$, the value of σ_x/σ_x^0 is unity, which is in conformity with the boundary condition of the problem

Figures 4.6 and 4.7 exhibit the distribution of normalized lateral stress versus normalized position at different sections of the panel for $n = 3$ and $b/a = 3.0$. Figure 4.7 is plotted to show the detail characteristics of the stress variation at the sections other than the right lateral end where the magnitude of the stress is much higher than those of other sections. The stress distribution is symmetric. However, the nature of distribution is quite different at different sections. At the section $x/b = 0$, the stress is tensile whose magnitude is not so significant. At $x/b = 0.5$, the stress is negative that represent compressive stress. At the section $x/b = 0.9$, the central region of the panel ($0.24 < y/a < 0.76$) is under tension i.e. the stress is positive while the remaining region of the panel is under compression (negative stress). At the right lateral end ($x/b = 1.0$) the lateral stress is the maximum, which is tensile in nature. At all the sections, the lateral stress is only a fraction to the applied load. Moreover, the stress components are zero at the stiffened edges, which satisfies the boundary condition as well.

The distribution of normalized shearing stresses σ_{xy}/σ_x^0 as a function of x and y is shown in Fig. 4.8. At $x/b = 1$, i.e. at the right lateral edge, the shearing stress is zero

which is in conformity with the boundary condition of the problem. The distribution of shear stress at all sections, other than $x/b = 1$, is anti-symmetric. Further, it is observed that the magnitude of the shear stress increases with the increase of x/b except at $x/b = 1$, where it is zero.

Figure 4.9 displays the longitudinal displacement as a function of ply number for $b/a = 3.0$ and $x/b = 0.5$. The results are calculated at three points, $y/a = 0.2, 0.4$, and 0.95 along the section $x/b = 0.5$. It is observed that the magnitude of displacement decreases with the increase in ply number for same resultant applied load at $x/b = 1.0$.

Figure 4.10 shows the effect of ply number on the lateral displacement u_y/a for the same values of different parameters as stated for Fig. 4.9. As longitudinal displacement, the magnitude of lateral displacement also decreases as the number of plies increases.

Figure 4.11 represents the change in longitudinal stress component with the change in ply number. The figure shows that for the same resultant load the magnitude of stress reduces with the increase in ply number. This characteristic conforms with the obvious fact that the greater the number of plies gives the larger cross-sectional area over which the load is distributed. The magnitude of lateral and shear stress also decreases with the increase of ply number as can be seen from Figs. 4.12 and 4.13.

The effect of panel aspect ratio b/a on the longitudinal displacement u_x/b is portrayed in Fig. 4.14. The results correspond to $n = 3$ and $x/b = 0.5$. The results are calculated at three points along the section $x/b = 0.5$. It is to be noted that the magnitude of the longitudinal displacement, for a particular value of y/a , decreases as the aspect ratio increases. This is due to the fact that the section $x/b = 0.5$ is getting away from the loading section $x/b = 1.0$ as the aspect ratio b/a increases. Obviously, the effect of load will diminish as the distance of a point rises. Due to the same reason, the aspect ratio, in general, has the same effect on all other displacement and stress components as can be seen from Figs. 4.15 to 4.18.



The results presented so far show the characteristics of cross-ply laminate. For the same boundary and loading conditions, angle-ply laminated composite panel is also considered in order to analyze the elastic field. Figure 4.19 shows the geometry of the problem.

Figure 4.20 to Fig. 4.36 present different characteristics of the angle-ply laminated composite panel. The nature of the curves resembles to those discussed for cross-ply laminated panel. Therefore the discussions of the curves are not repeated here for the purpose of brevity.

Figure 4.37 demonstrates the effect of fiber angle on the longitudinal displacement of angle-ply laminates. It shows that for fiber angles near zero to a higher value of angles, within the range $0^\circ < \theta < 20^\circ$, the deflection reduces with the increase of angle and vice versa for the range $70^\circ < \theta < 90^\circ$. It happens due to the stiffened edges. On the other hand Fig. 4.38 shows that the magnitude of normalized lateral deflection increases with the increase in fiber angle within the range $0^\circ < \theta < 20^\circ$ and vice versa for the range $70^\circ < \theta < 90^\circ$. So an optimization can be suggested for design problems.

Like longitudinal deflection the normalized longitudinal stress decreases with increase in fiber angle, depicted in Fig. 4.39. So, for design problems these characteristics can become useful. Again analyzing Fig. 4.40 shows that the magnitude of the normalized lateral stress increases with increase in fiber angle for an angle ply composite laminate. On the other hand the normalized shear stress has no effect on the fiber angle, shown in Fig. 4.41, as the load applied here is only the tensile load.

4.2 Results of the problem of article 3.2

The problem at article 3.2 refers to a rectangular panel of symmetric cross-ply laminated composite. The panel is subjected to a parabolic tensile load $\sigma_x^0 = 4P/a^2 (ay - y^2)$, at one lateral end while the other lateral end is fixed. The

two longitudinal edges of the panel are stiffened. The geometry and the type of the loading of the problem are shown in Fig. 3.2.

The variation of the normalized longitudinal displacement component u_x/b as a function of normalized position y/a at different sections of the panel is shown in Fig. 4.42. The distribution of the longitudinal displacement is parabolic and symmetric with respect to the line $y/b = 0.5$. The magnitude of the longitudinal displacement increases with the increase of x/b . It is zero at the fixed end ($x/b = 0$) and two stiffened ends ($y/a = 0$, and 1.0), which satisfies the physical boundary conditions to the problem. The results corresponds to the number of plies $n = 3$ and aspect ratio $b/a = 3.0$.

Figures 4.43 and 4.44 illustrate the variation of normalized lateral displacement component u_y/a at different sections of the panel for $n = 3$ and $b/a = 3.0$. The lateral displacement varies anti-symmetrically with respect to the line $y/a = 0.5$. For any particular value of x/b , the lateral displacement is the maximum at the two stiffened edges ($y/a = 0$ and 1) and zero at the mid plane ($y/a = 0.5$). The lateral displacement is also zero for any y/a at the section $x/b = 0$, i.e. at the left lateral boundary. This conforms to the physical phenomenon of the problem. The characteristics of lateral displacement are similar for all the sections apart from the right lateral end $x/b = 1$, i.e. the displacement varies from a positive value at the bottom surface $y/a = 0$ to negative value at the top surface $y/a = 1$. The reverse characteristics are obtained at the section $x/b = 1$ and its few adjoining section. The magnitude of the lateral displacement is much higher at section $x/b = 1$ than those of the other sections ($x/b < 1$). Therefore, the detail characteristics of variation of the displacement at the sections of $x/b < 1$ can not be obtained from Fig. 4.43. To observe detail characteristics, the results of these sections ($x/b < 1$) only are plotted in Fig. 4.44

Figure 4.45 shows the original and the deformed shape of the panel, which is obtained, from Fig. 4.42, and Fig. 4.43. It represents the combined effect of deformations in both the x -and y -directions. The lateral displacement component u_y/a , which expresses expansion or contraction in y -direction, shows the

intuitively expected behavior. But at the same time some part of the deformed panel shows some unexpected shape. Tensile loading in axial direction should have normally led to contraction in the y -direction due to the effect of Poisson's ratio, which is found to be true over the range of $0 < x/b < 0.9$. But, for the small region, $x/b \geq 0.9$, the bar is observed to be expanding in the y -direction and the explanation is that, it may be attributed to the physical conditions of the stiffened boundary under tension. The solutions for both the displacement components u_x and u_y are found to be zero at the fixed support, which is also expected for the physical characteristic of the problem.

Figure 4.46 illustrates the distribution of normalized longitudinal stress component σ_x/P at different sections of the panel for $n = 3$ and $b/a = 3.0$. The stress distribution is symmetric with respect to the mid longitudinal section $y/a = 0.5$. The magnitude of the stress increases as the right lateral end approaches, i.e. as the value of x/b increases. At $x/b = 1$, the maximum value of σ_x/P is unity, which is in conformity with the boundary condition of the problem

Figures 4.47 and 4.48 exhibit the distribution of normalized lateral stress versus normalized position due to parabolic tensile load at different sections of the panel for $n = 3$ and $b/a = 3.0$. Figure 4.7 is plotted to show the detail characteristics of the stress variation at the sections other than the right lateral end where the magnitude of the stress is much higher than those of other sections. The stress distribution is symmetric. However, the nature of distribution is quite different at different sections. At the section $x/b = 0$, the stress is tensile whose magnitude is not so significant. At $x/b = 0.5$, the stress is negative that represent compressive stress. At the section $x/b = 0.9$, the panel is in tension. But the magnitude closer to the stiffened edges is not significant while at $y/a = 0.5$, tension is much higher, although not that high compared to the applied load. At all the sections the lateral stress is only a fraction to the applied load. Moreover, the stress components are zero at the stiffened edges, which satisfies the boundary condition as well.

The distributions of normalized shearing stress σ_{xy}/P as a function of x and y is shown in Fig. 4.49. At $x/b = 1$, i.e. at the right lateral edge, the shearing stress is zero which is in conformity with the boundary condition of the problem. The distribution of shear stress at all sections, other than $x/b = 1$, is anti-symmetric. Further, it is observed that the magnitude of the shear stress increases with the increase of x/b except at $x/b = 1$, where it is zero.

Figure 4.50 explores the longitudinal displacement as a function ply number for $b/a = 3.0$ and $x/b = 0.5$. The results are calculated at three points $y/a = 0.2, 0.4,$ and 0.95 along the section $x/b = 0.5$. It is observed that the magnitude of displacement decreases with the increase of ply number for the same resultant applied load at $x/b = 1.0$.

Figure 4.51 shows the effect of ply number on the lateral displacement u_y/a , for the same values of different parameters as stated for Fig. 4.50. As longitudinal displacement, the magnitude of lateral displacement also decreases as the number of plies increases.

Figure 4.52 represents the change in longitudinal stress component with the change in ply number. The figure shows that for the same resultant load the magnitude of stress reduces with the increase in ply number. This characteristic conforms to the obvious fact that the greater the number of plies gives the larger cross-sectional area over which the load is distributed. The magnitude of lateral and shear stress also decreases with the increase of ply number as can be seen from Figs. 4.53 and 4.54.

The effect of panel aspect ratio b/a on the longitudinal displacement u_x/b is portrayed in Fig. 4.55. The results correspond to $n = 3$ and $x/b = 0.5$. The results are calculated at three points along the section $x/b = 0.5$. It is to be noted that the magnitude of the longitudinal displacement, for a particular value of y/a , decreases as the aspect ratio increases. This is due to the fact that the section $x/b = 0.5$ is getting away from the loading section $x/b = 1.0$ as the aspect ratio b/a increases. Obviously, the effect of load will diminish as the distance of a point rises. Due to the same reason, the aspect

ratio, in general, has the same effect on all other displacement and stress components as can be seen from Figs. 4.56 to 4.59.

The results presented so far show the characteristics of cross-ply laminate. For the same boundary and loading conditions, angle-ply laminated composite panel is also considered in order to analyze the elastic field. Figure 4.60 shows the geometry of the problem.

Figures 4.61 to Fig. 4.77 present different characteristics of the angle-ply laminated composite panel. The nature of the curves resembles to those discussed for cross-ply laminated panel. Therefore the discussions of the curves are not repeated here for the purpose of brevity.

Figure 4.78 demonstrates the effect of fiber angle on the longitudinal displacement of angle-ply laminates. It shows that for fiber angles near zero to a higher value of angles, within the range $0^\circ < \theta < 20^\circ$, the magnitude of the deflection decreases with the increase of angle and vice versa for the range $70^\circ < \theta < 90^\circ$. It happens due to the stiffened edges. On the other hand Fig. 4.79 shows that the magnitude of the normalized deflection along the lateral direction increases with the increase in fiber angle within the range $0^\circ < \theta < 20^\circ$ and vice versa for the range $70^\circ < \theta < 90^\circ$. So an optimization can be suggested for design problems.

Like longitudinal deflection the normalized longitudinal stress decreases with increase in fiber angle, depicted in Fig. 4.80. So, for design problems these characteristics can become useful. Again analyzing Fig. 4.81 shows that the magnitude of the normalized lateral stress increases with increase in fiber angle for an angle ply composite laminate. On the other hand the normalized shear stress has no effect on the fiber angle, shown in Fig. 4.82, as the load applied here is only the tensile load.

4.3 Results of the problem of article 3.3

The problem at article 3.3 refers to a rectangular panel of symmetric cross-ply laminated composite. The panel is subjected to a parabolic shear load $\sigma_x^0 = 4P/a^2 (y^2 - ay)$, at one lateral end while the other lateral end is fixed. The two longitudinal edges of the panel are stiffened. The geometry and the type of the loading of the problem are shown in Fig. 3.3.

Shown in Fig. 4.83 is the normalized longitudinal displacement component u_x/b as a function of normalized position y/a at different sections of the panel. The distribution of the longitudinal displacement is anti-symmetric with respect to the line $y/a = 0.5$. It varies from zero, at $y/a = 0, 0.5$, and 1 , to the maximum, at $y/a = 0.25$, and 0.75 . Further, the magnitude of the longitudinal displacement increases with the increase of x/b . It is zero at the fixed end ($x/b = 0$), two stiffened edges and the mid plane ($y/a = 0, 0.5$, and 1.0), which satisfies the physical boundary conditions of the problem. The results corresponds to the number of plies $n = 3$ and the aspect ratio $b/a = 3.0$.

Figure 4.84 illustrates the variation of the lateral displacement component u_y/a at different sections of the panel for $n = 3$ and $b/a = 3.0$. The lateral displacement varies symmetrically. For any particular value of x/b , the magnitude of displacement is the maximum at transversely mid section ($y/a = 0.5$). The displacement is zero at the fixed end ($x/b = 0$). This conforms to the physical phenomenon of the problems. The two edges ($y/a = 0$ and 1) move parallel to each other while mid plane ($y/a = 0.5$) deflection is the maximum which resembles with the applied load. However, the maximum deflection is at the right lateral edge ($x/b = 1.0$). One thing should be noted that the deflection is in the negative direction as the applied load is negative in direction.

Figure 4.85 shows the original and the deformed shape of the panel under parabolic shear loading. The deformations are obtained from Fig. 4.86, and Fig. 4.87. Here it is observed that the deformation along y direction is quite natural and expected but the

deformation along x direction is so small, with respect to the size of the panel, that it actually could not be visualized.

Figures 4.86 and 4.87 illustrate the distribution of the longitudinal stress component σ_x/P at different sections of the panel for $n = 3$ and $b/a = 3.0$. The stress distribution is anti-symmetric with respect to mid longitudinal section $y/a = 0.5$. But at right lateral edge ($x/b = 1$), the value of σ_x/P is zero, depicted in Fig. 4.86. This satisfies the boundary condition. And in Fig. 4.87 it is observed that the magnitude increases with the increase in x/b for $x/b < 1$. Moreover, it is also observed that the upper part of the panel is in tension while the lower part of the panel is in compression.

Figures 4.88 and 4.89 show the distribution of lateral stress at different section of the panel for $n=3$ and $b/a = 3.0$. The stress distribution is anti-symmetric with respect to the mid plane ($y/a = 0.5$). Its magnitude increases with the increase in x/b . But in Fig. 4.88, the pattern of the curves shows different behavior at different sections. At $x/b = 0$ the stress is almost zero, where as at $x/b = 0.5$ the stress is significant, but the direction of the stress is opposite in upper and lower half of the panel. Now looking at the plane $x/b = 0.9$ a very complicated condition is observed where at $0.88 < y/a < 1.0$ the stress is negative and at $0.88 > y/a > 0.5$ the stress is positive. A similar characteristic is observed for the lower half ($y/a < 0.5$) of the panel. Moreover, the stress components are zero at the stiffened edges, which satisfies the boundary condition as well. The Fig. 4.89 shows the lateral stress distribution in the panel at $x/b = 1.0$.

The distribution of the shearing stresses σ_{xy}/P as a function of x and y is shown in Fig. 4.90. At $x/b = 1$, i.e. at the right lateral edge, the magnitude of the shearing stress is maximum and the maximum value is unity which is in conformity with the loading condition. The distribution of shear stress at all sections is symmetric. The variation in shear stress along the width of the panel is very small at any point nearer to the fixed support. But at $x/b = 0.9$ the magnitude of the stress is minimum at the mid

plane, which is opposite to the applied load. One thing is to be noted that the shear stress for any particular x/b is same for $y/a = 0.2$ and 0.8 .

Figure 4.91 shows the longitudinal displacement as a function of ply number for $b/a = 3.0$ and $x/b = 0.5$. The results are calculated at three points $y/a = 0.2, 0.4,$ and 0.95 along the section $x/b = 0.5$. It is observed that the magnitude of displacement decreases with the increase of ply number for the same resultant applied load at $x/b = 1.0$.

Figure 4.92 also shows the non-linear and inverse characteristics for the relation between lateral deflection u_y/a and ply number for the same values of different parameters as stated for Fig. 4.91. Like the longitudinal displacement, the magnitude of lateral displacement also decreases as the number of plies increases. One thing is noticeable that for any particular x/b the amount of deflection is same at all y/a . So, all the curves become a single one for a particular x/b .

Figure 4.93 represents the change in longitudinal stress component with the change in ply number. The figure shows that for the same resultant load the magnitude of stress reduces with the increase in ply number. This characteristic conforms to the obvious fact that the greater the number of plies gives the larger cross-sectional area over which the load is distributed. The magnitude of lateral and shear stress also decreases with the increase of ply number as can be seen from Figs. 4.94 and 4.95. Again one thing is noticeable in Fig. 4.95 that for any particular x/b the amount of deflection is same at all y/a . So, all the curves become a single one for a particular x/b .

The effect of panel aspect ratio b/a on the longitudinal displacement u_x/b is portrayed in Fig. 4.96. The results correspond to $n = 3$ and $x/b = 0.5$. The results are calculated at three points along the section $x/b = 0.5$. It is to be noted that the magnitude of the longitudinal displacement, for a particular value of y/a , decreases as the aspect ratio increases. This is due to the fact that the section $x/b = 0.5$ is getting away from the loading section $x/b = 1.0$ as the aspect ratio b/a increases. Obviously, the effect of

load will diminish as the distance of a point rises. Due to the same reason, the aspect ratio, in general, has the same effect on all other displacement and stress components as can be seen from Figs. 4.97 to 4.100.

The results presented so far show the characteristics of cross-ply laminate. For the same boundary and loading conditions, angle-ply laminated composite panel is also considered in order to analyze the elastic field. Figure 4.101 shows the geometry of the problem.

Figure 4.102 to Fig. 4.119 present different characteristics of the angle-ply laminated composite panel. The nature of the curves resembles to those discussed for cross-ply laminated panel. Therefore the discussions of the curves are not repeated here for the purpose of brevity.

Figure 4.120 demonstrates the effect of fiber angle on the longitudinal displacement of angle-ply laminates. It shows that for fiber angles near zero to a higher value of angles, within the range $0^\circ < \theta < 20^\circ$, the magnitude of the deflection reduces with the increase of angle and vice versa for the range $70^\circ < \theta < 90^\circ$. It happens due to the stiffened edges. On the other hand Fig. 4.121 shows that the normalized deflection along the magnitude of the lateral direction decreases with the increase in fiber angle within the range $0^\circ < \theta < 20^\circ$ and vice versa for the range $70^\circ < \theta < 90^\circ$. So an optimization can be suggested for design problems.

Like longitudinal deflection the magnitude of the normalized longitudinal stress decreases with increase in fiber angle, depicted in Fig. 4.122. So, for design problems these characteristics can become useful. Again analyzing Fig. 4.123 shows that the magnitude of the normalized lateral stress decreases slightly with increase in fiber angle for an angle ply composite laminate. But the amount of change in stress is negligible. On the other hand the magnitude of the normalized shear stress decreases with increase in fiber angle, shown in Fig. 4.124.

4.4 Results of the problem of article 3.4

The problem at article 3.4 refers to a rectangular panel of symmetric cross-ply laminated composite. The panel is subjected to a parabolic shear load $\sigma_v^0 = (P - 2Py/a)$. The load is applied at one lateral end and within the range $0 \leq y \leq a/2$ while the other lateral end is fixed. The two longitudinal edges of the panel are stiffened. The geometry and the type of the loading of the problem are shown in Fig. 3.4.

Shown in Fig. 4.125 is the normalized longitudinal displacement component u_x/b as a function of normalized position at different sections of the panel. The distribution of the longitudinal displacement is non-symmetric. It varies from a minimum, at $y/a = 1$, to the maximum, at $y/a = 0$ which resembles with the load. Further, the magnitude of normalized longitudinal displacement increases with the increase of x/b .

Figure 5.126 illustrates the variation of normalized lateral displacement component due to linearly varying tensile load at different sections of the panel. The lateral displacement also varies non-symmetrically. For any value of x/b , displacement is the maximum at some where bellow mid section. The displacement is zero for any y/a at the section $x/b = 0$, i.e. at the left lateral boundary. This conforms to the physical phenomenon of the problems. Deflection at the two edges ($y/a = 0$ and 1) are also zero. However, the maximum deflection is at the right lateral edge ($x/b = 1.0$). One thing should be noted that some deflections are in the negative direction like problem 3.1.

Figure 4.127 shows the original and the deformed shape of the panel under parabolic shear loading. The deformations are obtained form Fig. 4.125, and Fig. 4.126. Here it is observed that the deformation at the lower part of the panel is greater, where the load is applied. Moreover, the contraction in the width of the panel is not significant as the load is applied only in a part of the panel.

Figure 4.128 illustrates the distribution of normalized longitudinal stress component due to linearly varying tensile load at different sections of the panel. The stress distribution is non-symmetric and the magnitude increases as the reference point is moved toward the load. At $x/b = 1$, and $y/a = 0$, the value of σ_x/P is unity, which satisfies the boundary condition.

Figure 4.129 is the distribution of normalized lateral stress vs. normalized position due to linearly varying tensile load at different sections of the panel. The stress distribution is non-symmetric. The stress is the maximum at the right lateral end where the load is applied. Here lateral stresses at different points are very small. Only at $x/b = 1$ the stress is almost 60% of the applied load.

The distribution of normalized shearing stresses due to linearly varying tensile load is shown in Fig. 4.130. At $x/b = 1$, i.e. at the right lateral edge, the shearing stress is zero which satisfies the boundary condition. Further, it is observed that the magnitude of the shear stress increases with increase of x/b at any particular y/a of the panel except at $x/b = 1$. Again the variation in shear stress along the width of the panel is very small at any point nearer to the fixed support. One thing should be noted that the shear stress developed in the panel is all through negative.

Figure 4.131 shows the change in longitudinal displacement with a change in ply number. The figure represents the non-linear and inverse characteristic due to linearly varying tensile load for all three planes ($y/a = 0.2, 0.4, \text{ and } 0.95$). So, it is observed that the increase in ply number decreases the deflection along the length of the panel, which is quite natural.

Figure 4.132 also shows the non-linear and inverse characteristics for the relation between lateral deflection and ply number due to linearly varying tensile load. It is also observed that the deflections are negative in direction and the magnitude of the displacements decrease with increase in ply number.

Figure 4.133 represents the change in longitudinal stress pattern, in a roller guided cross-ply laminated panel under linearly varying tensile load, with change in ply number. The figure shows that under same load the amount of stress reduces with an increase in ply number. Similar phenomena can be seen from Fig. 4.134.

In case of shear stress developed in the laminated panel due to linearly varying tensile, shown in Fig. 4.135, it is also observed here that the magnitude of the stress is reducing with increase in ply number and again all through the stress is negative.

The effect of panel aspect ratio b/a on the longitudinal displacement u_x/b is portrayed in Fig. 4.136. The results correspond to $n = 3$ and $x/b = 0.5$. The results are calculated at three points along the section $x/b = 0.5$. It is to be noted that the magnitude of the longitudinal displacement, for a particular value of y/a , decreases as the aspect ratio increases. This is due to the fact that the section $x/b = 0.5$ is getting away from the loading section $x/b = 1.0$ as the aspect ratio b/a increases. Obviously, the effect of load will diminish as the distance of a point rises. Due to the same reason, the aspect ratio, in general, has the same effect on all other displacement and stress components as can be seen from Figs. 4.137 to 4.140.

The results presented so far show the characteristics of cross-ply laminate. For the same boundary and loading conditions, angle-ply laminated composite panel is also considered in order to analyze the elastic field. Figure 4.141 shows the geometry of the problem.

Figure 4.142 to Fig. 4.157 present different characteristics of the angle-ply laminated composite panel. The nature of the curves resembles to those discussed for cross-ply laminated panel. Therefore the discussions of the curves are not repeated here for the purpose of brevity.

Figure 4.158 demonstrates the effect of fiber angle on the longitudinal displacement of angle-ply laminates. It shows that for fiber angles near zero to a higher value of angles. On the other hand Fig. 4.159 shows that the magnitude of the normalized

deflection along the lateral direction increases with the increase in fiber angle within the range $0^\circ < \theta < 20^\circ$. So an optimization can be suggested for design problems.

The normalized longitudinal stress decreases with increase in fiber angle at lower half of the panel and at the upper half the stress increases with increase in fiber angle, depicted in Fig. 4.160. So, for design problems these characteristics can become useful. Again analyzing Fig. 4.161 shows that the normalized lateral stress increases with increase in fiber angle for an angle ply composite laminate. On the other hand the normalized shear stress slightly decreases in magnitude with increase in fiber angle but no effect at the right lateral edge, shown in Fig. 4.162, as the load applied here is only the tensile load.

4.5 Verification of equilibrium of forces

In the preceding article, analytical results of elastic field have been discussed. It is observed from the results that all the boundary conditions of the problems are satisfied identically, which may clarify the accuracy and reliability of the results. However, in the preceding articles, equilibrium of forces acting on the body is not stated which is equally important for the results to be accepted as accurate and reliable. In this article, an attempt is made to verify the equilibrium of forces for a problem discussed earlier.

Problem of article 3.1

Article 3.1 describes a rectangular panel of laminated composite with two stiffened edges, a fixed end, and a uniform tensile load at the other end. To verify the equilibrium of forces acting on the panel, it is cut along the fixed support and its free body diagram is shown in Fig. 4.163. It is acted upon by the applied uniform tensile load (F_1) at the right lateral surface, reaction force (F_2) from the fixed support at the left lateral surface, and shear loads (F_3 and F_4) at the remaining two surfaces. Equilibrium of forces in the direction of applied load must satisfy that

$$F_1 = F_2 + F_3 + F_4 \quad (4.1)$$

Here, $F_1 = \int_0^a \sigma_x^0 dy = \int_0^a f(y) dy$, where $f(y) = \sigma_x^0$. The thickness of the panel is assumed to be unity. The integral can be evaluated numerically by using the trapezoidal rule as

$$F_1 = \frac{l}{2} (f_0 + 2f_1 + 2f_2 + \dots + 2f_{n-1} + f_n) \quad (4.2)$$

where $l = (a - 0) / N$ and $N =$ number of strips. For numerical calculation, the size of the strip is taken as $a = 100\text{mm}$, $b = 100\text{mm}$, and $N = 16$ for tensile stresses and 11 for shear stresses. With these values, Eq. (4.2) is evaluated as

$$F_1 = \frac{100}{2 \times 16} [0 + 2(1.001933 + 1.007559 + 0.998309 + 0.996134 + 1.001828 + 1.002678 + 0.997879 + 0.997878 + 1.002677 + 1.001829 + 0.996134 + 0.998308 + 1.007559 + 1.001934) - 6.421351 \times 10^{-5}] \sigma_x^0 = 87.58 \sigma_x^0 \text{N}$$

Similarly,

$$F_2 = \frac{100}{2 \times 16} [0 + 2(0.177667 + 0.341491 + 0.481406 + 0.592481 + 0.673833 + 0.726655 + 0.752555 + 0.752555 + 0.726655 + 0.673833 + 0.592481 + 0.481406 + 0.34149 + 0.177666) - 4.294468 \times 10^{-7}] \sigma_x^0 = 46.82 \sigma_x^0 \text{N}$$

The shear force F_3 is given by $F_3 = \int_0^b \sigma_{xy} dx = \int_0^b f(x) dx$. By trapezoidal rule, it is computed as

$$F_3 = \frac{100}{2 \times 11} [0.087854 + 2(0.086072 + 0.107393 + 0.141154 + 0.182743 + 0.229885 + 0.281076 + 0.334518 + 0.38624 + 0.415274) + 1.12 \times 10^{-5}] \sigma_x^0 = 20.07 \sigma_x^0 \text{N}$$

Similarly,

$$F_4 = \frac{100}{2 \times 11} [0.087854 + 2(0.086072 + 0.107393 + 0.141154 + 0.182743 + 0.229885 + 0.281076 + 0.334518 + 0.38624 + 0.415274) + 1.12 \times 10^{-5}] \sigma_x^0 = 20.07 \sigma_x^0 \text{N}$$

The total reaction force $F_1 + F_2 + F_3$ is $86.97 \sigma_x^0 \text{N}$ which is slightly less than the applied load $87.58 \sigma_x^0 \text{N}$. The small variation may be attributed to the numerical errors. Thus the above values of F 's satisfy the force equilibrium given by Eq. (4.1).

CHAPTER-5 CONCLUSIONS AND RECOMMENDATIONS

5.1 Conclusion

Due to their outstanding advantages over the conventional materials composites are being used increasingly for structural elements. Thus to make these materials more efficient a comprehensive method of analyzing the elastic field in structural elements of laminated composite has been developed. This method is a very effective and efficient one. It can be used to solve problems under any kind of boundary conditions whether they are prescribed in terms in terms of either stress or constraints or any combination of these two. As this method uses displacement potential function and all the boundary conditions can be represented in terms of the same single function, the procedure becomes very simple. Thus it reduces the problems into a single differential equation. The differential equation was solved with the help of an infinite series. It is true that the stress function formulation also seeks for the solution of a single function. But still the present method is superior as the stress function formulation can handle only the problems when the boundary condition is prescribed in terms of stress only.

Using this method elastic field in two different types of composite panel has been analyzed as a demonstration of this method, where various elastic properties have been calculated as a function of some other parameters. It is seen that the most of the results are expected and can be explained. Although some results are little confusing and those were explained from intuition. But it still needs more strong reasons to explain. After going through this method it seems that this method is capable of handling such type of problems. But as this is at an infant stage, it needs more development in future

5.2 Recommendation for future work

This is a new method and can successfully deal with composite lamina as well as with laminate. It can also deal with mixed mode boundary condition. Even then this method has some limitations. The method is suitable for a particular group of problems of stiffened and roller guided structures.

In addition, the method can handle cross-ply and angle-ply laminates. But in case of angle-ply laminate this method is applicable to a certain range of angle. It is observed that in the range $20^\circ \leq \theta \leq 70^\circ$ this method is unable to work with.

Moreover, this method is applicable for the cases of composite laminate where the coupling component of the stiffness matrix is absent for which the laminate must be a symmetric. For angle ply laminates the number of plies must be even above and below the mid plan. In addition to that two more elements (A_{16} and A_{26}) of matrix $[A]$ have to be zero to fit this method. So, these factors limit the application of the method. Thus the recommendation for future works may be;

- Modification of the method for dealing with all angles
- Rectification of the method to deal with all types of composites
- Rectification of the method to deal with all kinds of boundary conditions
- Using the results obtained from the method to optimize the design.

Figures

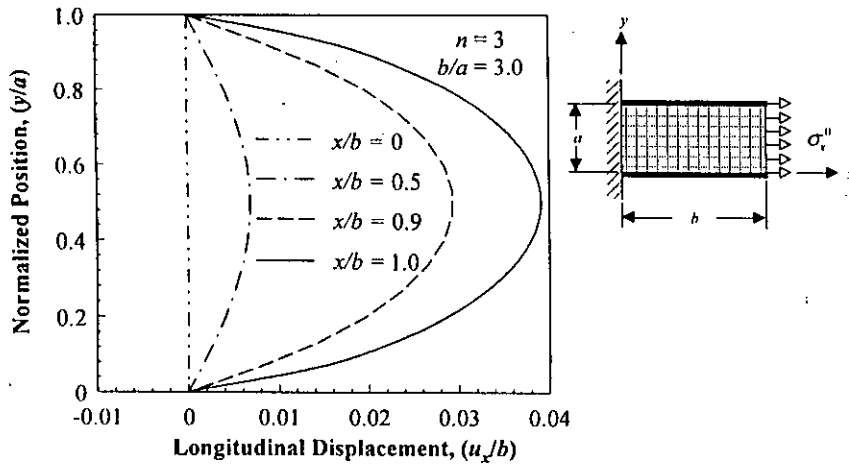


Fig. 4.1 Longitudinal displacement at different sections of the panel.

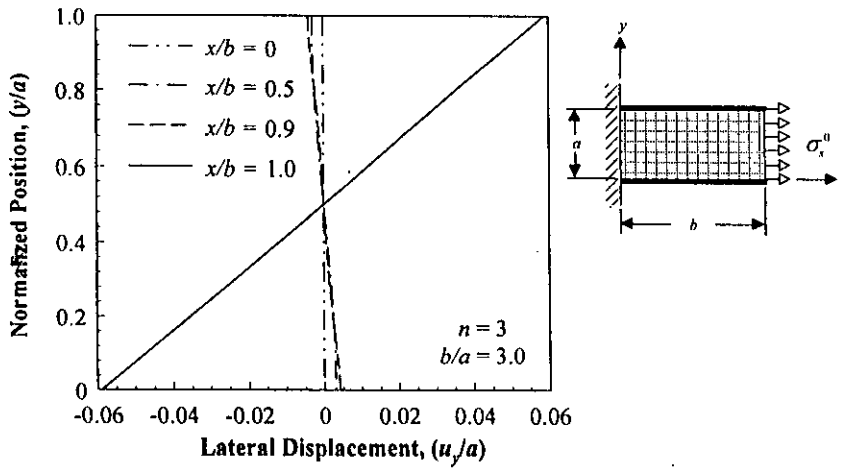


Fig. 4.2 Lateral displacement at different sections of the panel.

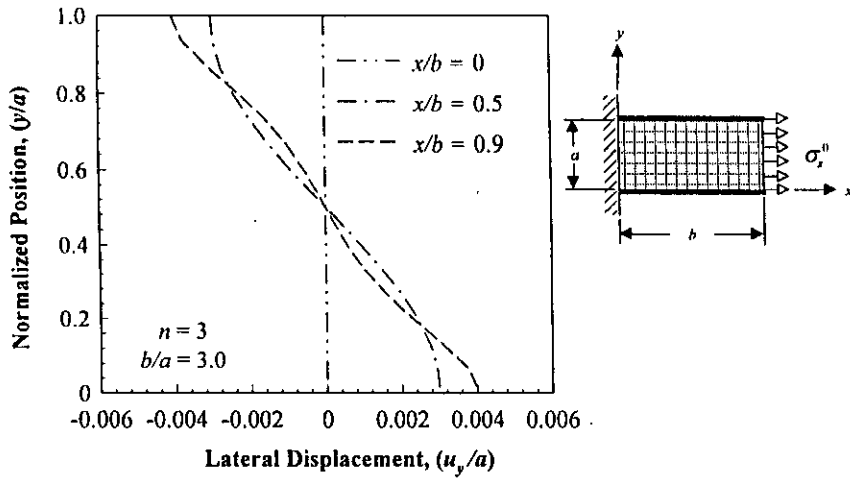


Fig. 4.3 Lateral displacement at different sections of the panel.

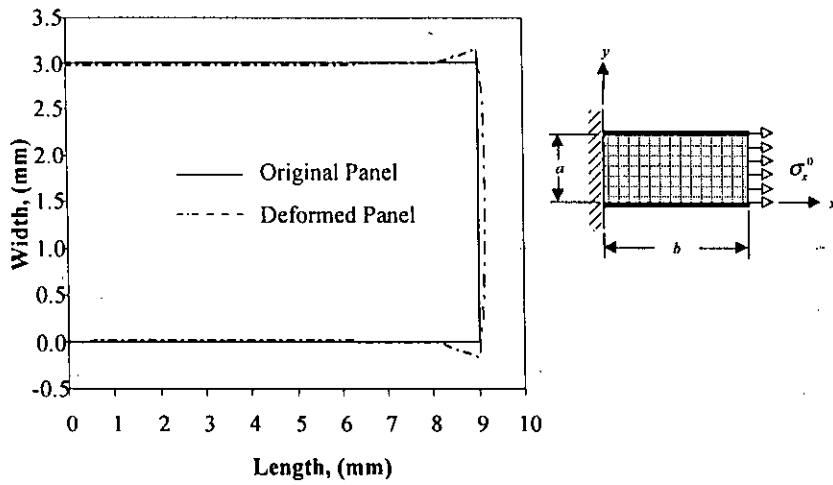


Fig. 4.4 Deformed and original shape of a cross-ply laminated composite panel under uniformly distributed tensile load.

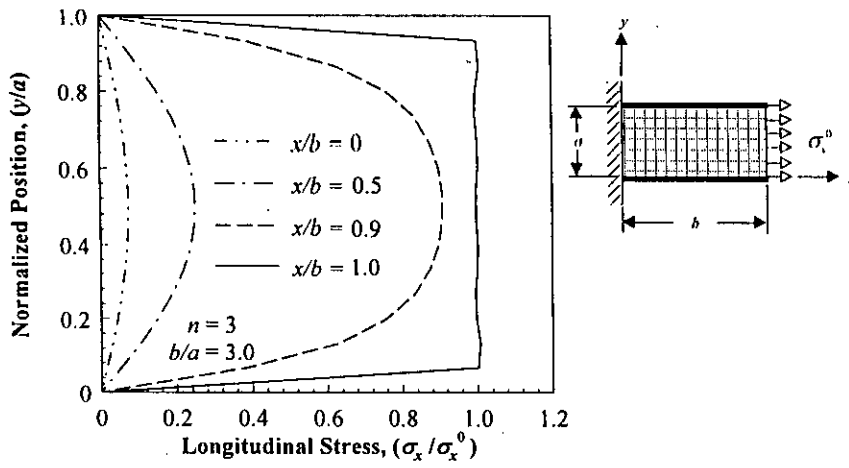


Fig. 4.5 Longitudinal stress at different sections of the panel.

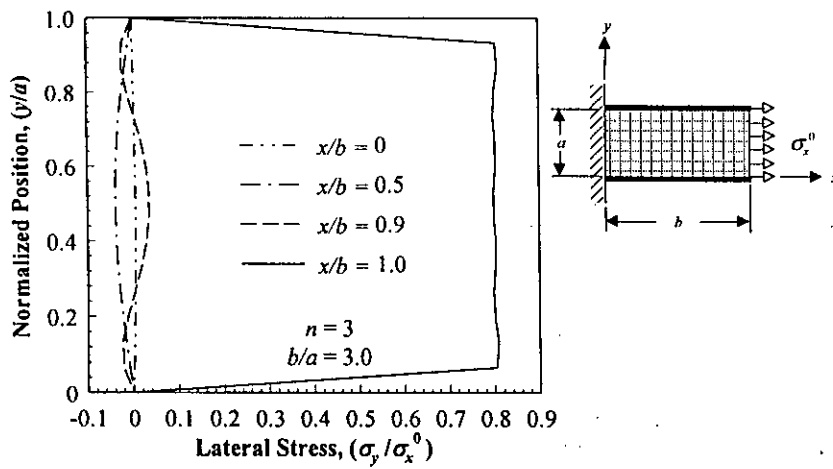


Fig. 4.6 Lateral stress at different sections of the panel.

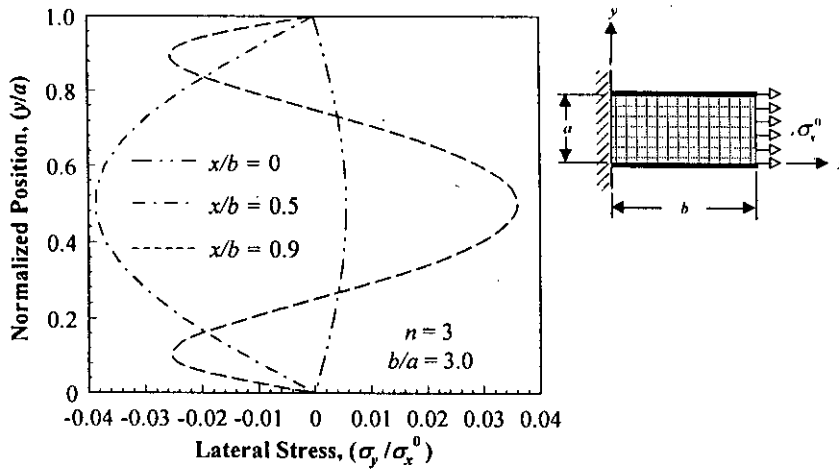


Fig. 4.7 Lateral Stress at different sections of the panel.

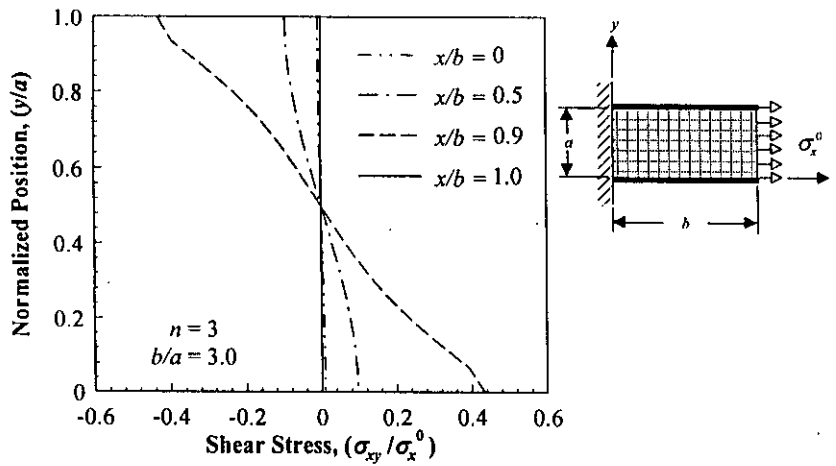


Fig. 4.8 Shear stress at different sections of the panel.

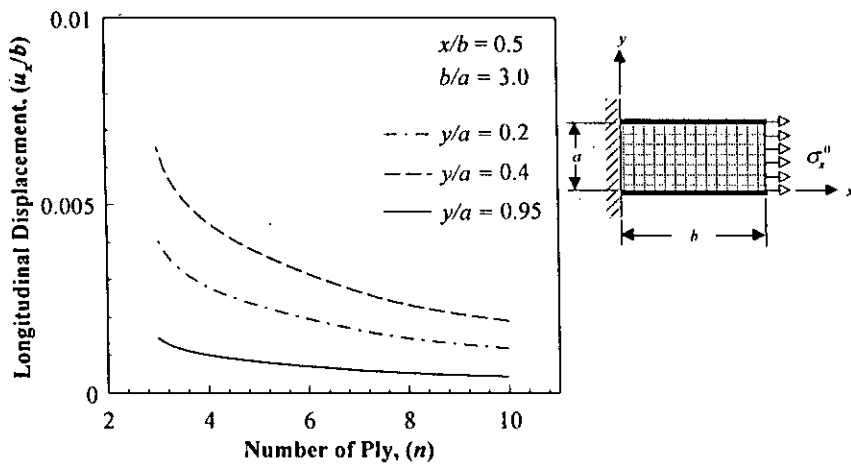


Fig. 4.9 Longitudinal displacement as a function of ply number.

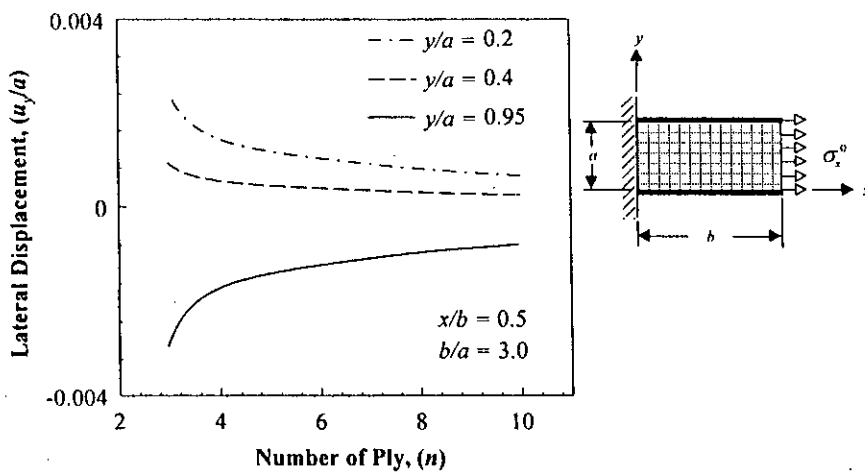


Fig. 4.10 Lateral displacement as a function of ply number.

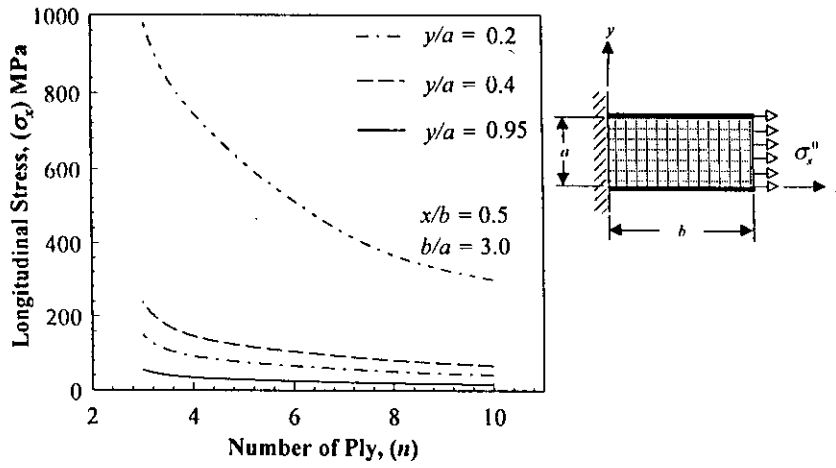


Fig. 4.11 Effect of ply number on the longitudinal stress component.

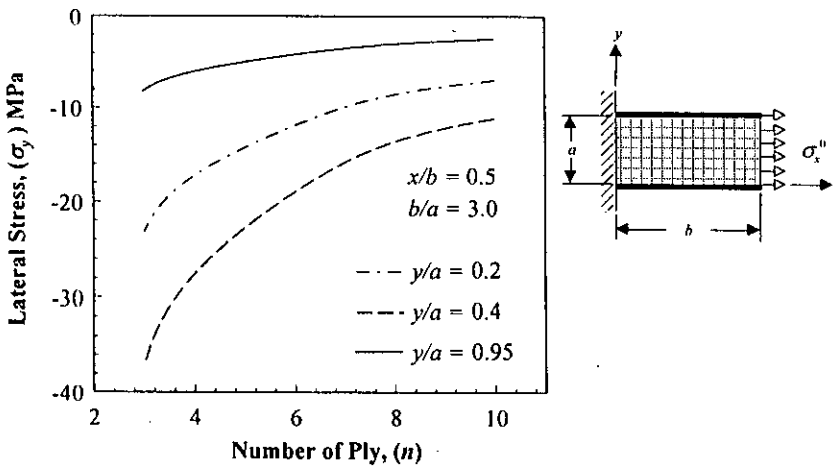


Fig. 4.12 Effect of ply number on the lateral stress component.

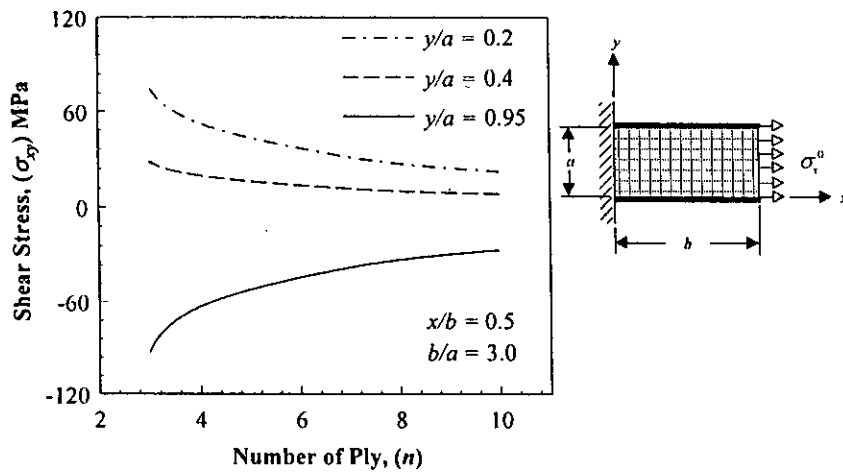


Fig. 4.13 Effect of ply number on the shear stress.

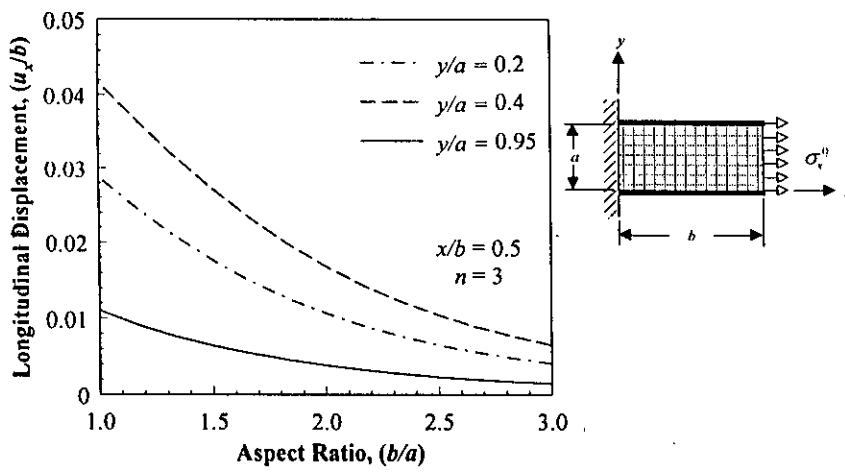


Fig. 4.14 Effect of aspect ratio on longitudinal displacement.

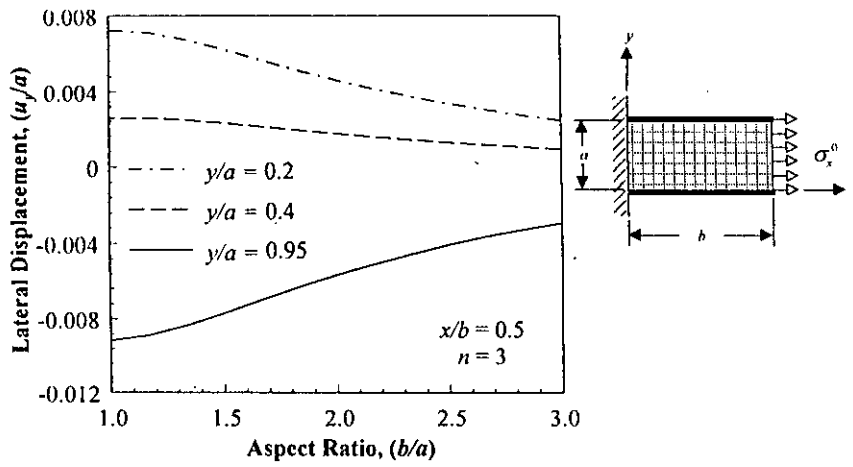


Fig. 4.15 Effect of aspect ratio on lateral displacement.

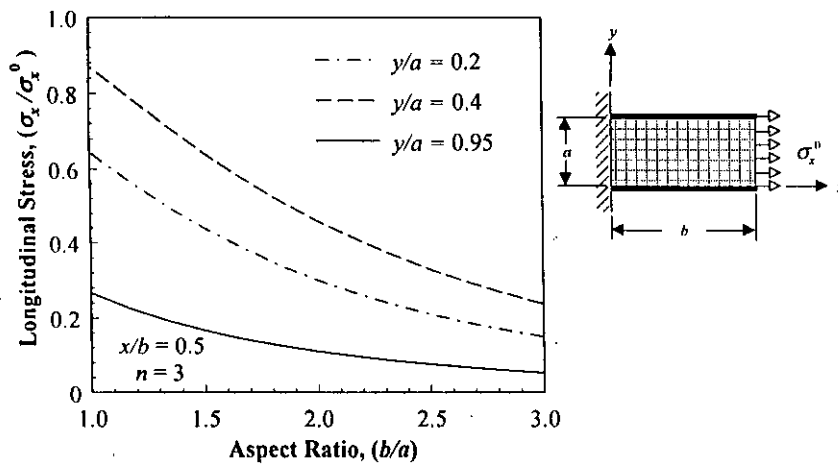


Fig. 4.16 Effect of aspect ratio on longitudinal stress component.

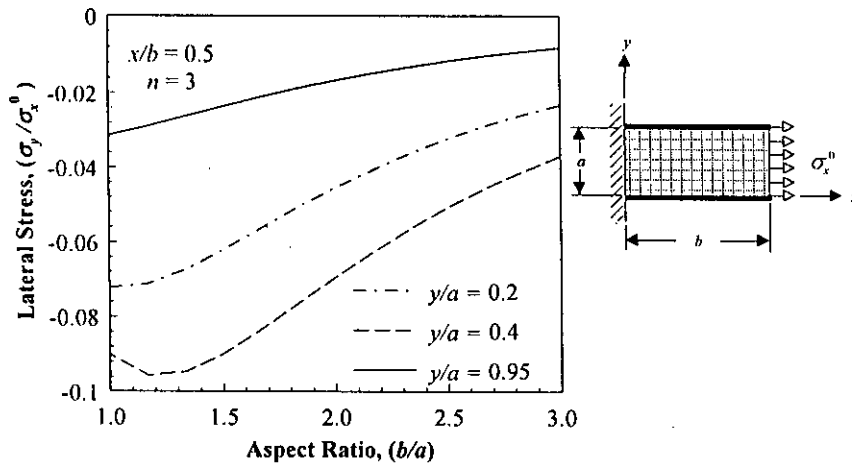


Fig. 4.17 Effect of aspect ratio on lateral stress component.

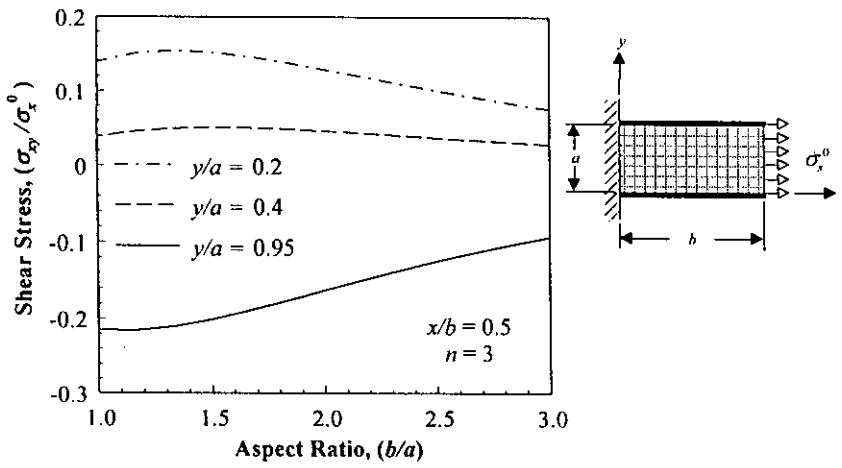


Fig. 4.18 Effect of aspect ratio on shear stress.

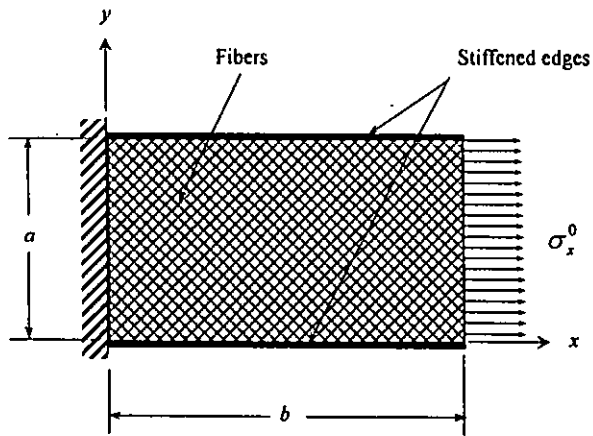


Fig. 4.19 A rectangular panel of angle-ply laminated composite under uniform tensile loading.

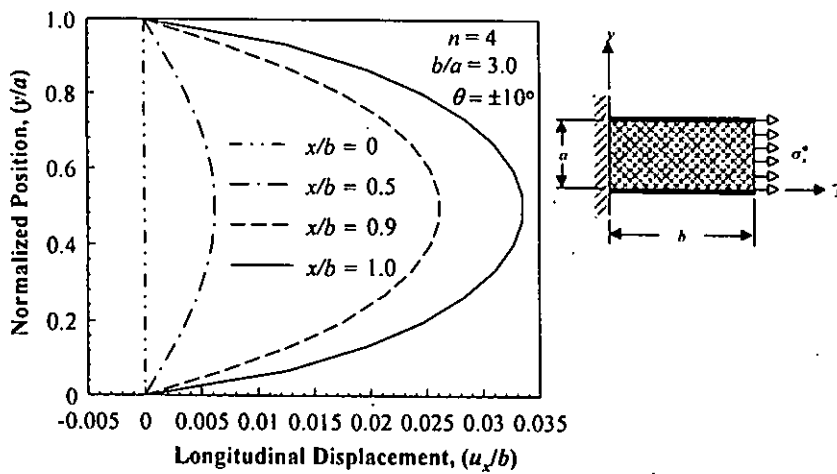


Fig. 4.20 Longitudinal displacement at different sections of the panel.

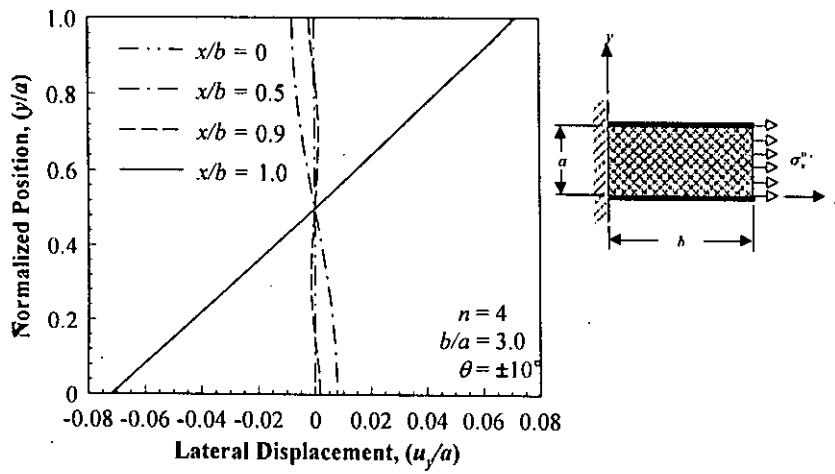


Fig. 4.21 Lateral displacement at different sections of the panel.

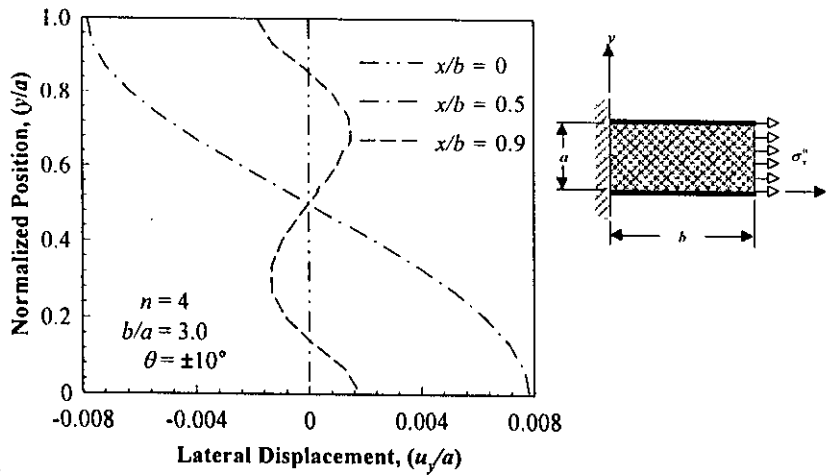


Fig. 4.22 Lateral displacement at different sections of the panel.

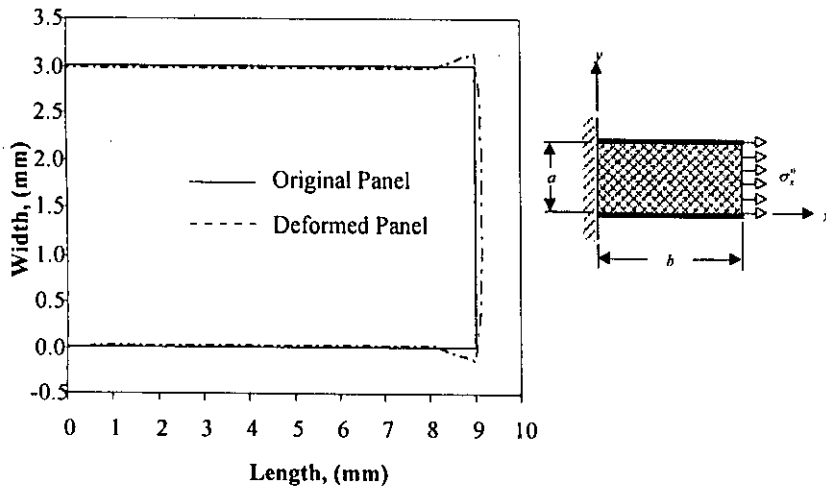


Fig. 4.23 Deformed and original shape of an angle-ply laminated composite panel under uniformly distributed tensile load.

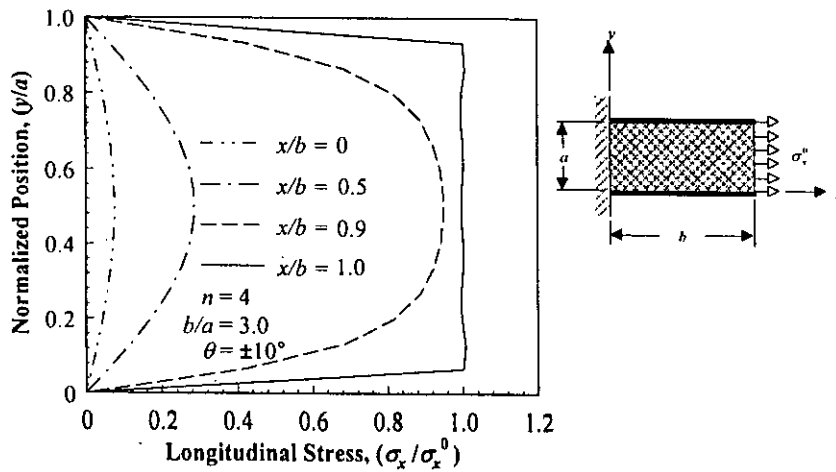


Fig. 4.24 Longitudinal stress at different sections of the panel.

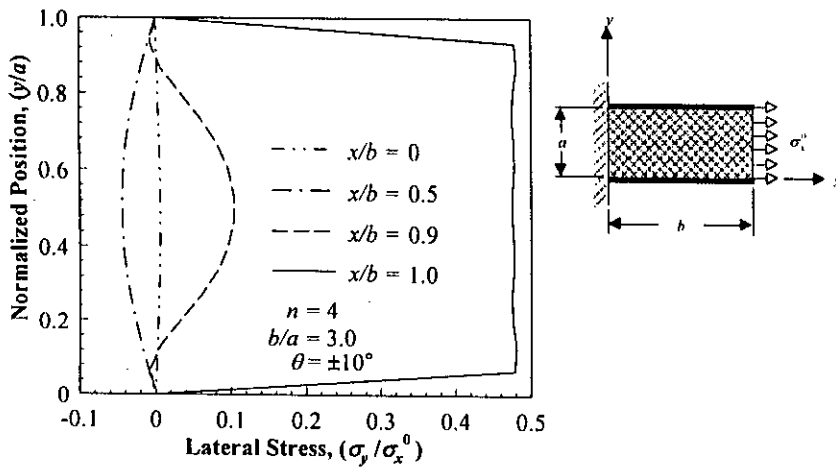


Fig. 4.25 Lateral stress at different sections of the panel.

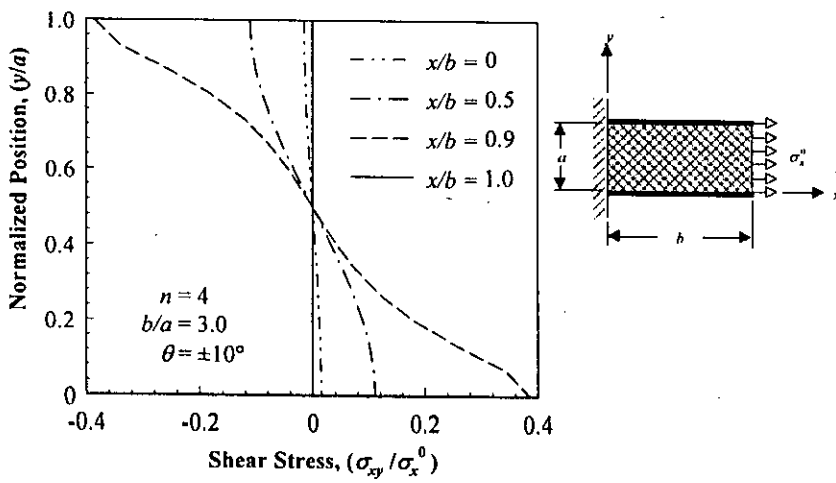


Fig. 4.26 Shear stress at different sections of the panel.

104322

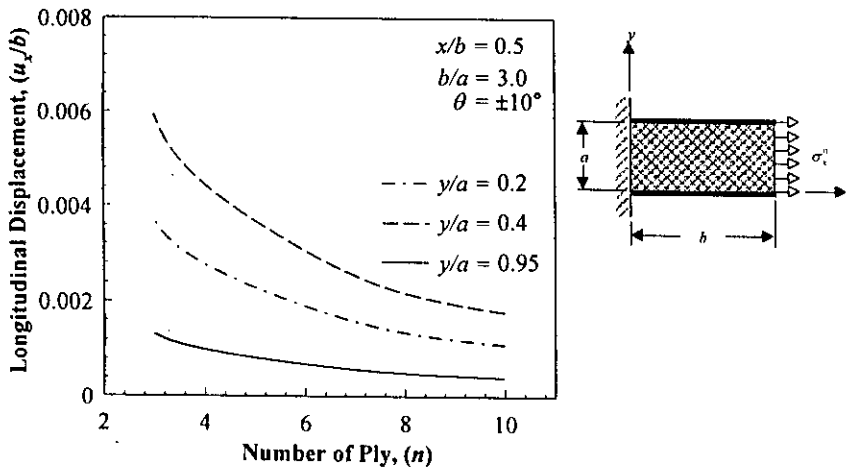


Fig. 4.27 Longitudinal displacement as a function of ply number.

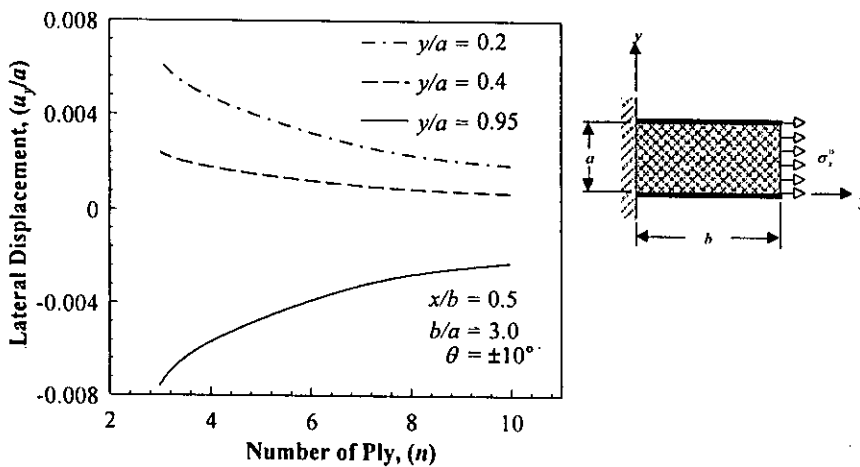


Fig. 4.28 Lateral displacement as a function of ply number.

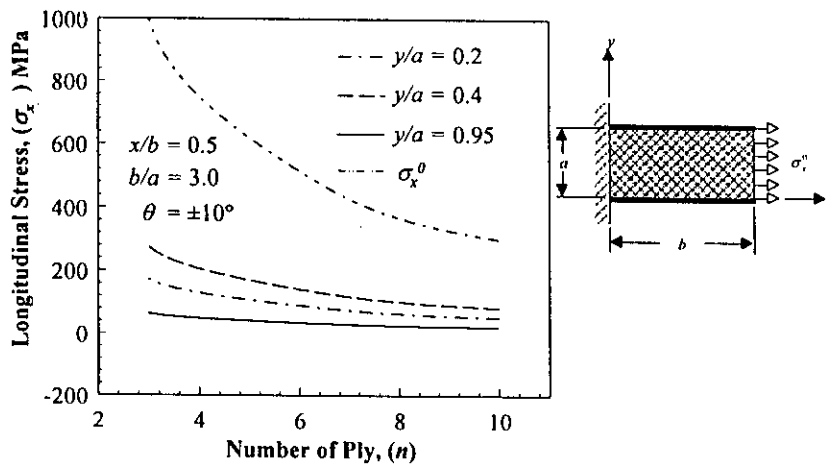


Fig. 4.29 Effect of ply number on the longitudinal stress component.

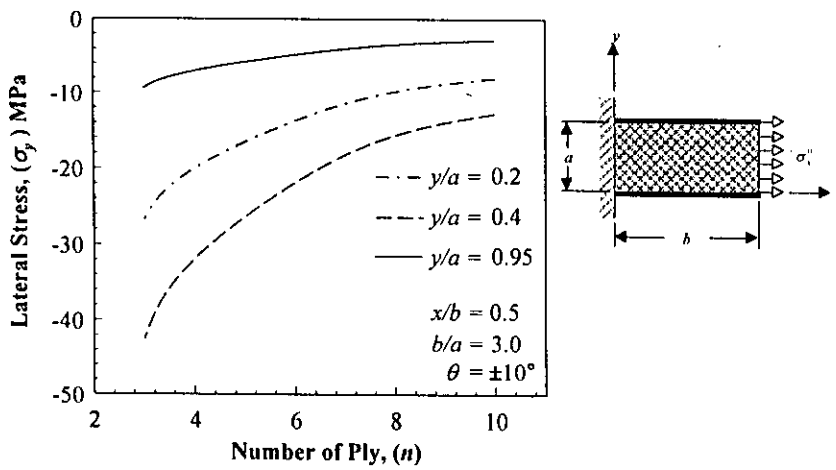


Fig. 4.30 Effect of ply number on the lateral stress component.

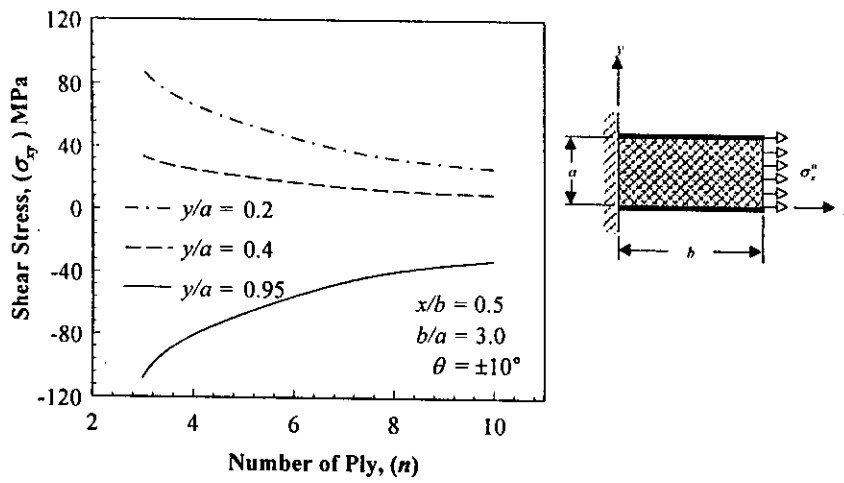


Fig. 4.31 Effect of ply number on the shear stress.

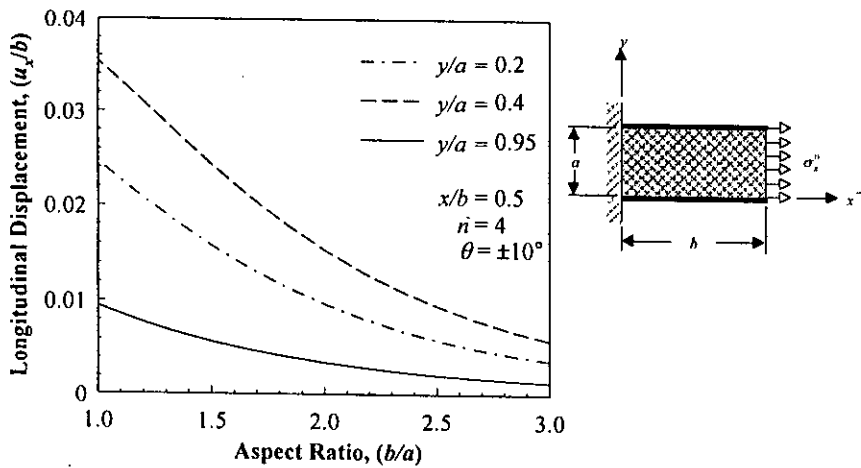


Fig. 4.32 Effect of aspect ratio on longitudinal displacement.

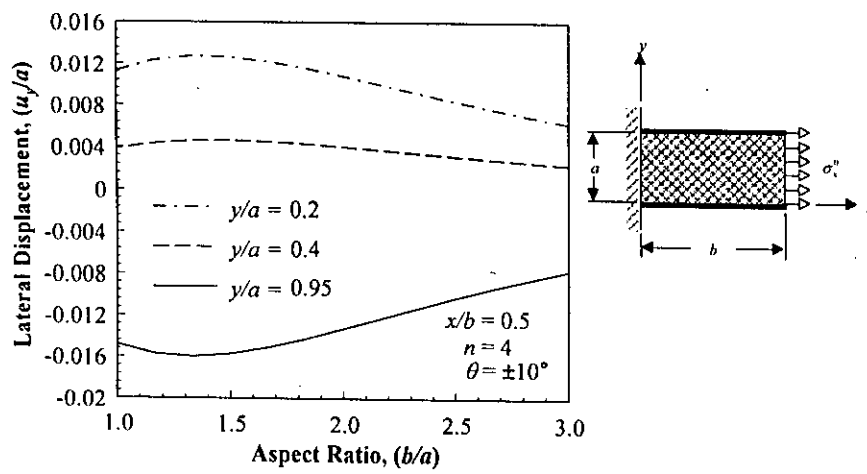


Fig. 4.33 Effect of aspect ratio on lateral displacement.

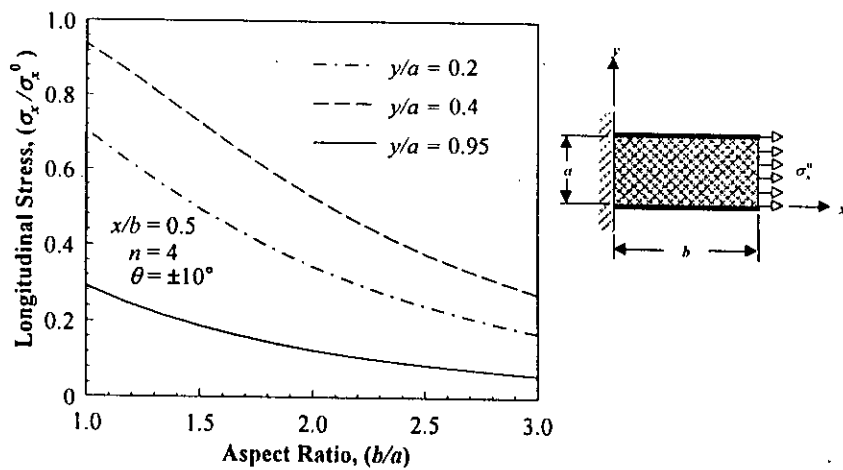


Fig. 4.34 Effect of aspect ratio on longitudinal stress component.

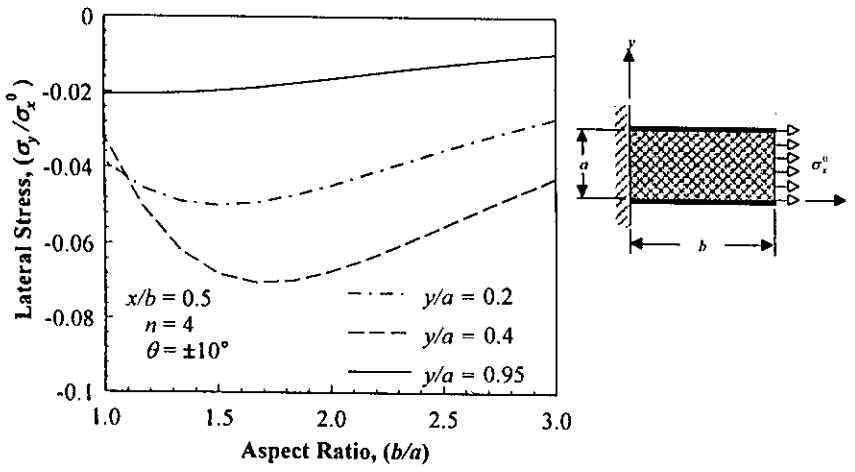


Fig. 4.35 Effect of aspect ratio on lateral stress component.

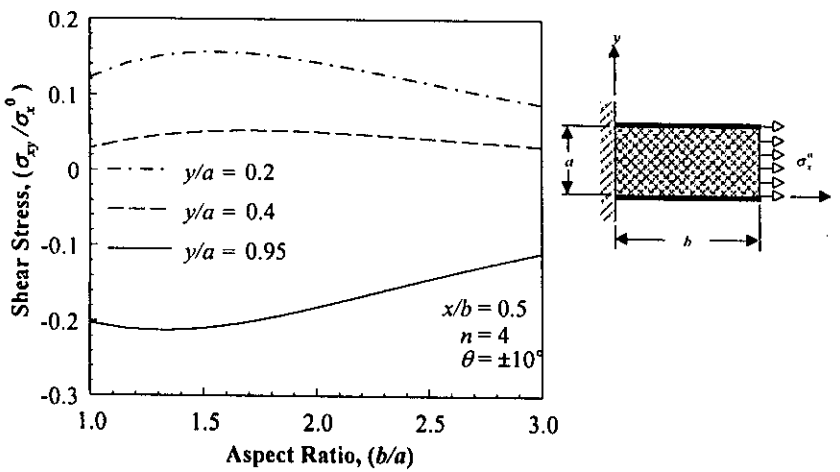


Fig. 4.36 Effect of aspect ratio on shear stress.

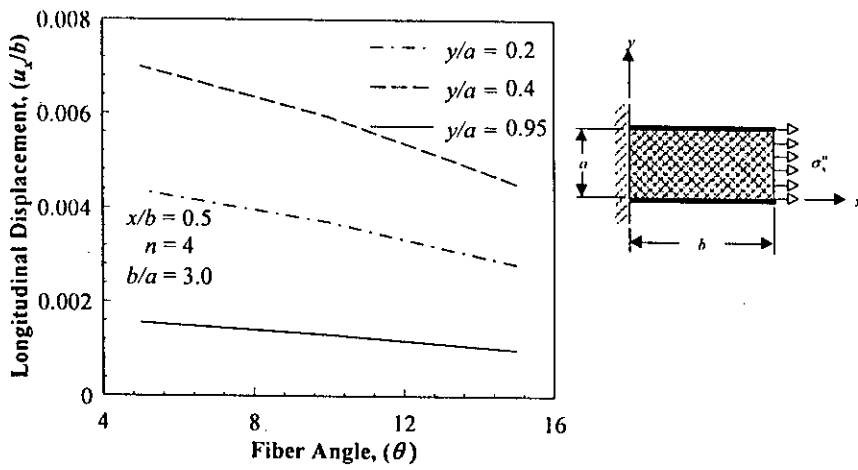


Fig. 4.37 Effect of fiber angle on longitudinal displacement.

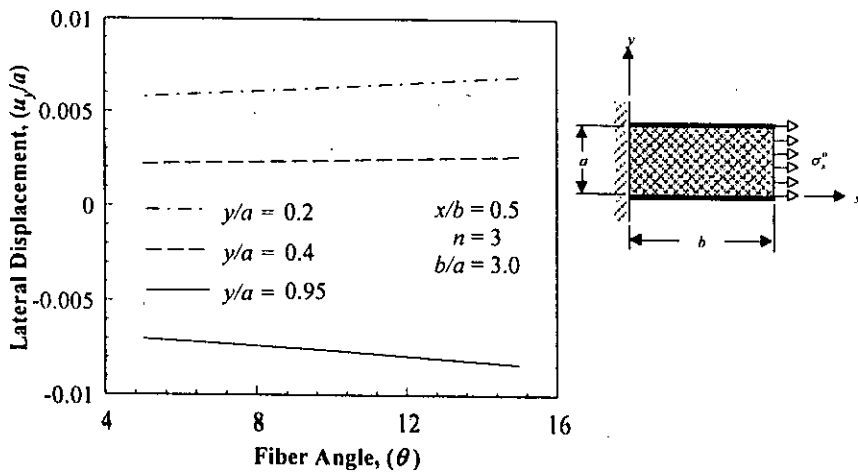


Fig. 4.38 Effect of fiber angle on lateral displacement.

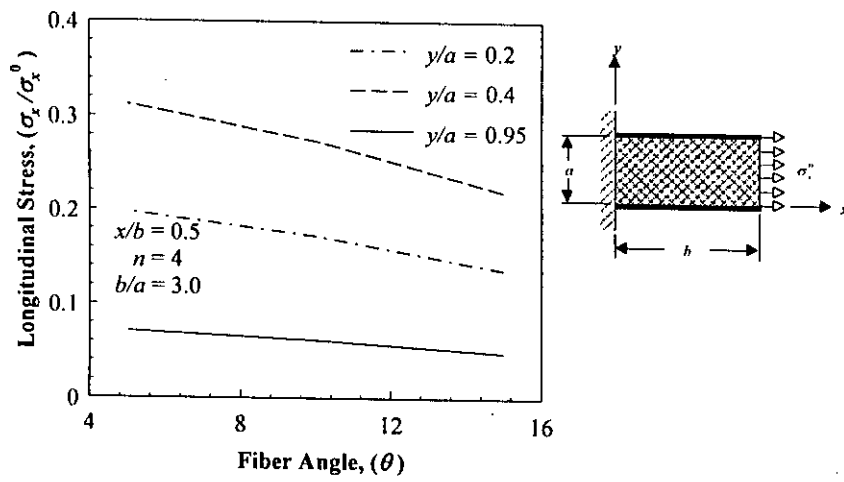


Fig. 4.39 Effect of fiber angle on longitudinal stress component.

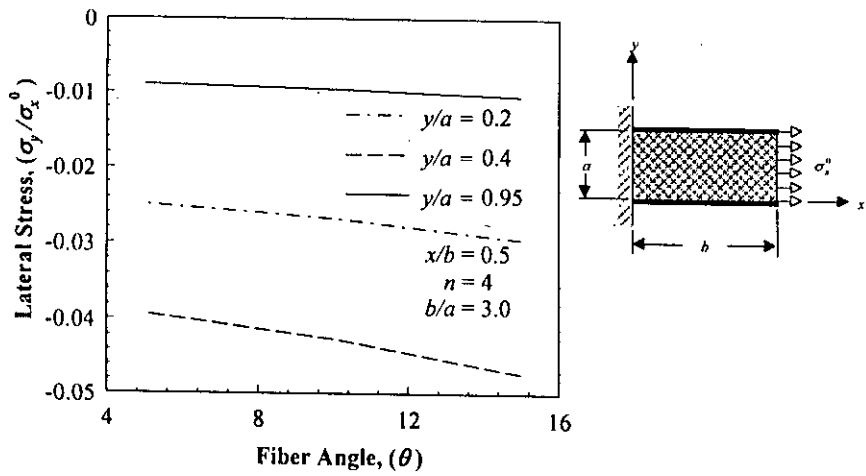


Fig. 4.40 Effect of fiber angle on lateral stress component.

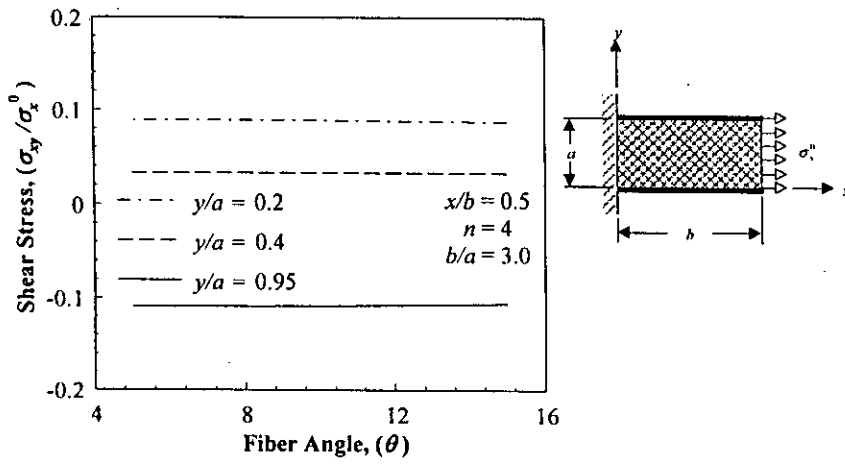


Fig. 4.41 Effect of fiber angle on shear stress.

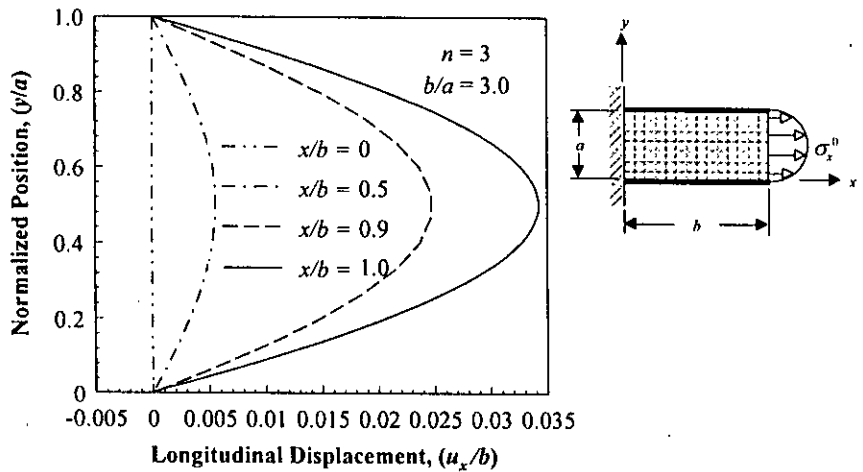


Fig. 4.42 Longitudinal displacement at different sections of the panel.

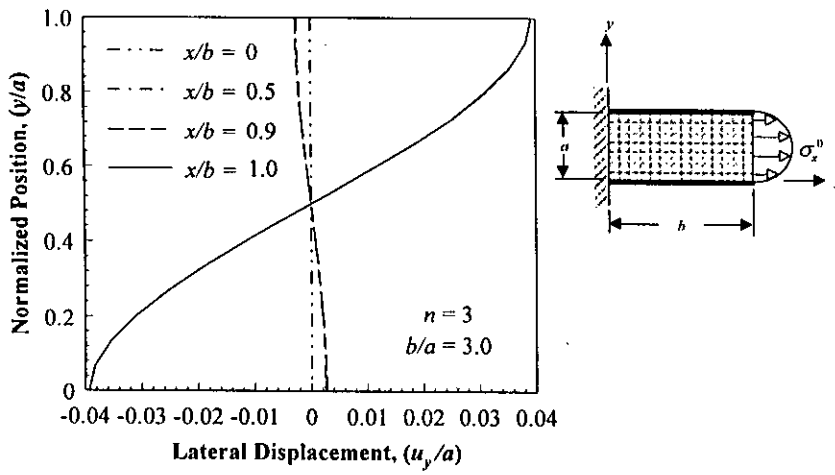


Fig. 4.43 Lateral displacement at different sections of the panel.

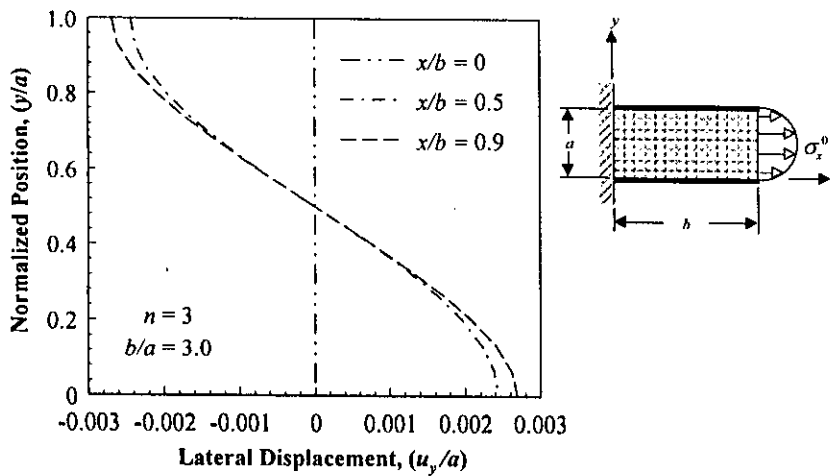


Fig. 4.44 Lateral displacement at different sections of the panel.

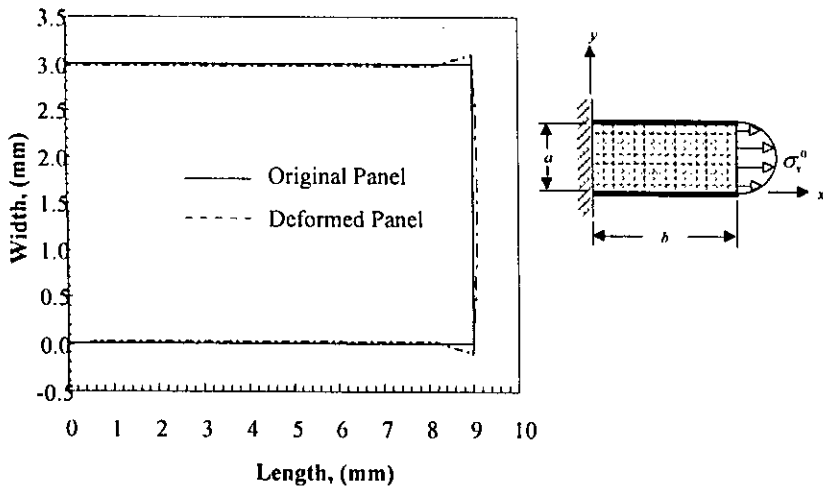


Fig. 4.45 Deformed and original shape of a cross-ply laminated composite panel under parabolic tensile load.

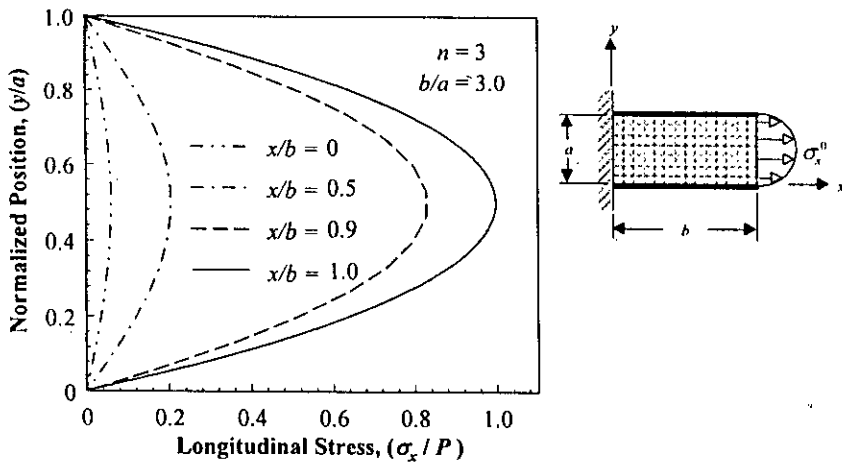


Fig. 4.46 Longitudinal stress at different sections of the panel.

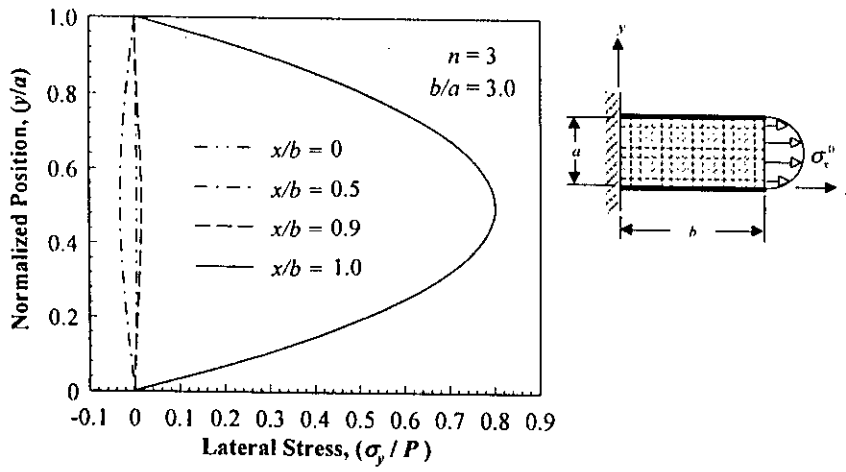


Fig. 4.47 Lateral stress at different sections of the panel.

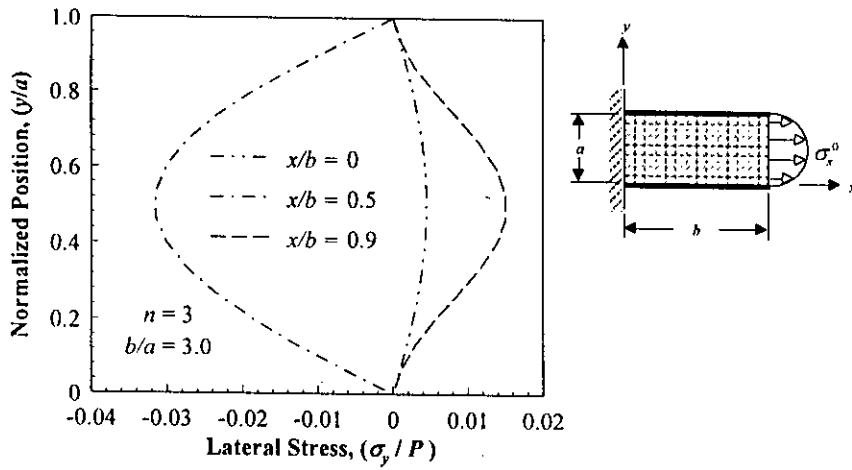


Fig. 4.48 Lateral stress at different sections of the panel.

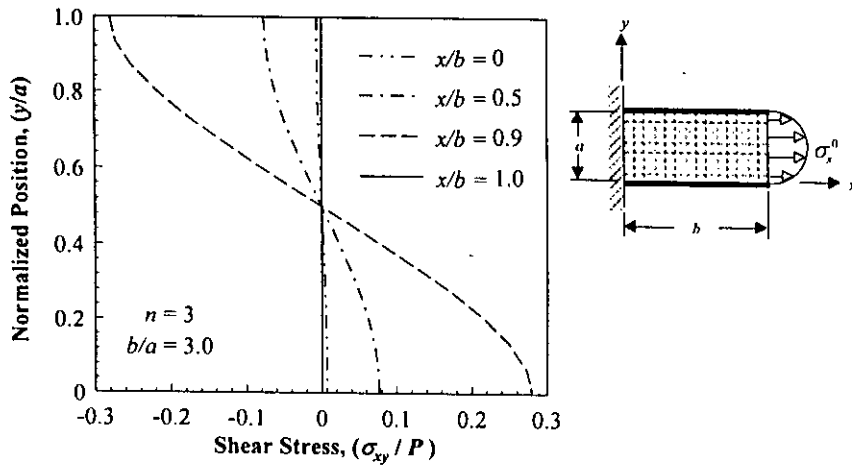


Fig. 4.49 Shear stress at different sections of the panel.

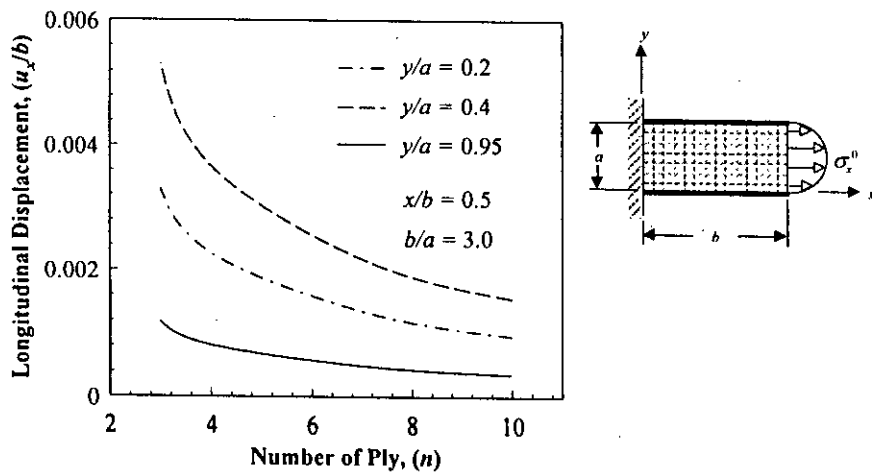


Fig. 4.50 Longitudinal displacement as a function of ply number.

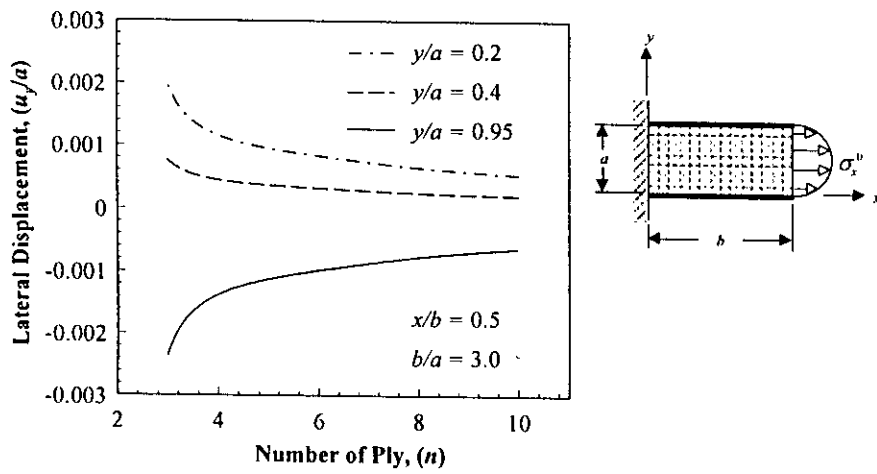


Fig. 4.51 Lateral displacement as a function of ply number.

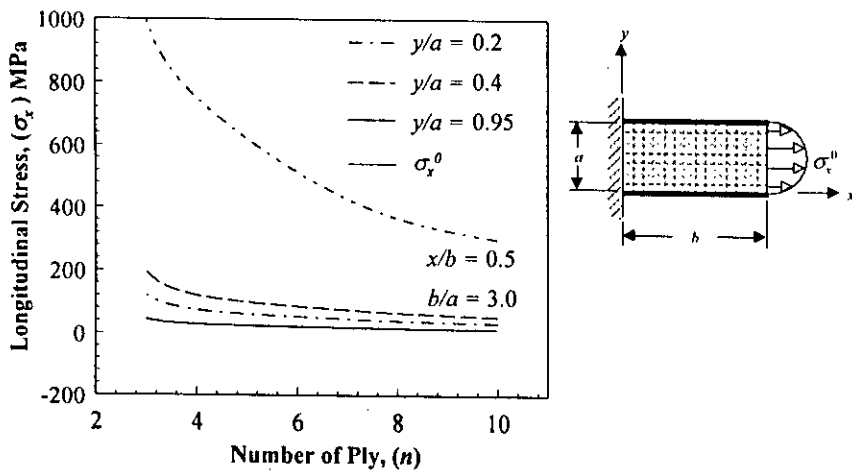


Fig. 4.52 Effect of ply number on the longitudinal stress component.

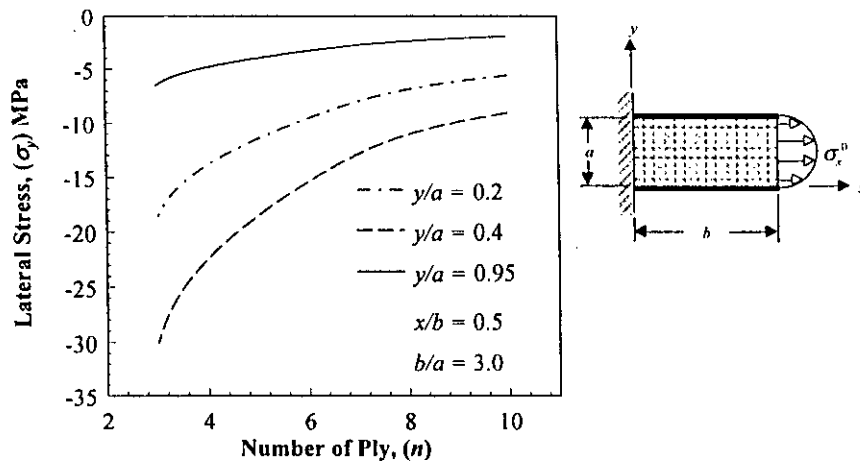


Fig. 4.53 Effect of ply number on the lateral stress component.

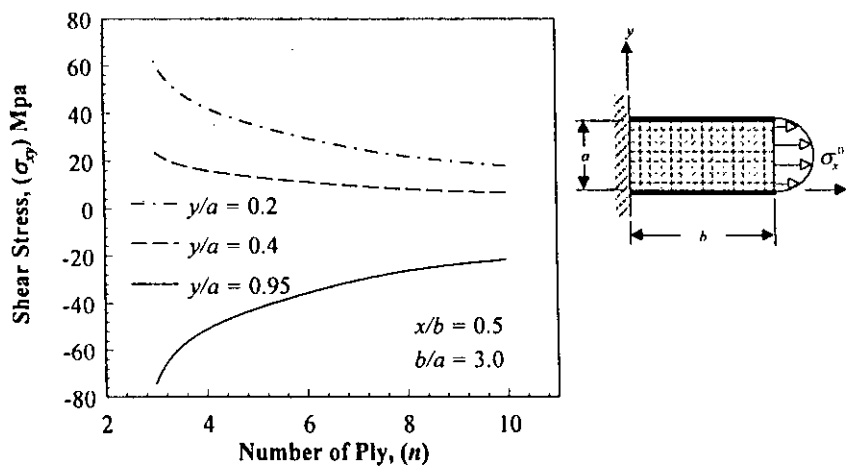


Fig. 4.54 Effect of ply number on the shear stress.

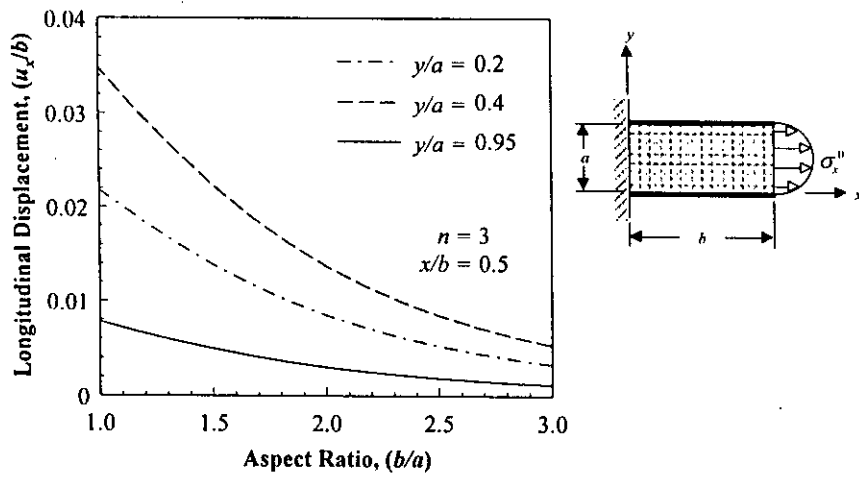


Fig. 4.55 Effect of aspect ratio on longitudinal displacement.

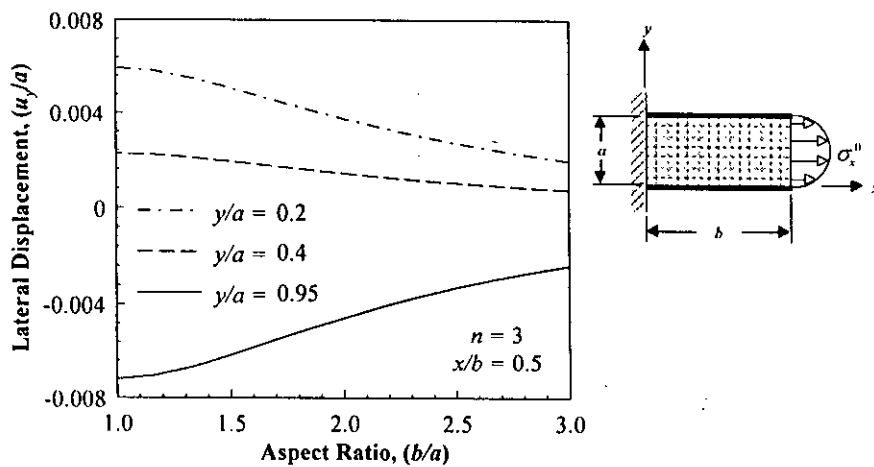


Fig. 4.56 Effect of aspect ratio on lateral displacement.

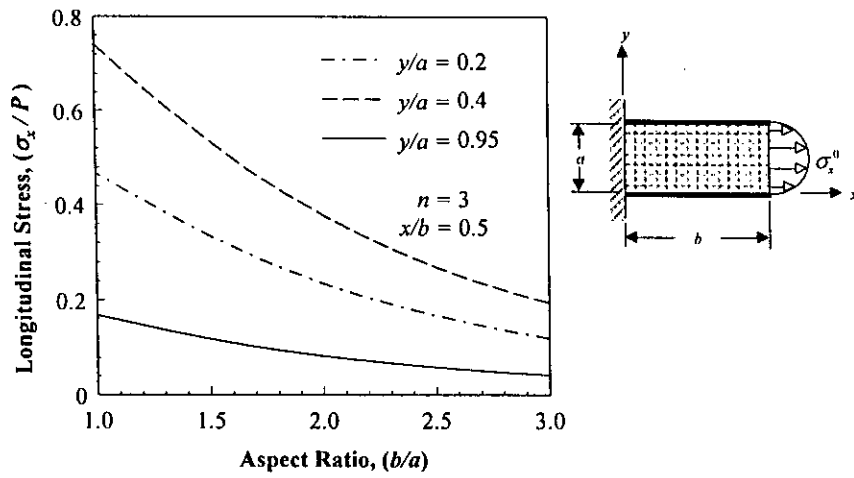


Fig. 4.57 Effect of aspect ratio on longitudinal stress component.

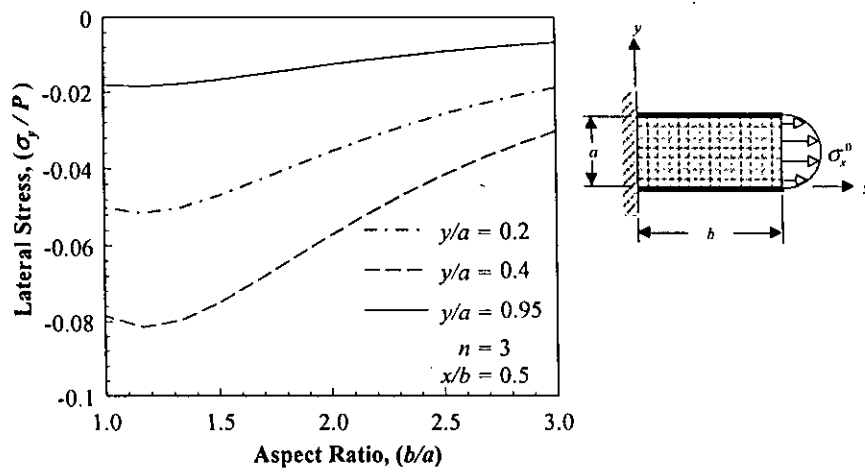


Fig. 4.58 Effect of aspect ratio on lateral stress component.

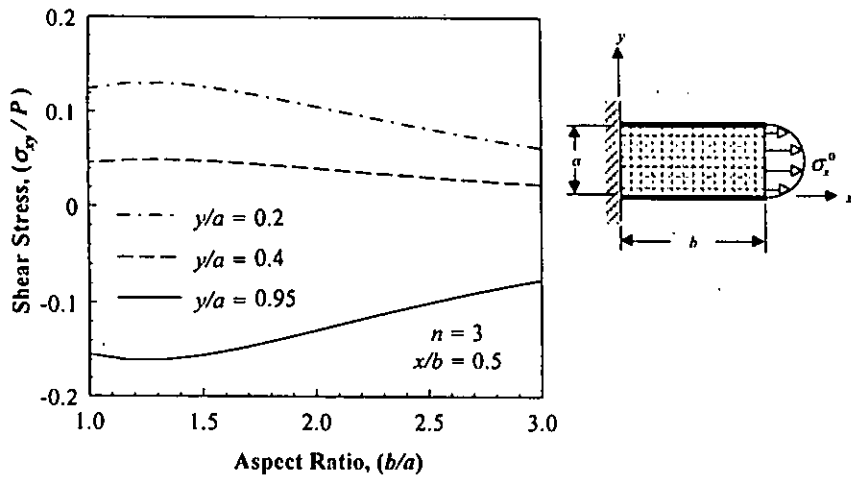


Fig. 4.59 Effect of aspect ratio on shear stress.

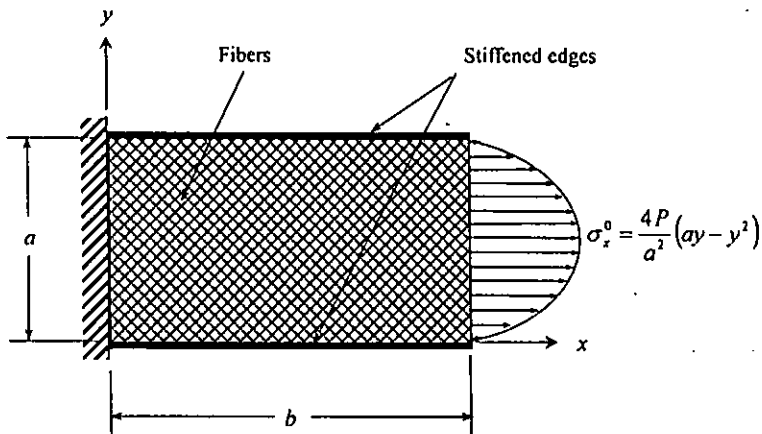


Fig. 5.60 A rectangular panel of angle-ply laminated composite under parabolic tensile loading.

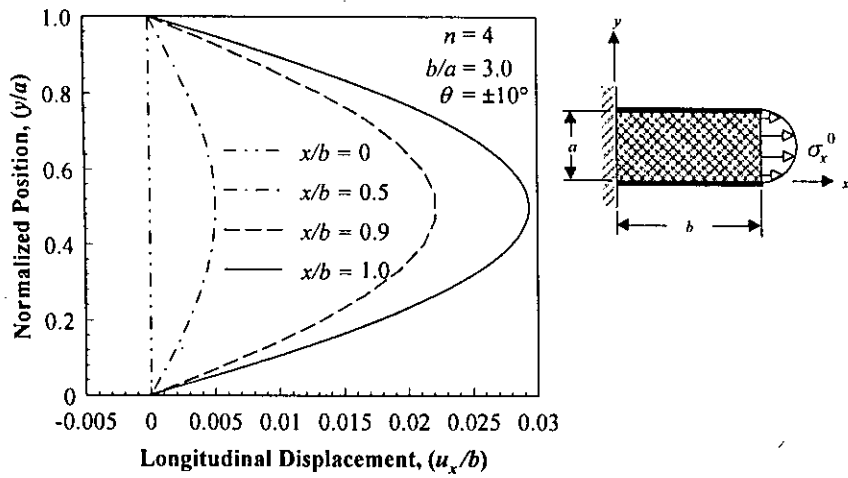


Fig. 4.61 Longitudinal displacement at different sections of the panel.

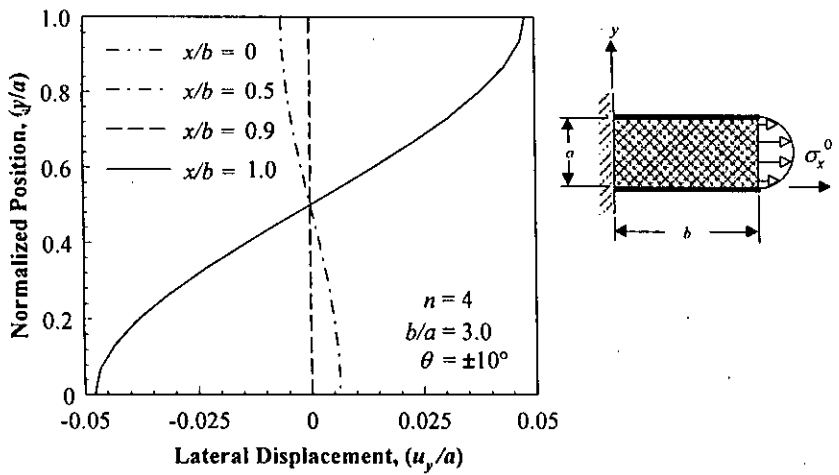


Fig. 4.62 Lateral displacement at different sections of the panel

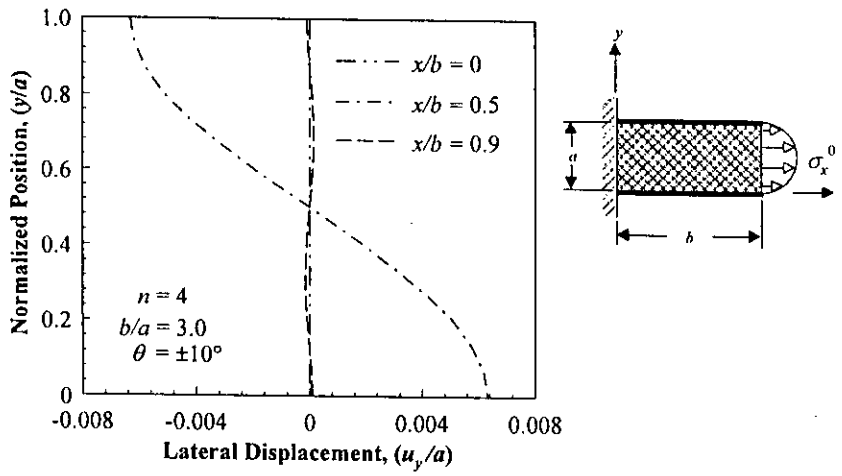


Fig. 4.63 Lateral displacement at different sections of the panel.

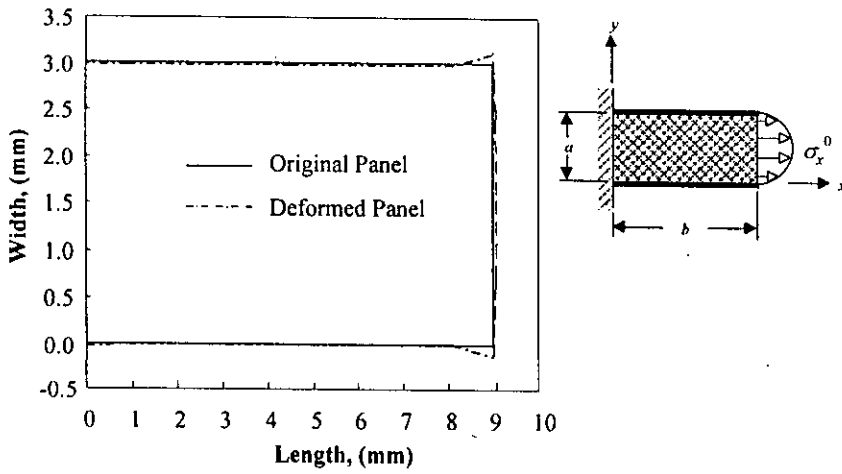


Fig. 4.64 Deformed and original shape of an angle-ply laminated composite panel under parabolic tensile load.

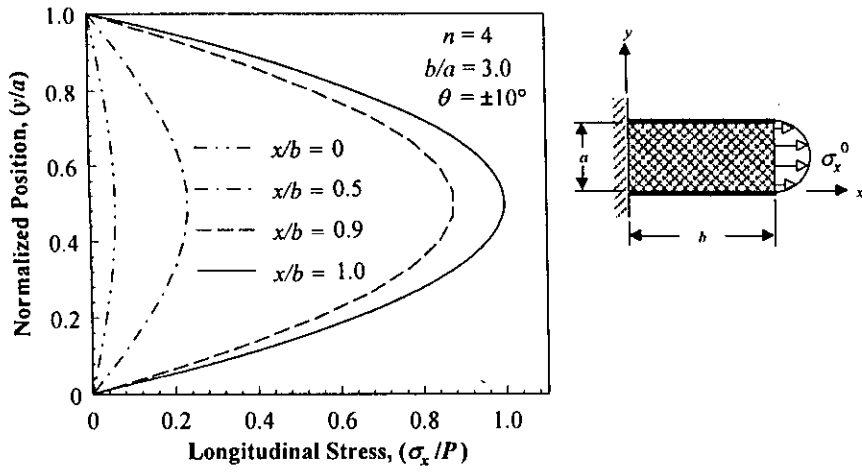


Fig. 4.65 Longitudinal stress at different sections of the panel.

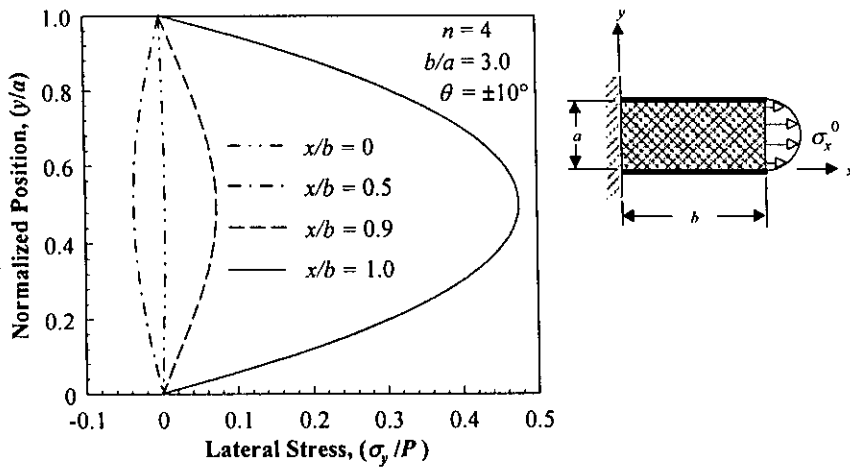


Fig. 4.66 Lateral stress at different sections of the panel.

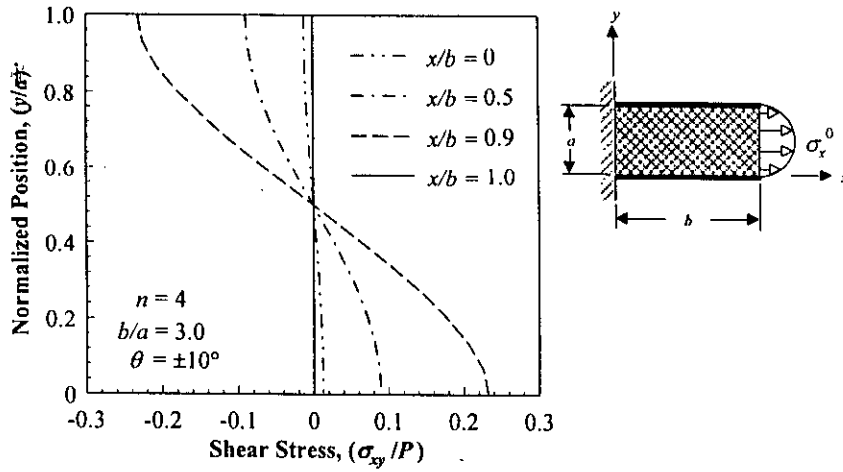


Fig. 4.67 Shear stress at different sections of the panel.

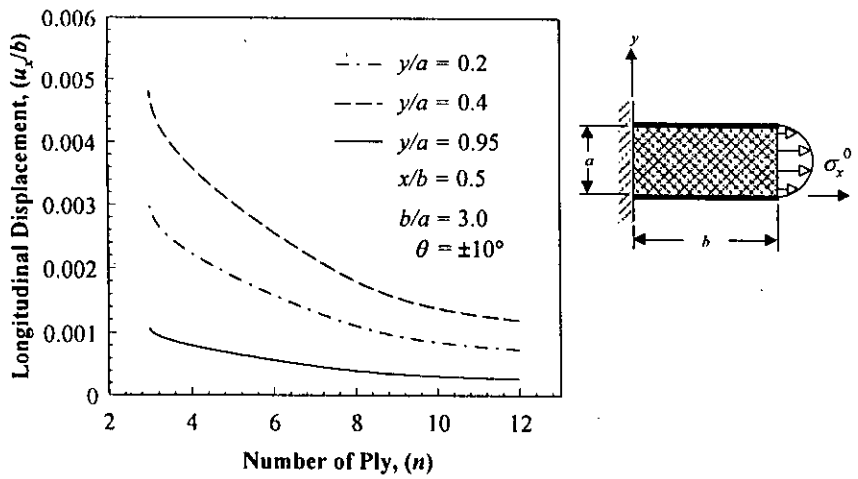


Fig. 4.68 Longitudinal displacement as a function of ply number.

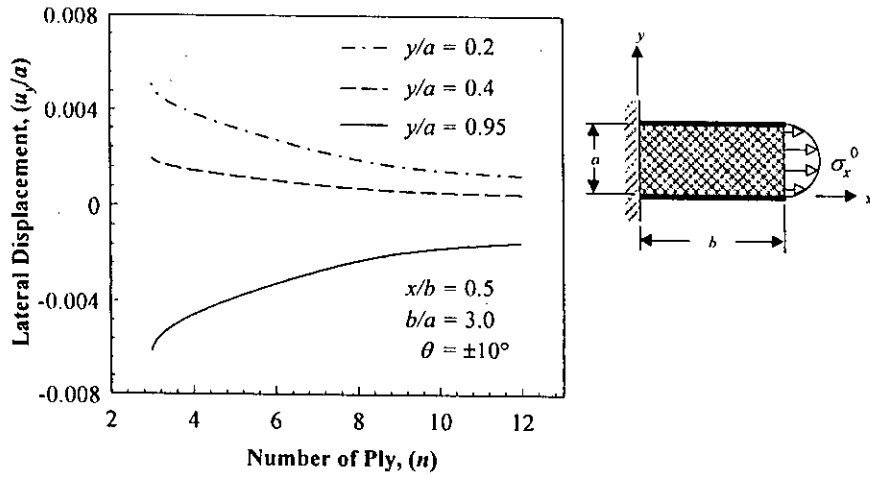


Fig. 4.69 Lateral displacement as a function of ply number.

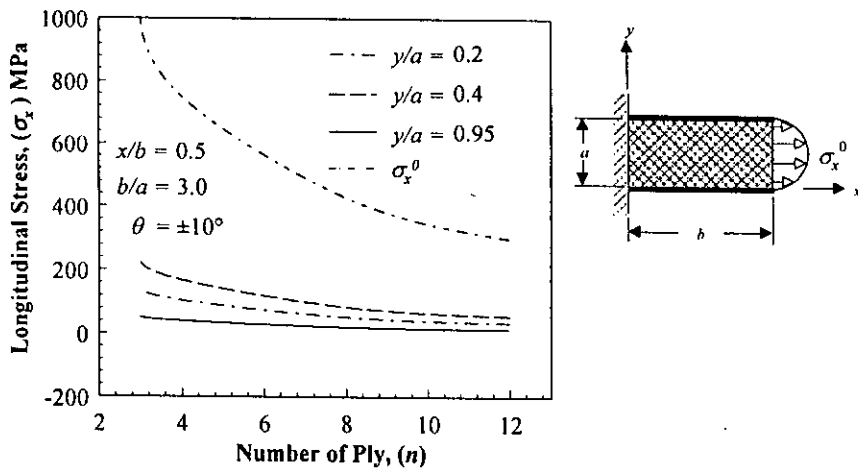


Fig. 4.70 Effect of ply number on the longitudinal stress component.

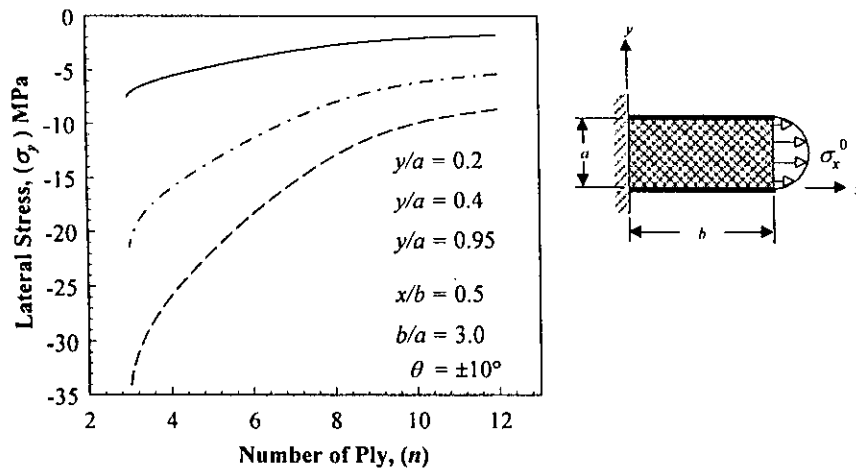


Fig. 4.71 Effect of ply number on the lateral stress component.

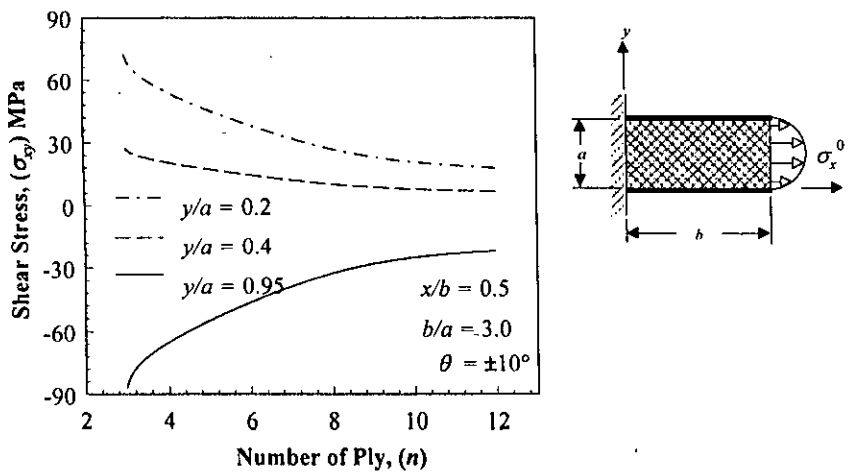


Fig. 4.72 Effect of ply number on the shear stress.

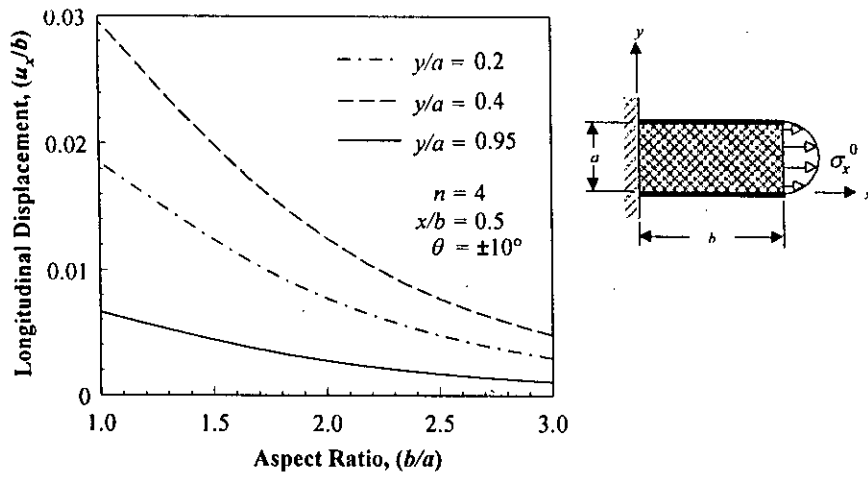


Fig. 4.73 Effect of aspect ratio on longitudinal displacement.

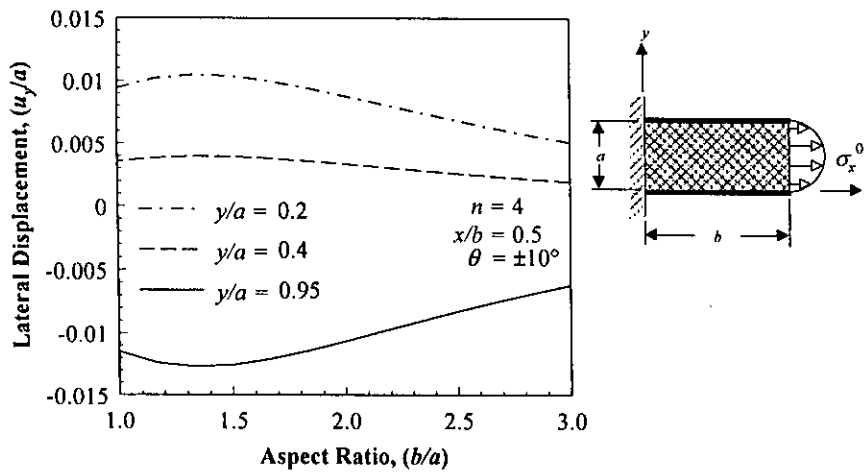


Fig. 4.74 Effect of aspect ratio on lateral displacement.

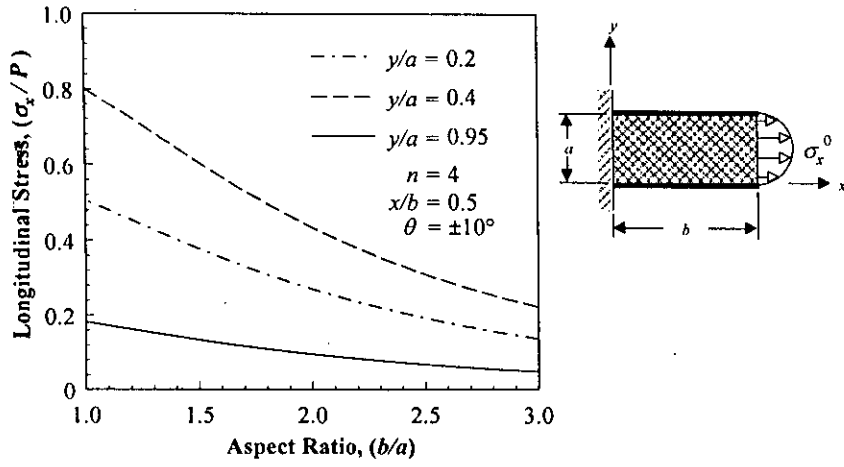


Fig. 4.75 Effect of aspect ratio on longitudinal stress component.

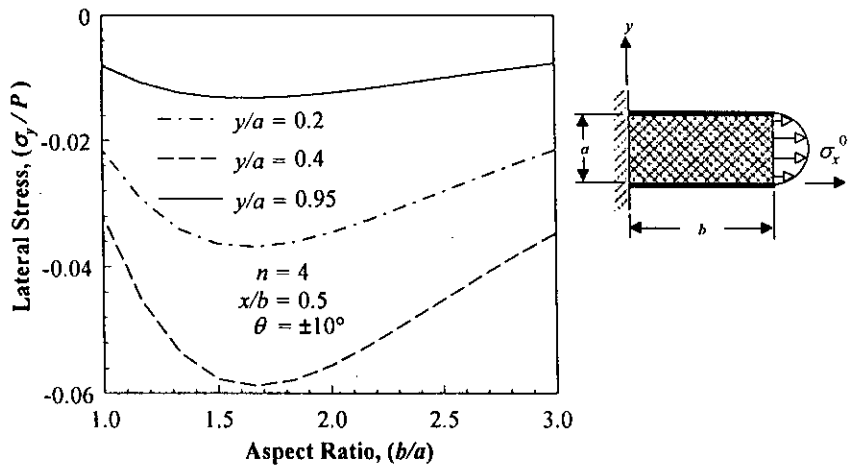


Fig. 4.76 Effect of aspect ratio on lateral stress component.

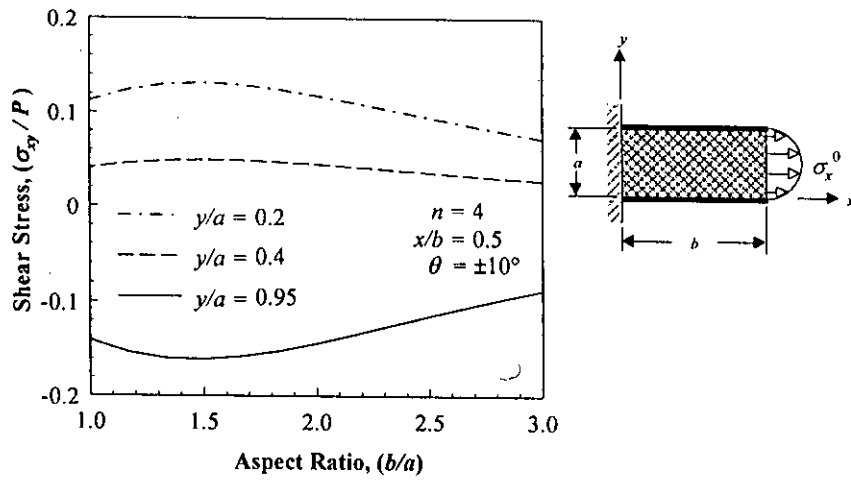


Fig. 4.77 Effect of aspect ratio on shear stress.

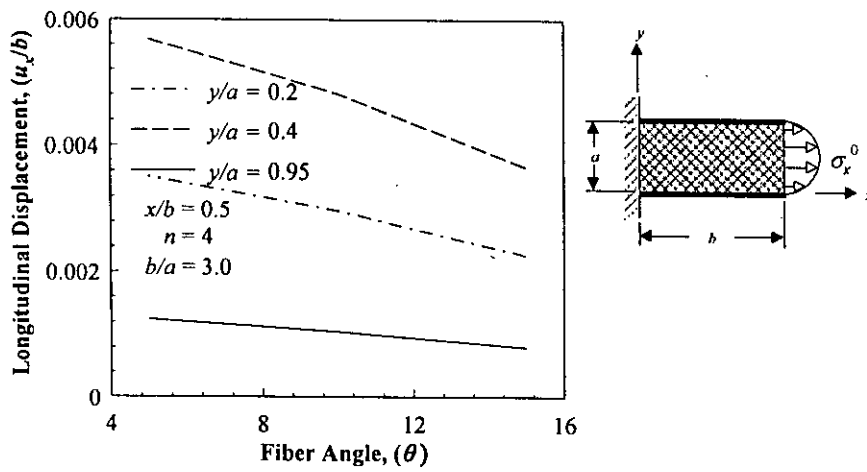


Fig. 4.78 Effect of fiber angle on longitudinal displacement.

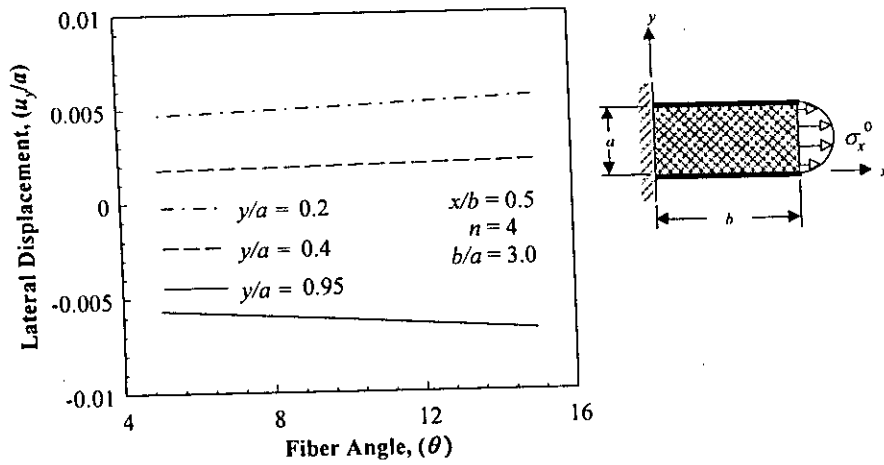


Fig. 4.79 Effect of fiber angle on lateral displacement.

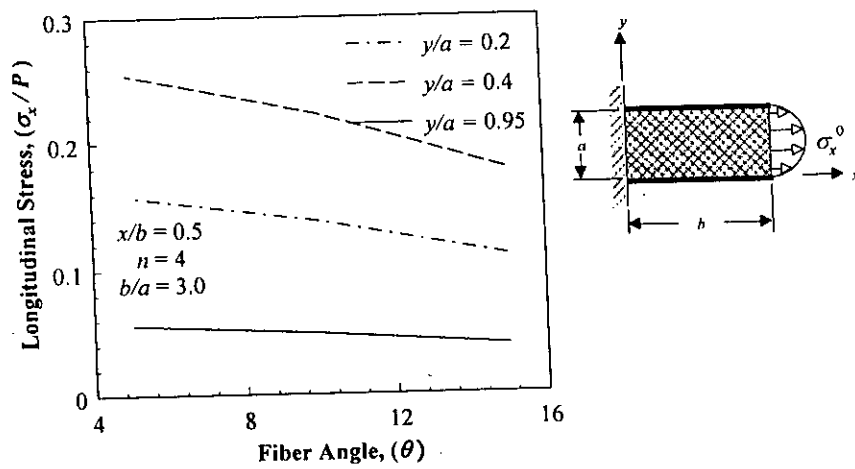


Fig. 4.80 Effect of fiber angle on longitudinal stress component.

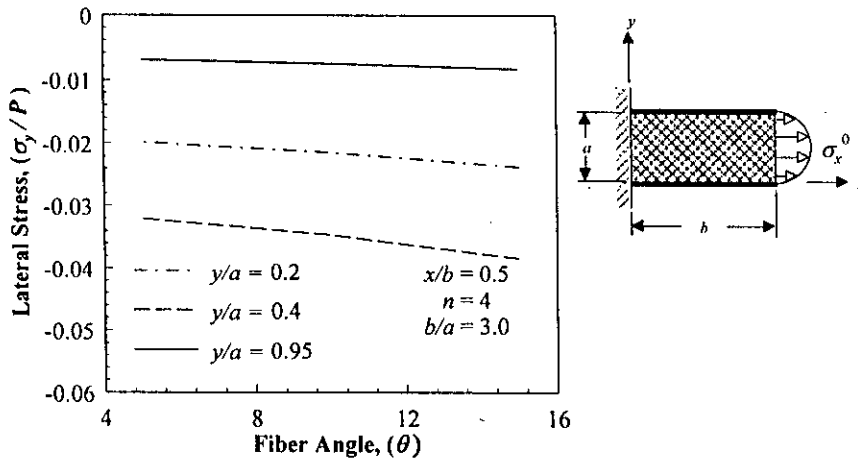


Fig. 4.81 Effect of fiber angle on lateral stress component.

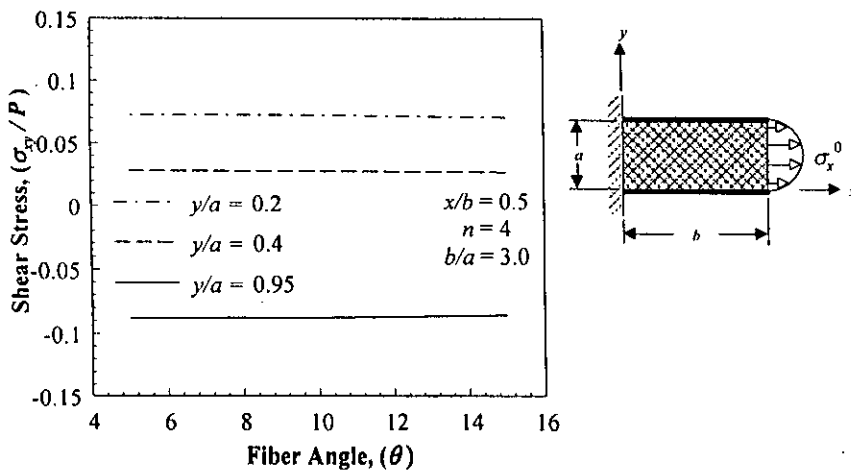


Fig. 4.82 Effect of fiber angle on shear stress.

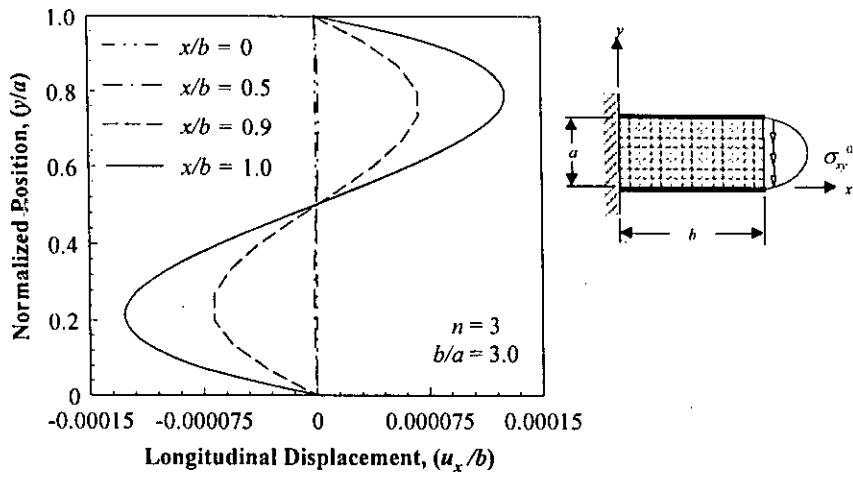


Fig. 4.83 Longitudinal displacement at different sections of the panel.

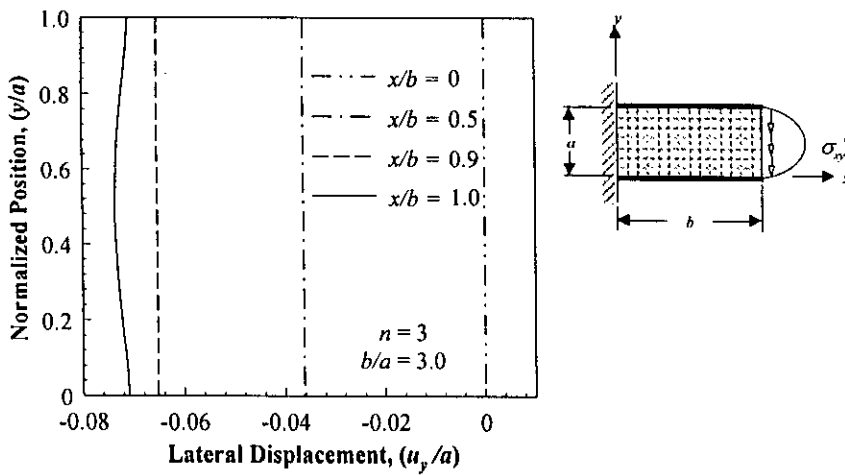


Fig. 4.84 Lateral displacement at different sections of the panel.

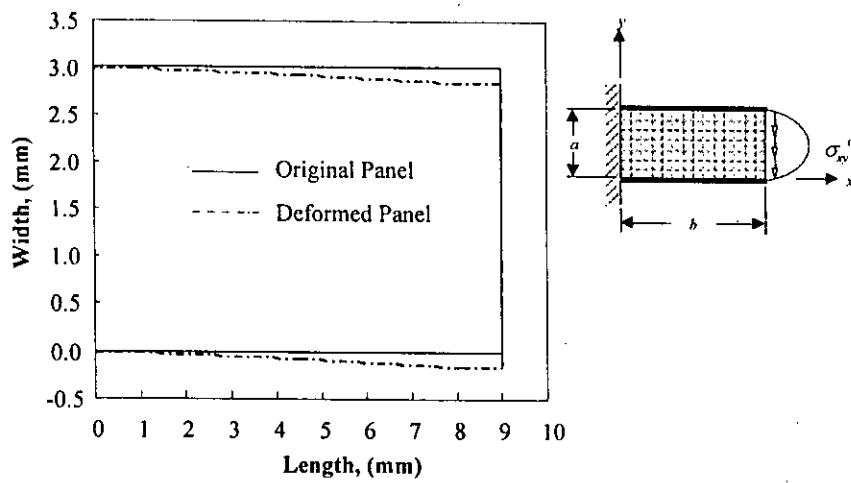


Fig. 4.85 Deformed and original shape of a cross-ply laminated composite panel under parabolic shear load.

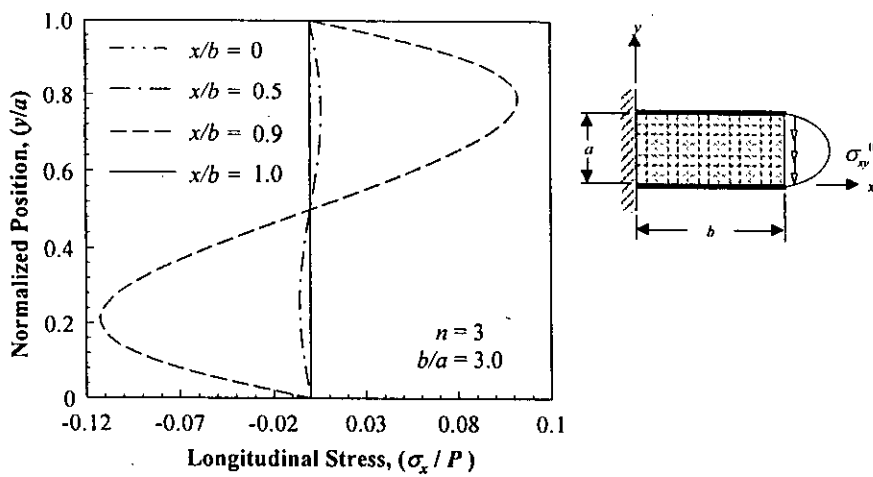


Fig. 4.86 Longitudinal stress at different sections of the panel.

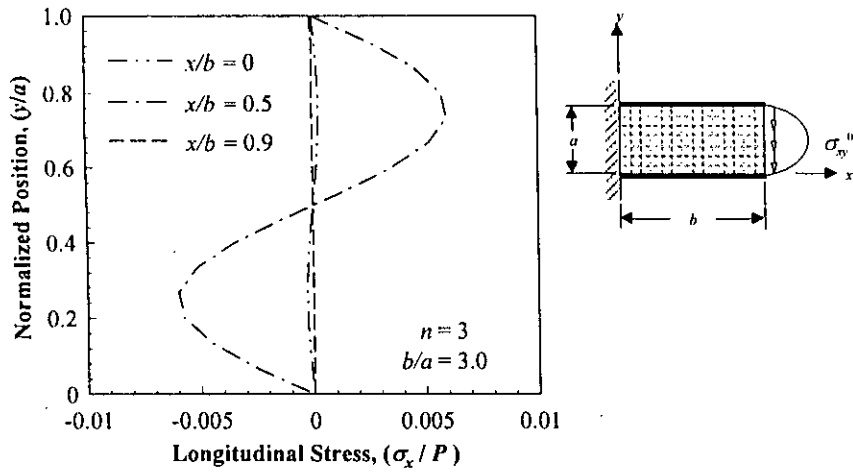


Fig. 4.87 Longitudinal stress at different sections of the panel.

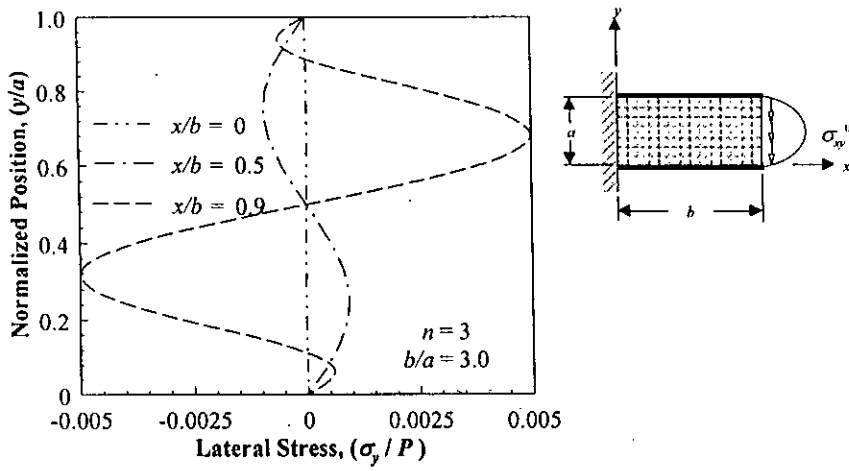


Fig. 4.88 Lateral stress at different sections of the panel.

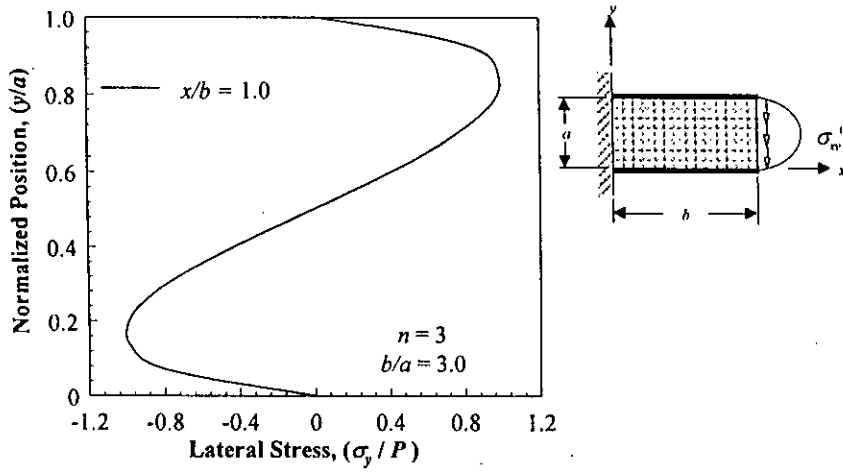


Fig. 4.89 Lateral Stress at section $x/b = 1$ of the panel.

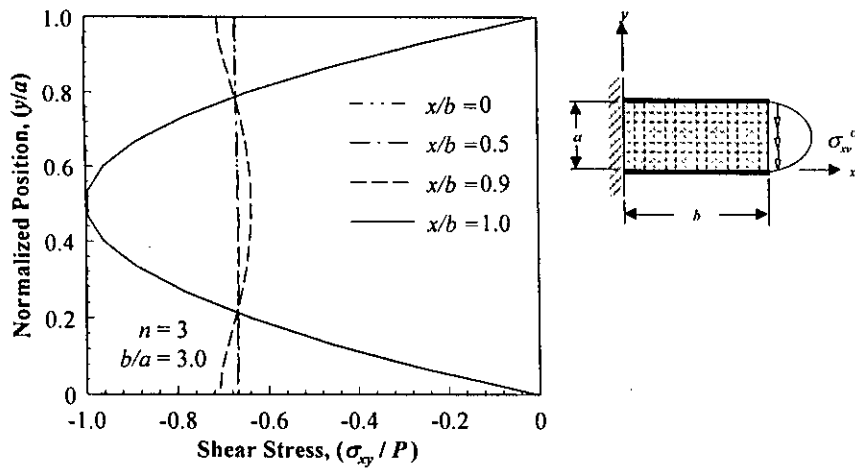


Fig. 4.90 Shear stress at different sections of the panel.

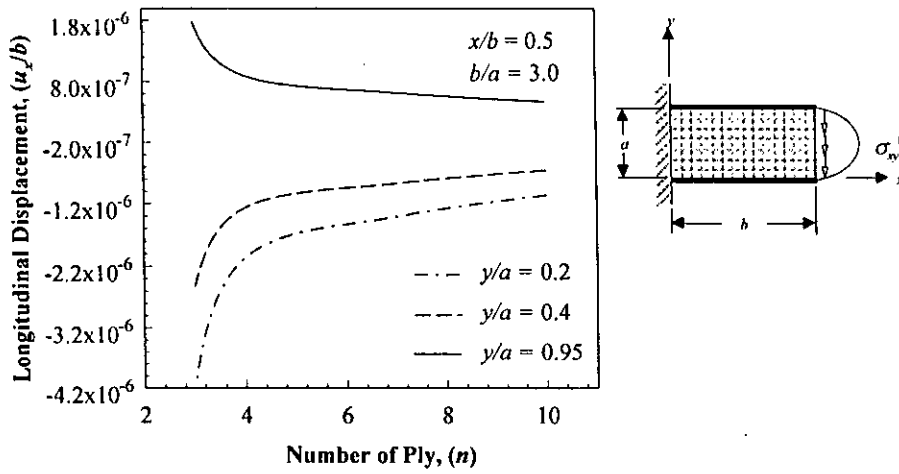


Fig. 4.91 Longitudinal displacement as a function of ply number.

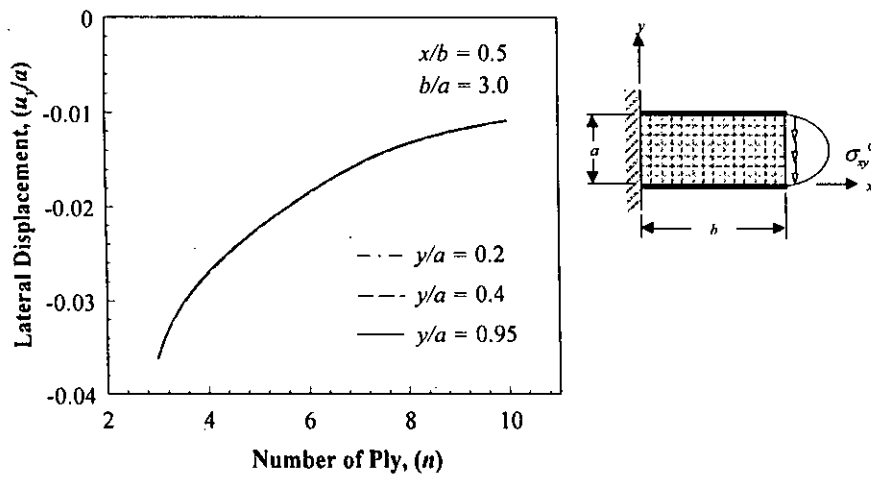


Fig. 4.92 Lateral displacement as a function of ply number.

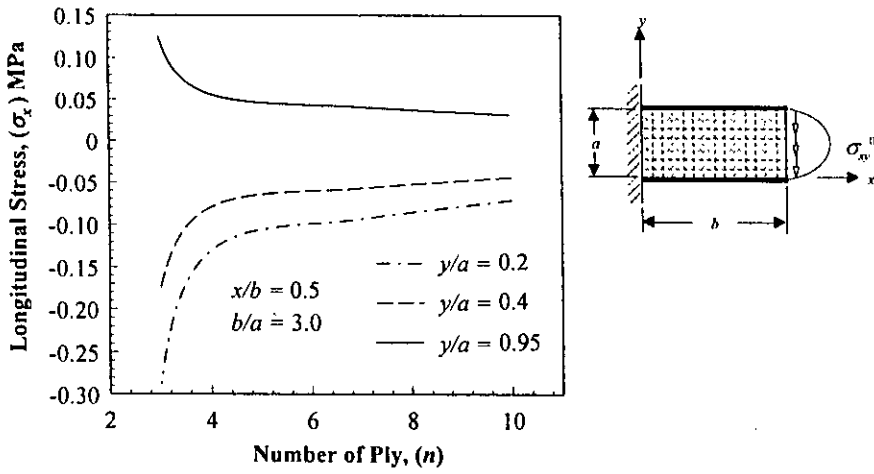


Fig. 4.93 Effect of ply number on the longitudinal stress component.

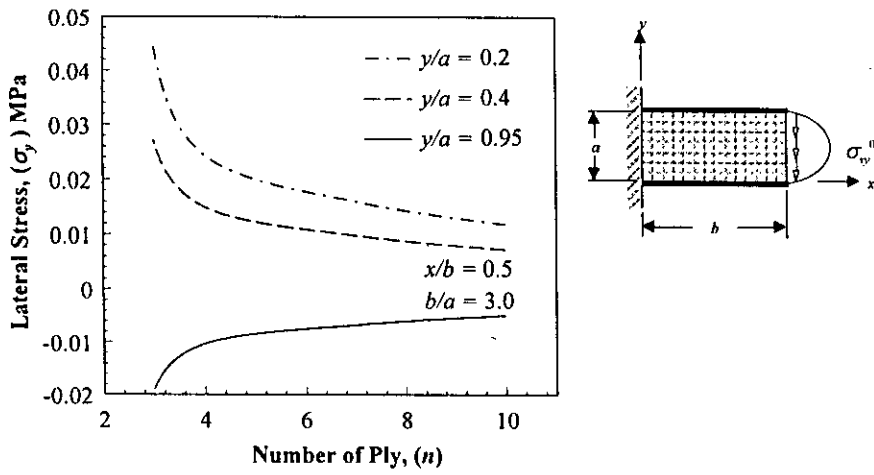


Fig. 4.94 Effect of ply number on the lateral stress component.

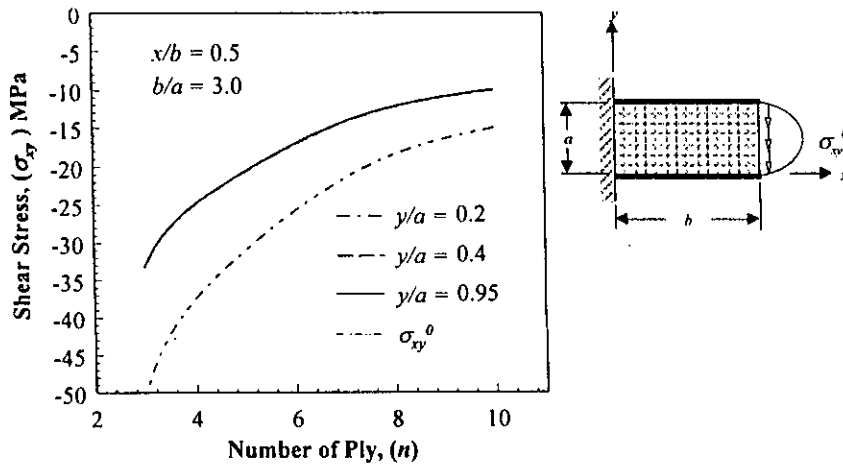


Fig. 4.95 Effect of ply number on the shear stress.

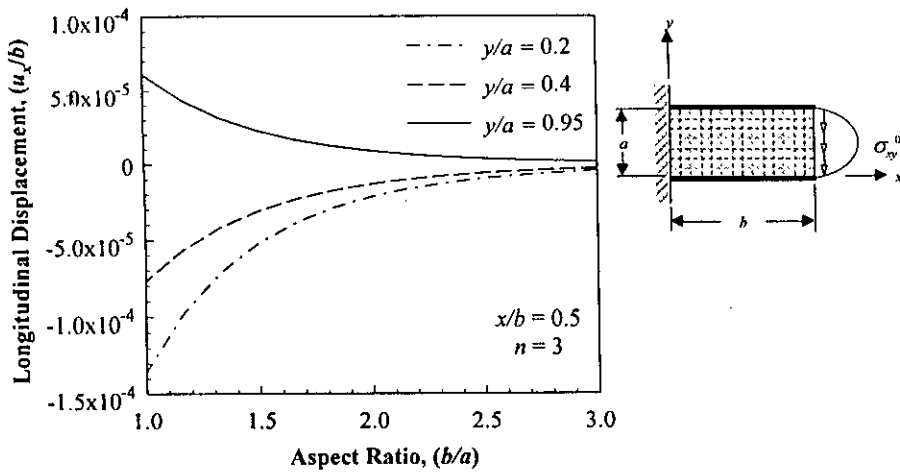


Fig. 4.96 Effect of aspect ratio on longitudinal displacement.

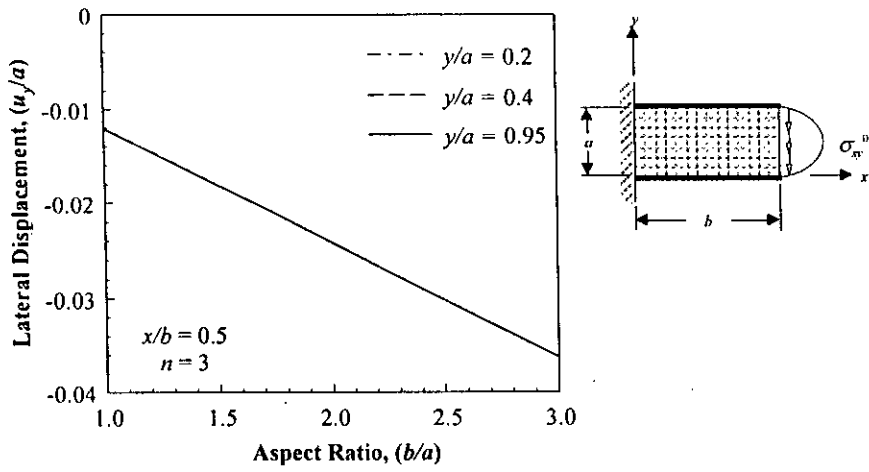


Fig. 4.97 Effect of aspect ratio on lateral displacement.

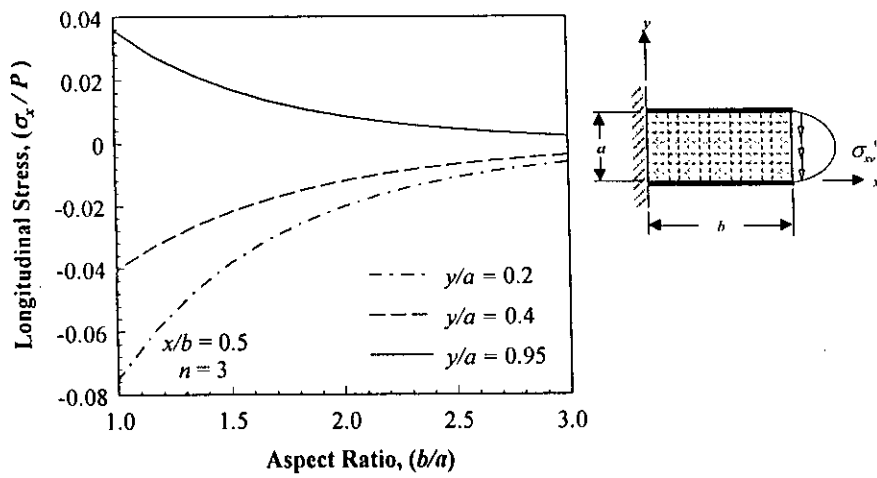


Fig. 4.98 Effect of aspect ratio on longitudinal stress component.

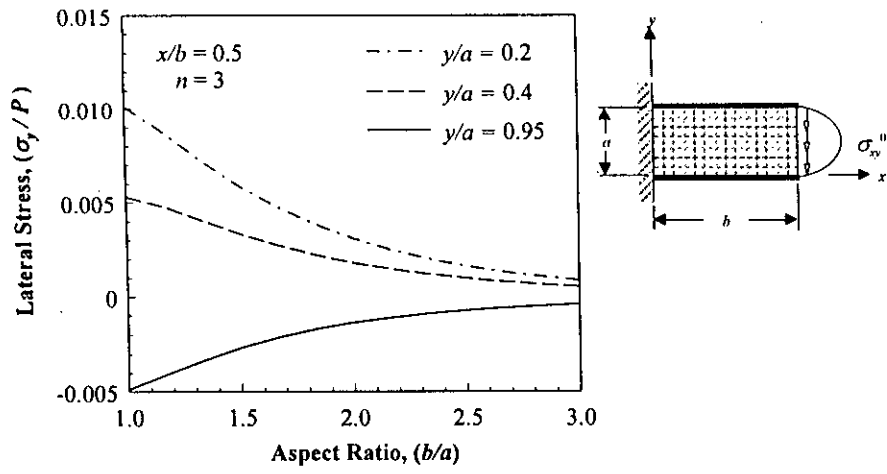


Fig. 4.99 Effect of aspect ratio on lateral stress component.

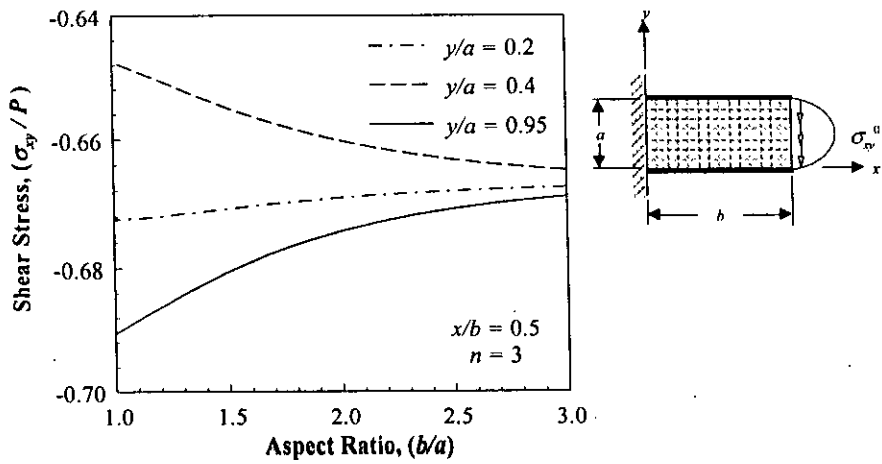


Fig. 4.100 Effect of aspect ratio on shear stress.

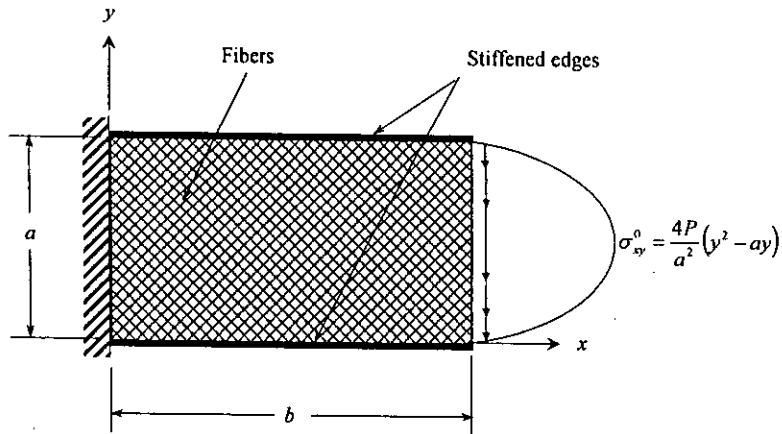


Fig. 4.101 A rectangular panel of angle-ply laminated composite under parabolic shear loading.

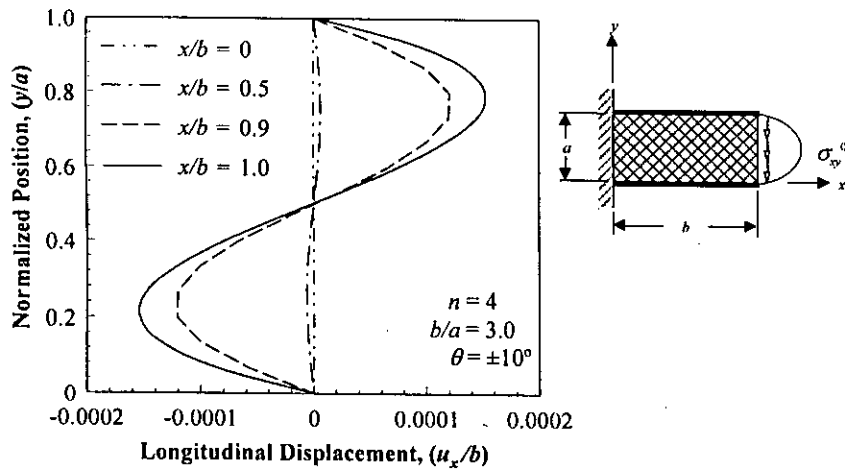


Fig. 4.102 Longitudinal displacement at different sections of the panel.

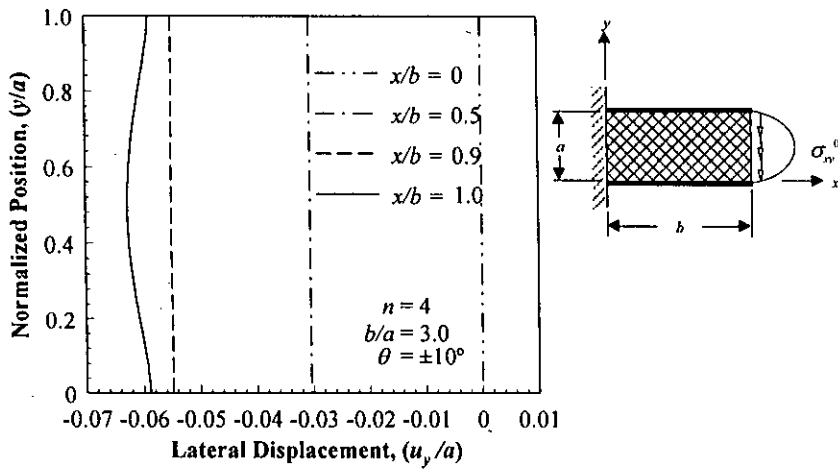


Fig. 4.103 Lateral displacement at different sections of the panel.

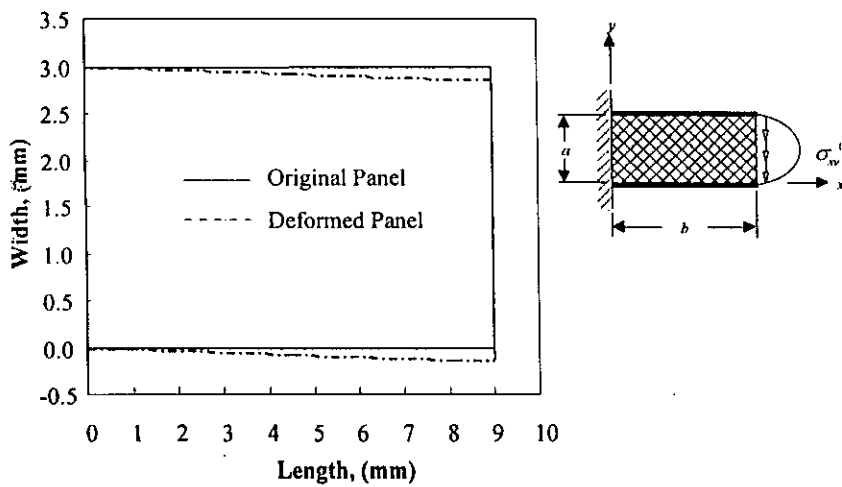


Fig. 4.104 Deformed and original shape of an angle-ply laminated composite panel under parabolic shear load.

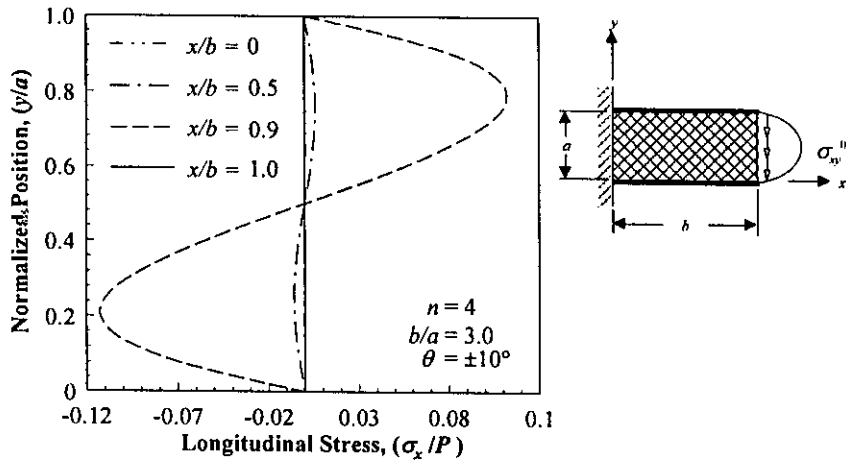


Fig. 4.105 Longitudinal stress at different sections of the panel.

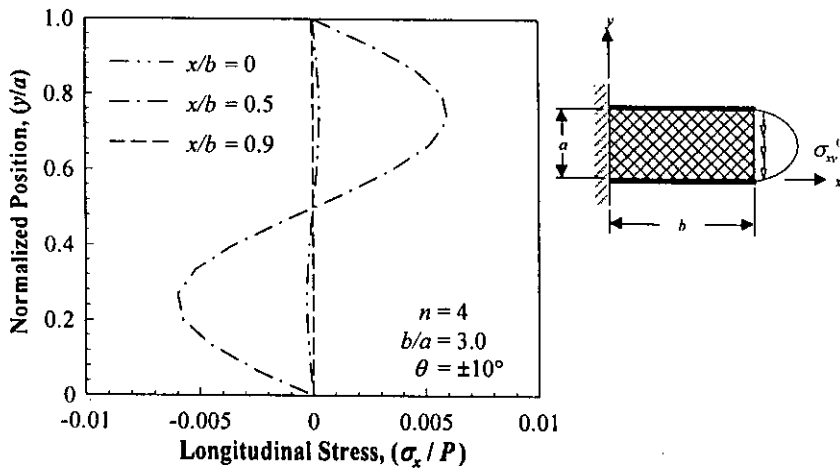


Fig. 4.106 Longitudinal stress at different sections of the panel

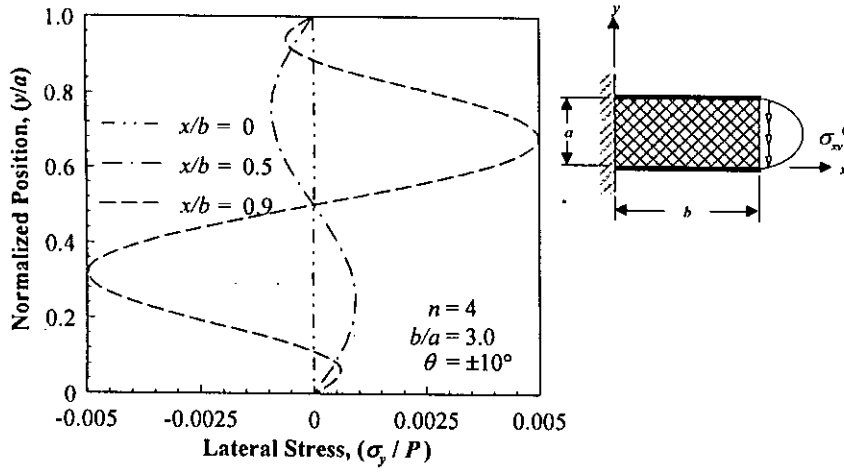


Fig. 4.107 Lateral stress at different sections of the panel.

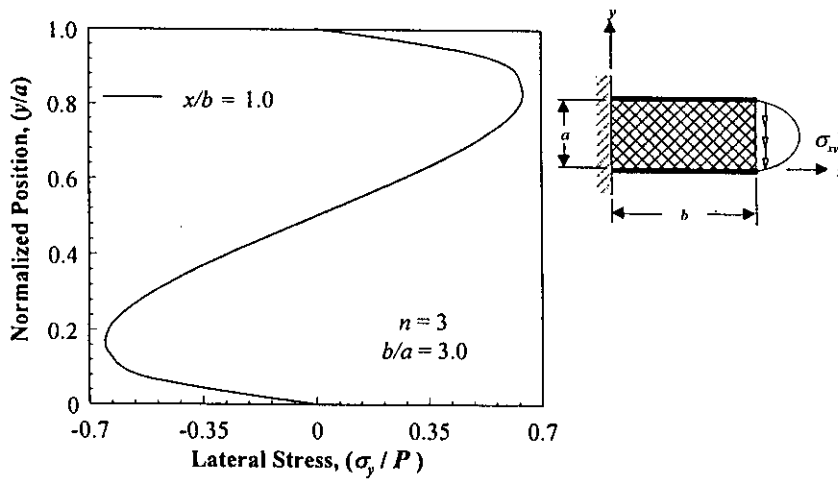


Fig. 4.108 Lateral Stress at section $x/b = 1$ of the panel.

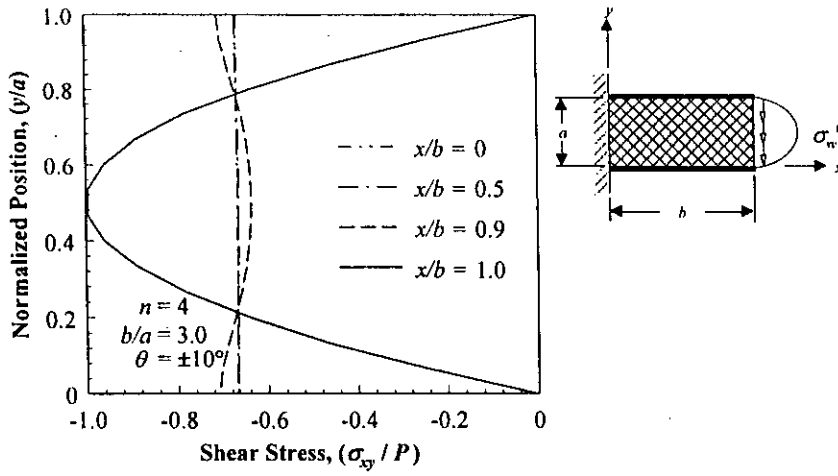


Fig. 4.109 Shear stress at different sections of the panel.

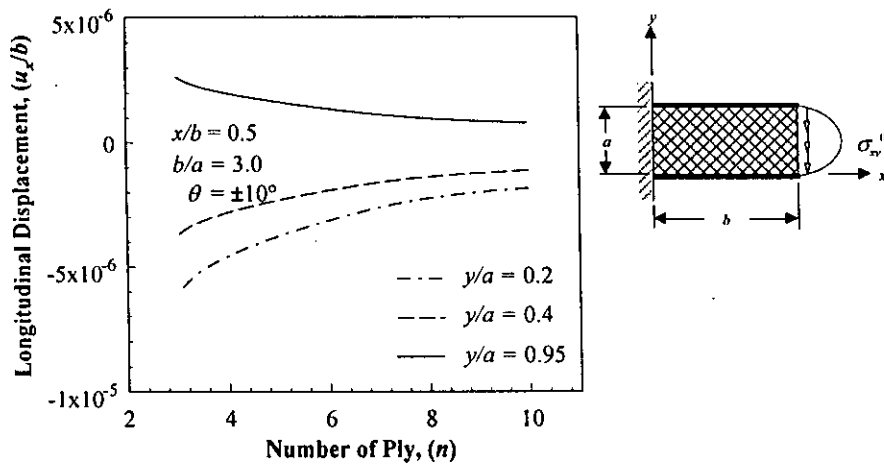


Fig. 4.110 Longitudinal displacement as a function of ply number.

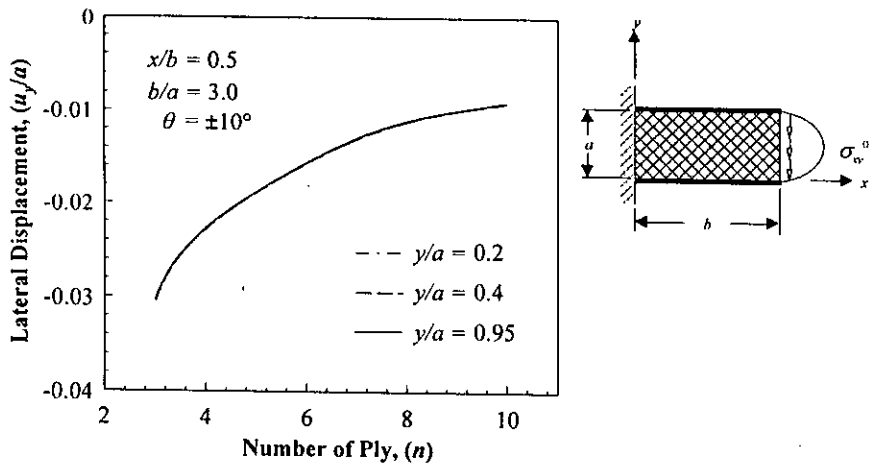


Fig. 4.111 Lateral displacement as a function of ply number.

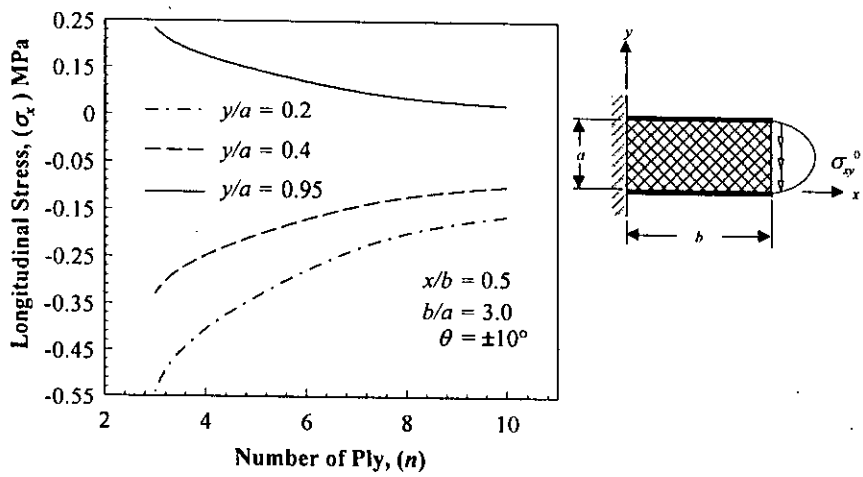


Fig. 4.112 Effect of ply number on the longitudinal stress component.

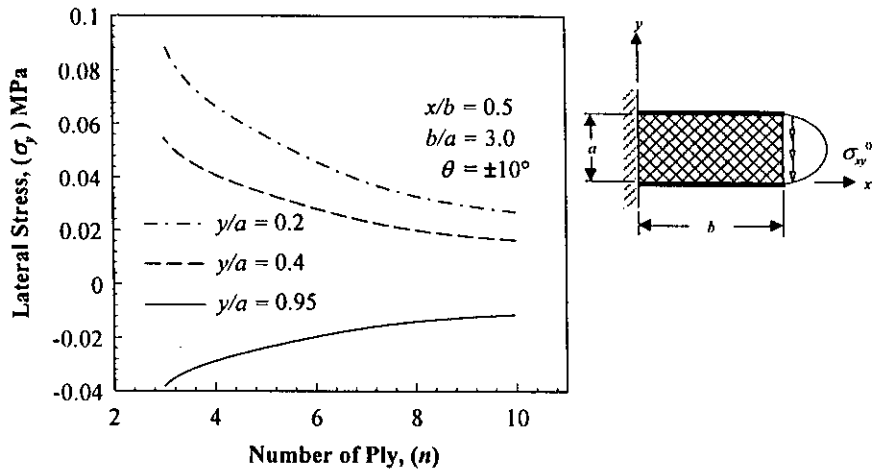


Fig. 4.113 Effect of ply number on the lateral stress component.

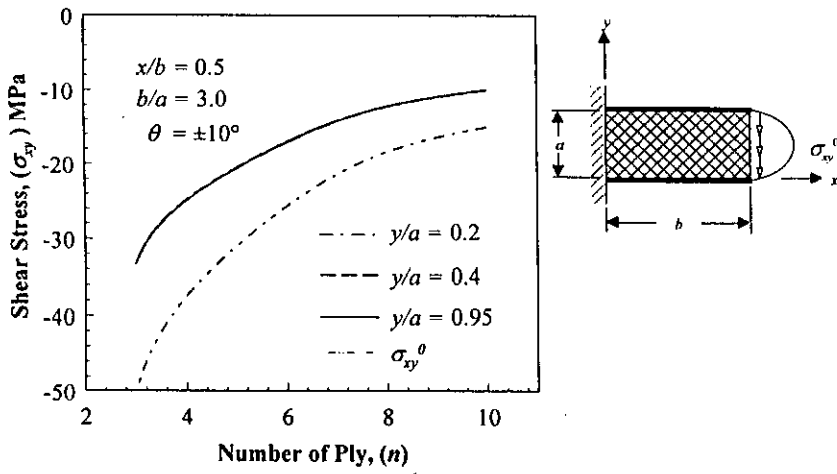


Fig. 4.114 Effect of ply number on the shear stress.

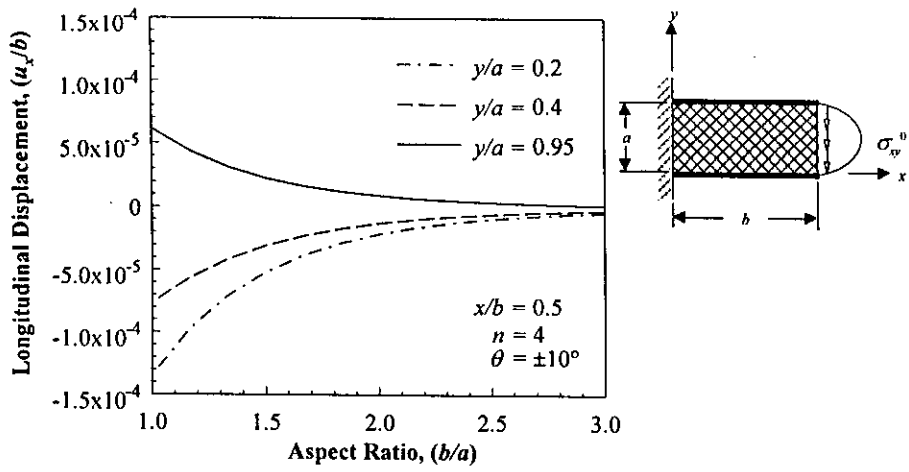


Fig. 4.115 Effect of aspect ratio on longitudinal displacement.

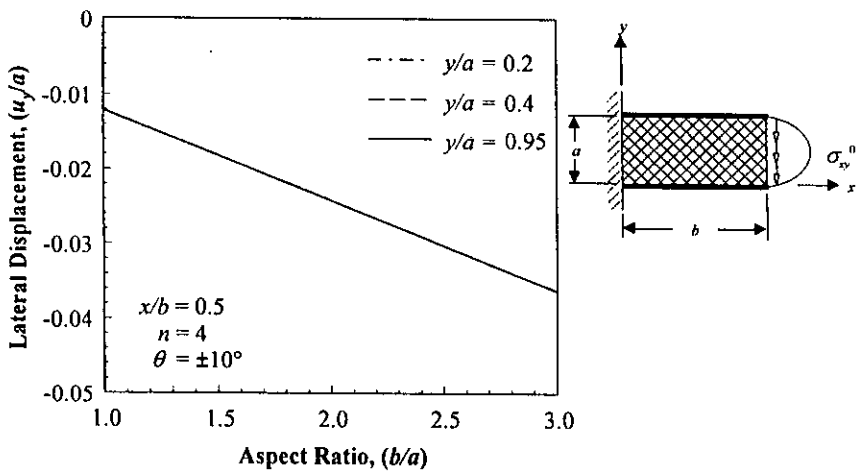


Fig. 4.116 Effect of aspect ratio on lateral displacement.

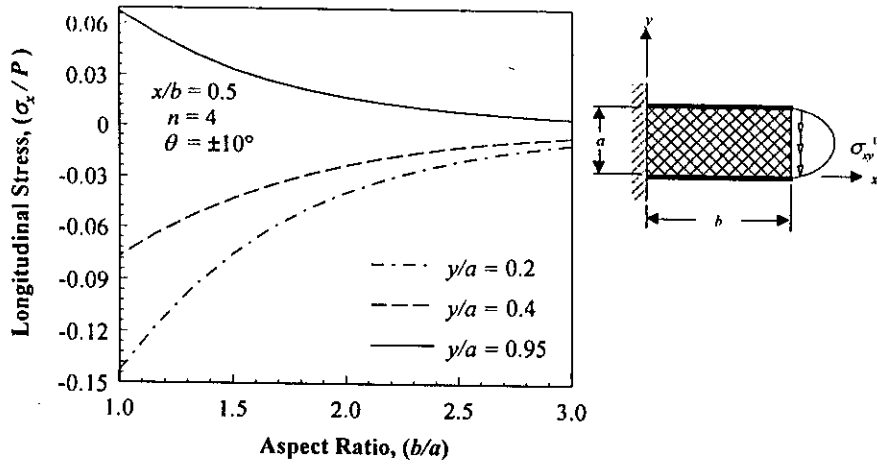


Fig. 4.117 Effect of aspect ratio on longitudinal stress component.

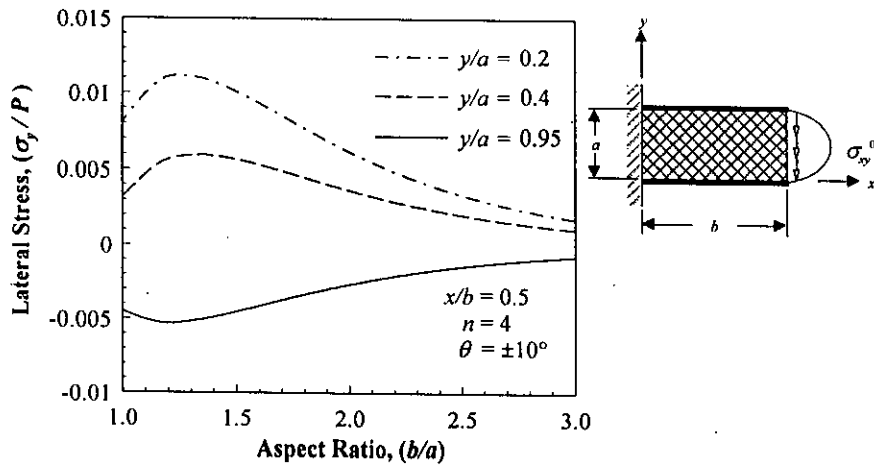


Fig. 4.118 Effect of aspect ratio on lateral stress component.

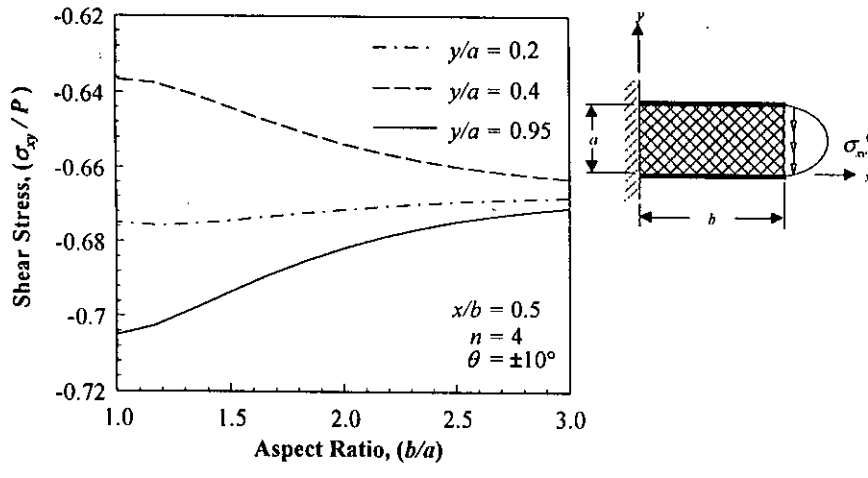


Fig. 4.119 Effect of aspect ratio on shear stress.

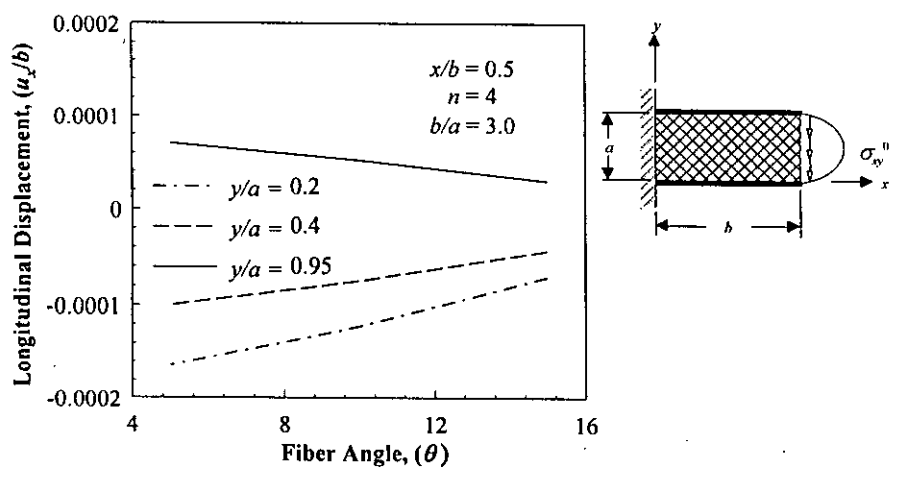


Fig. 4.120 Effect of fiber angle on longitudinal displacement.

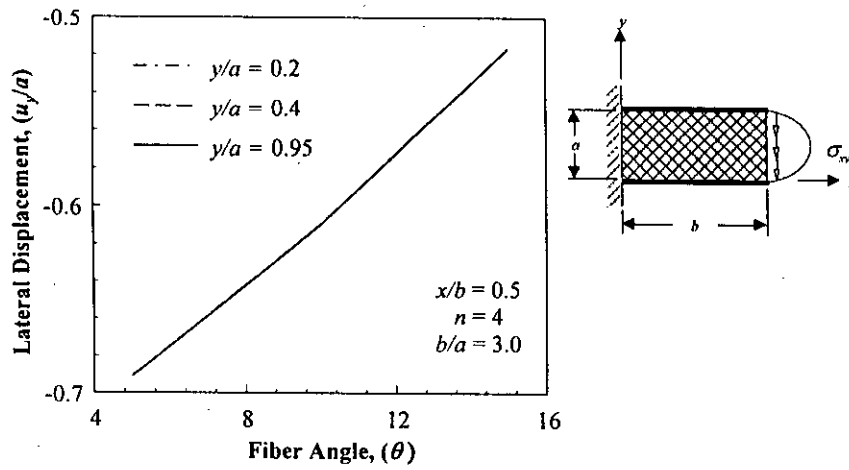


Fig. 4.121 Effect of fiber angle on lateral displacement.

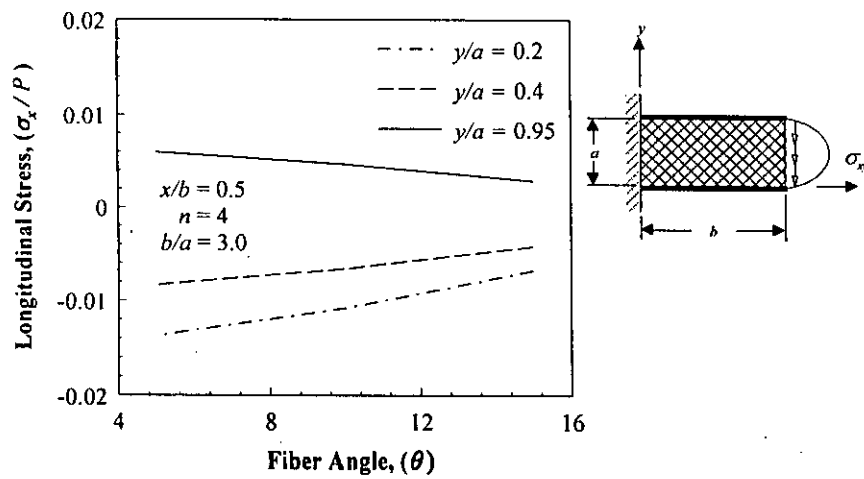


Fig. 4.122 Effect of fiber angle on longitudinal stress component.

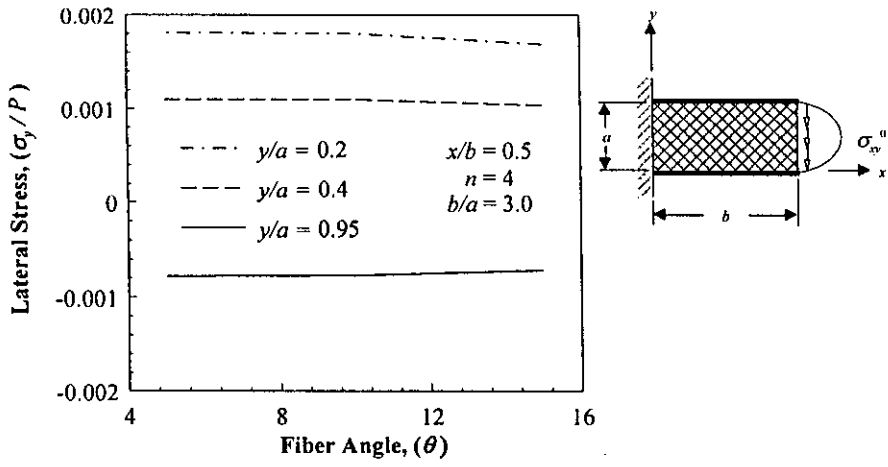


Fig. 4.123 Effect of fiber angle on lateral stress component.

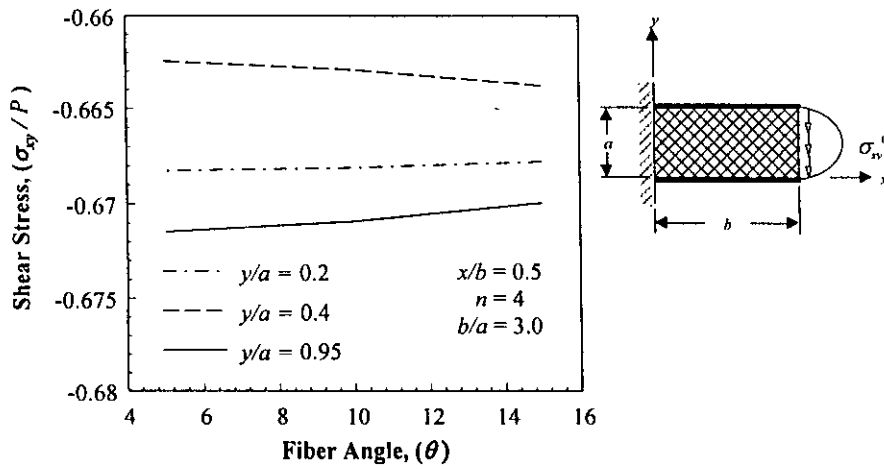


Fig. 4.124 Effect of fiber angle on shear stress.

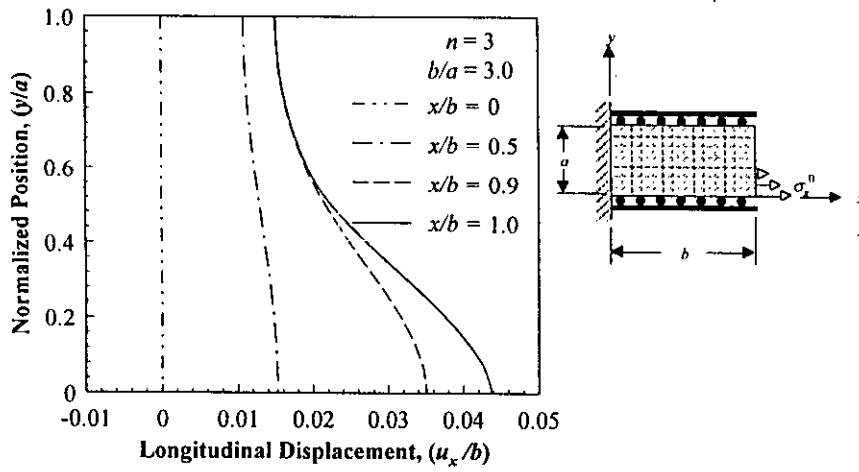


Fig. 4.125 Longitudinal displacement at different sections of the panel.

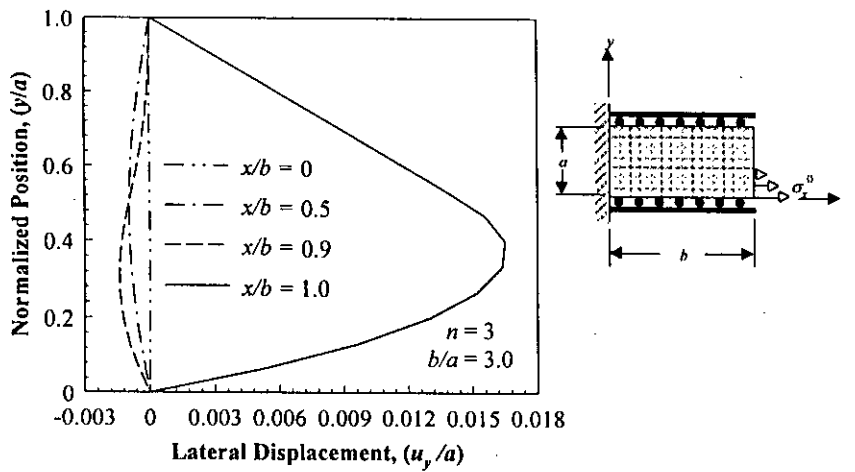


Fig. 4.126 Lateral displacement at different sections of the panel.

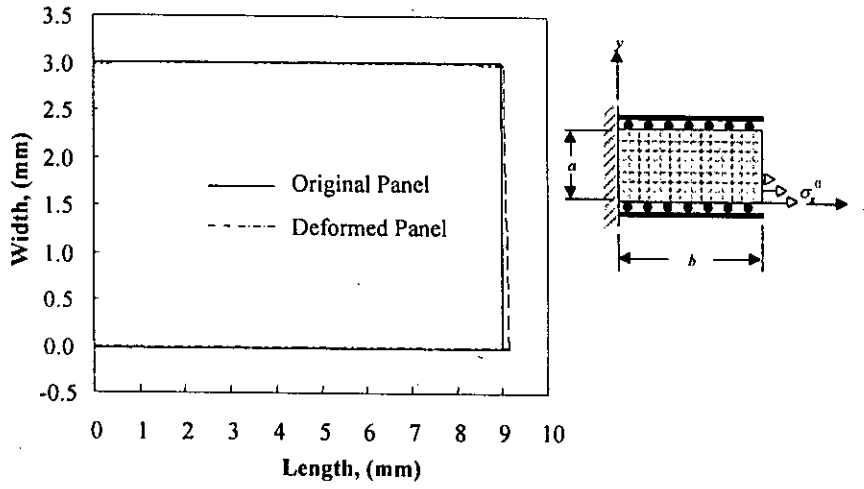


Fig. 4.127 Deformed and original shape of a cross-ply laminated composite panel under linearly varying tensile load.

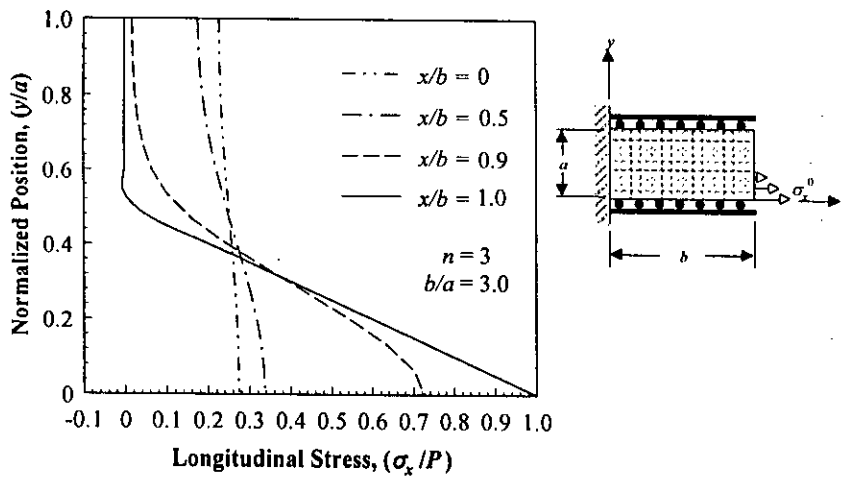


Fig. 4.128 Longitudinal stress at different sections of the panel.

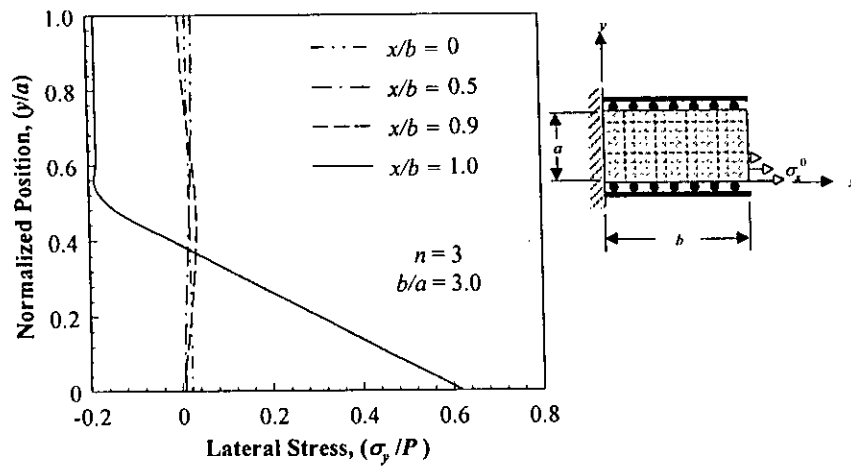


Fig. 4.129 Lateral stress at different sections of the panel.

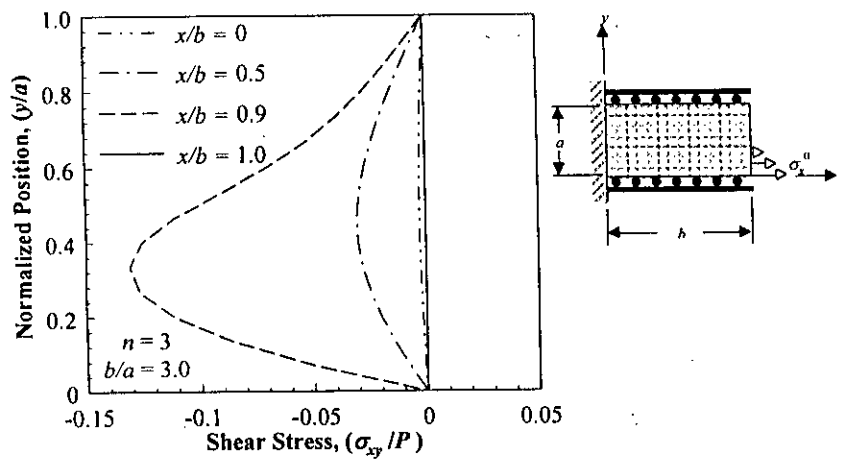


Fig. 4.130 Shear stress at different sections of the panel.

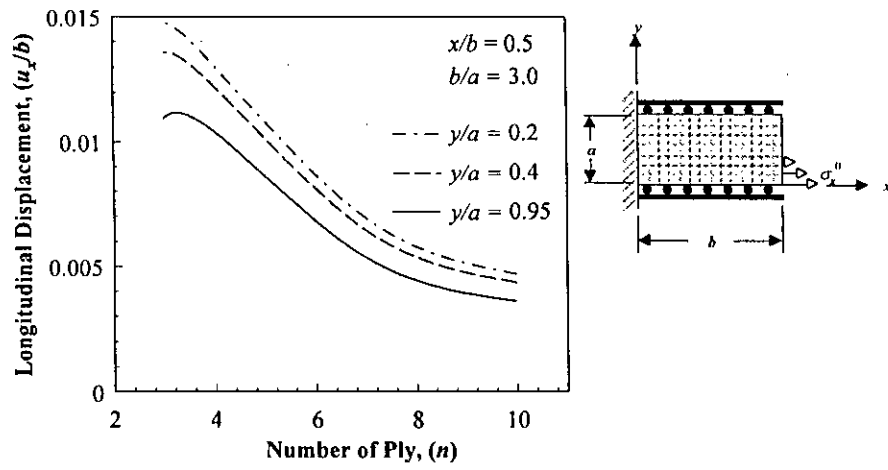


Fig. 4.131 Longitudinal displacement as a function of ply number.

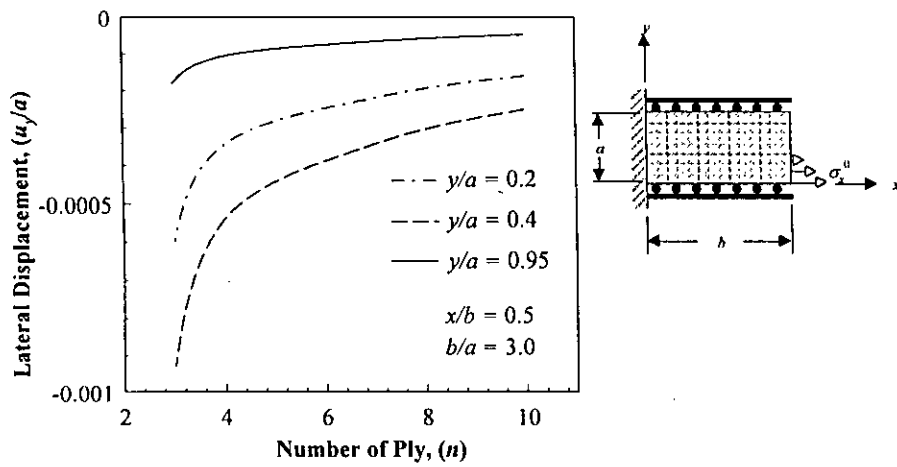


Fig. 4.132 Lateral displacement as a function of ply number.

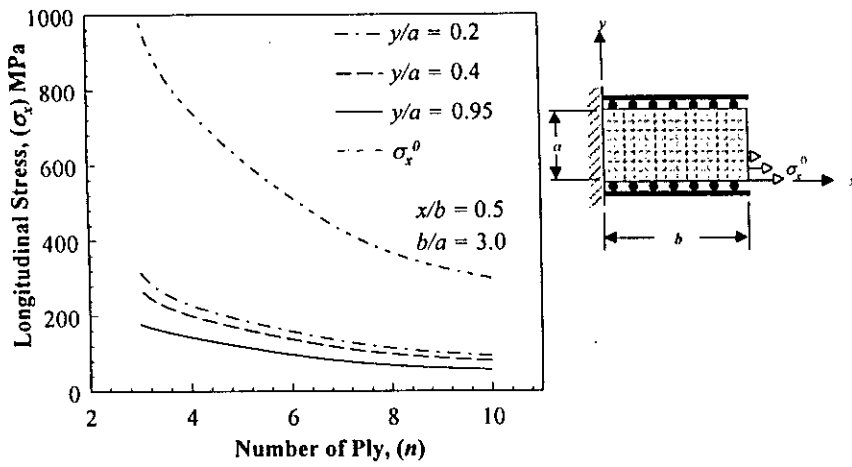


Fig. 4.133 Effect of ply number on the longitudinal stress component.

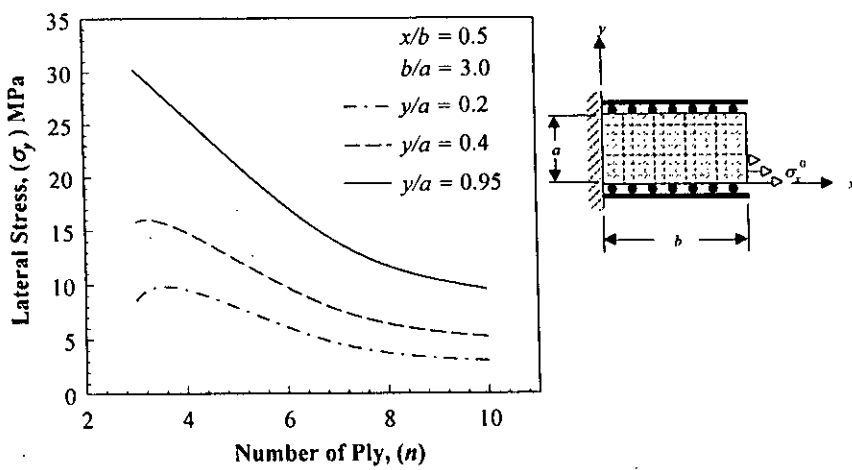


Fig. 4.134 Effect of ply number on the lateral stress component.

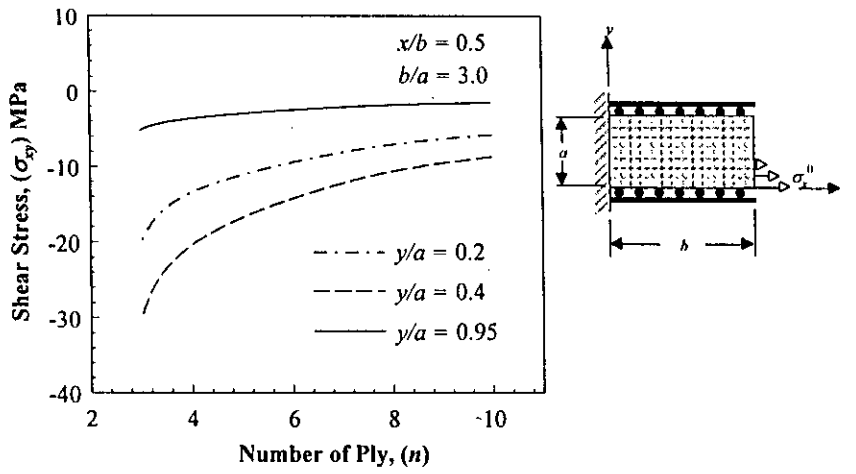


Fig. 4.135 Effect of ply number on the shear stress.

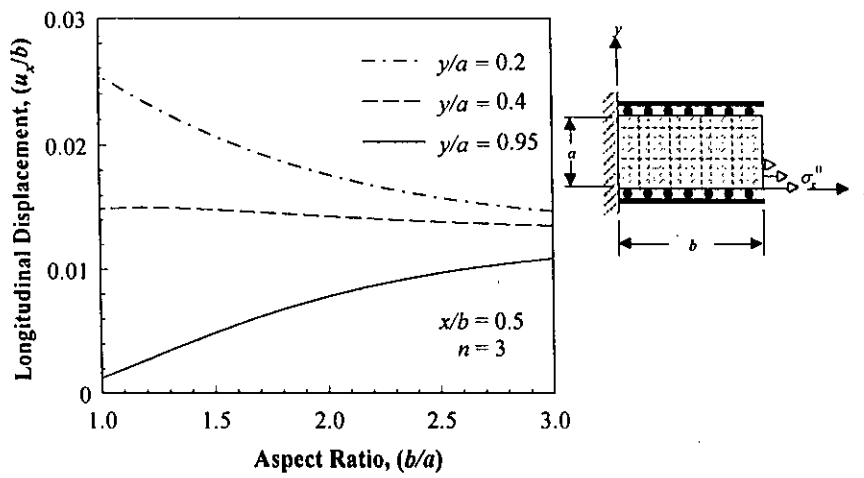


Fig. 4.136 Effect of aspect ratio on longitudinal displacement.

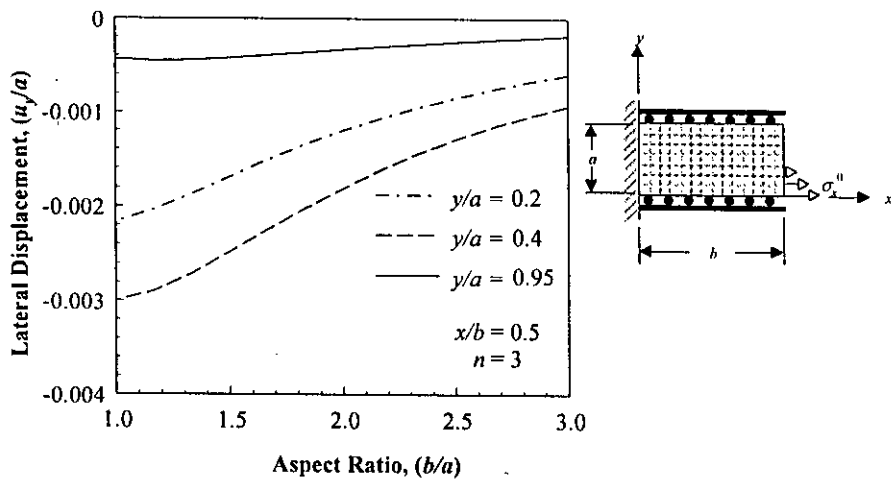


Fig. 4.137 Effect of aspect ratio on lateral displacement.

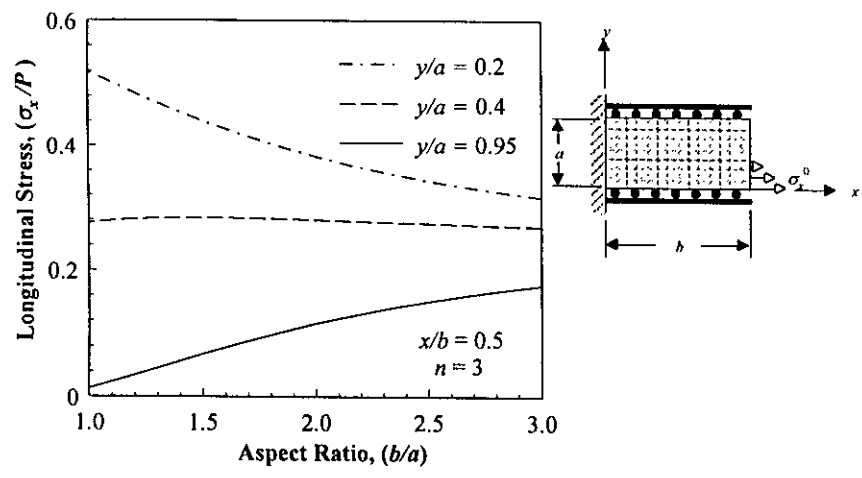


Fig. 4.138 Effect of aspect ratio on longitudinal stress component.

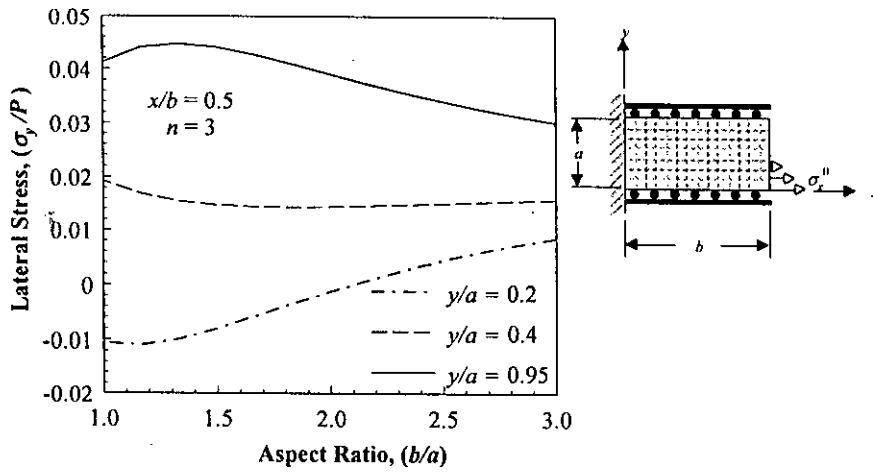


Fig. 4.139 Effect of aspect ratio on lateral stress component.

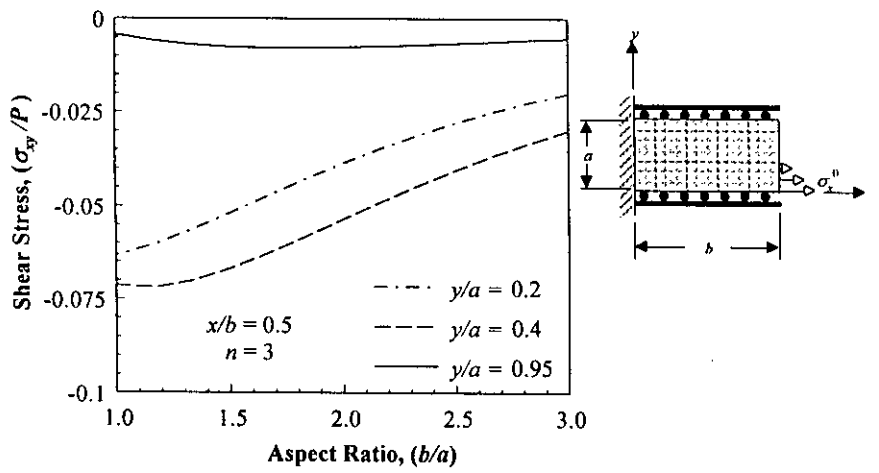


Fig. 4.140 Effect of aspect ratio on shear stress.

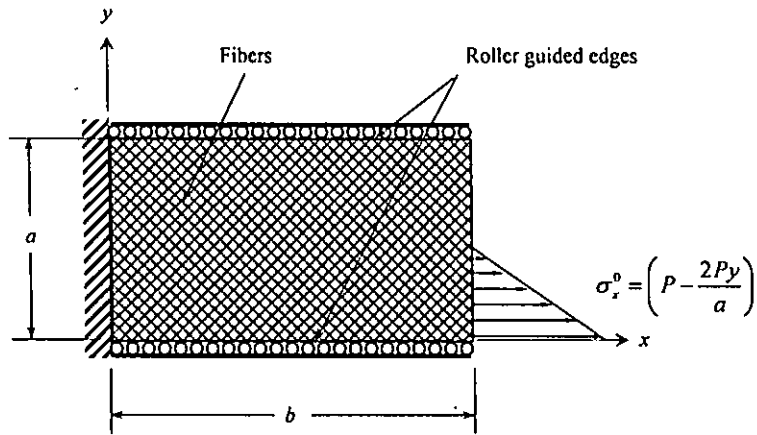


Fig. 4.141 A rectangular panel of angle-ply laminated composite under linearly varying tensile loading.

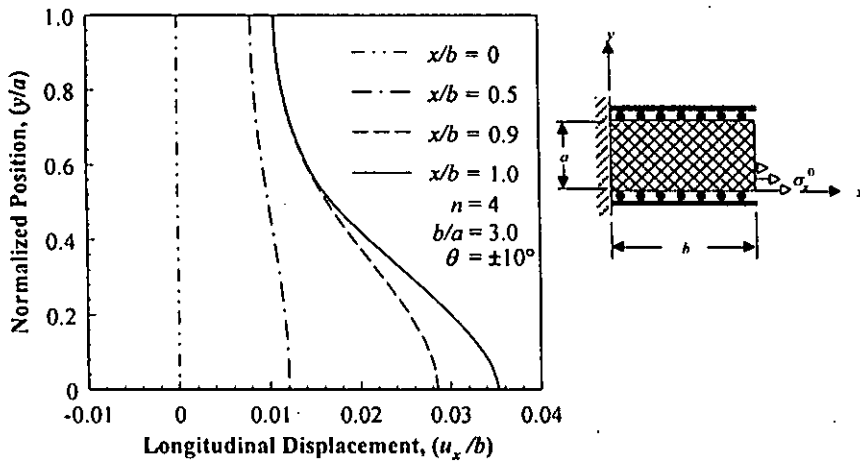


Fig. 4.142 Longitudinal displacement at different sections of the panel.

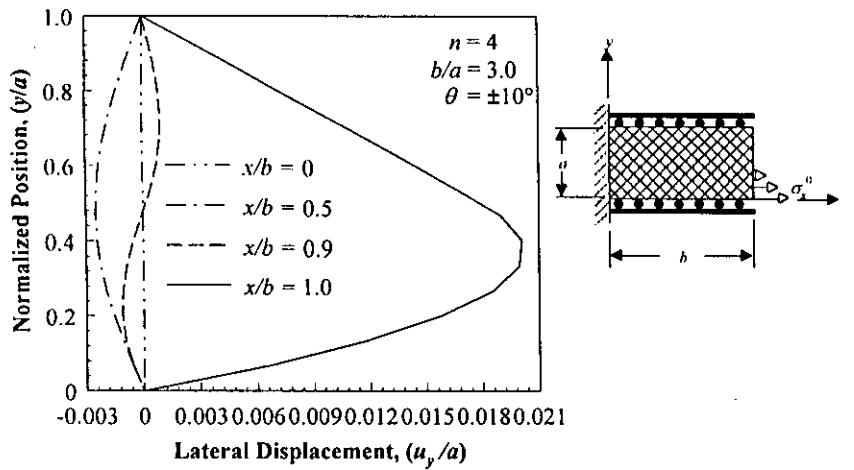


Fig. 4.143 Lateral displacement at different sections of the panel.

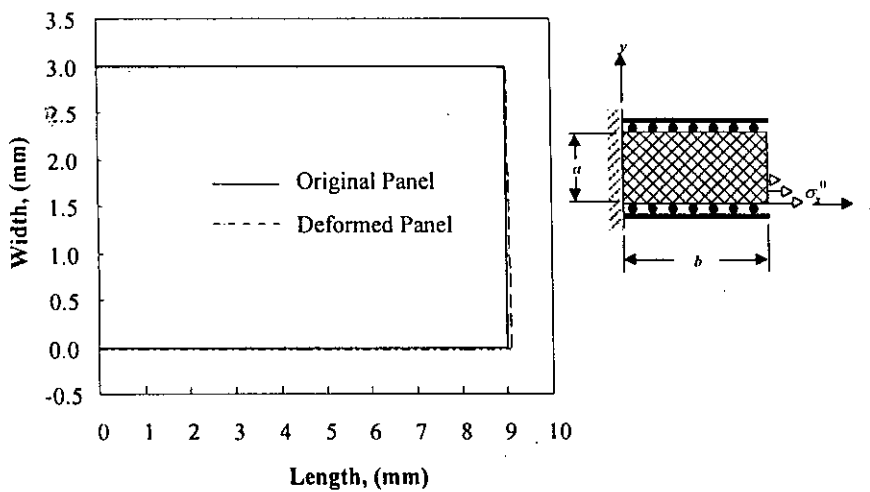


Fig. 4.144 Deformed and original shape of an angle-ply laminated composite panel under linearly varying tensile load.

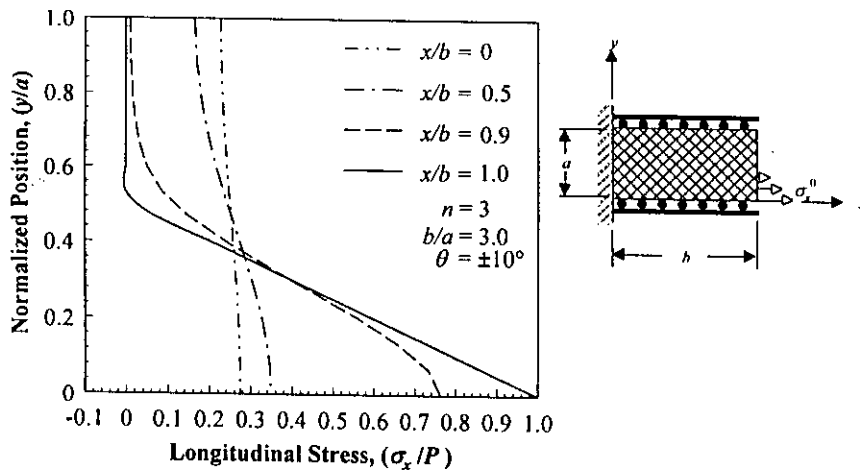


Fig. 4.145 Longitudinal stress at different sections of the panel.

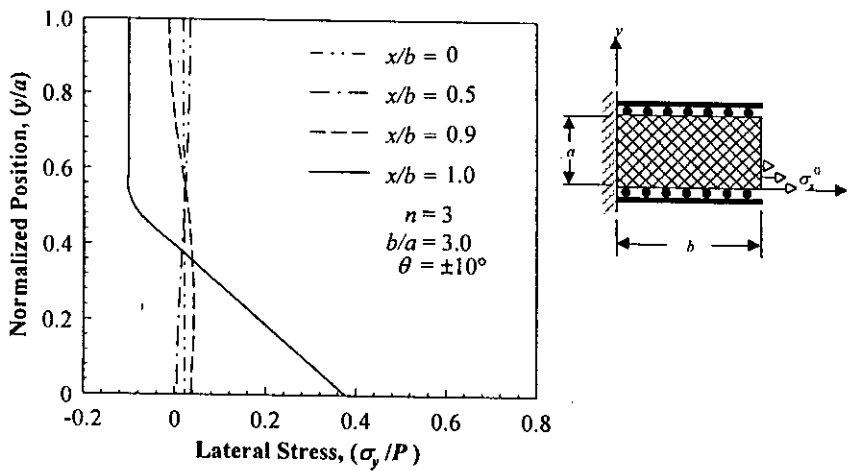


Fig. 4.146 Lateral stress at different sections of the panel.

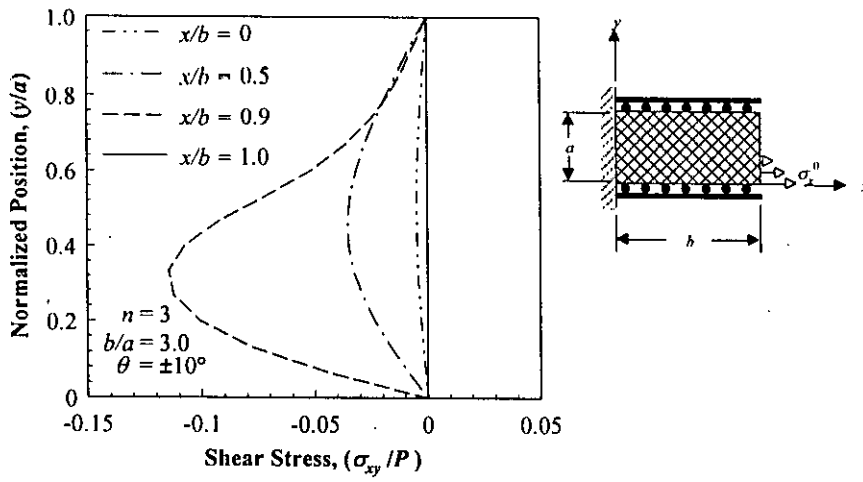


Fig. 4.147 Shear stress at different sections of the panel.

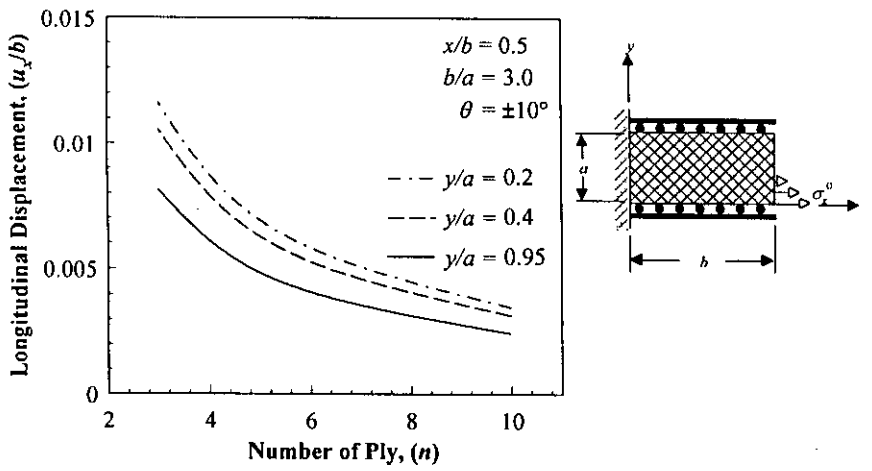


Fig. 4.148 Longitudinal displacement as a function of ply number.

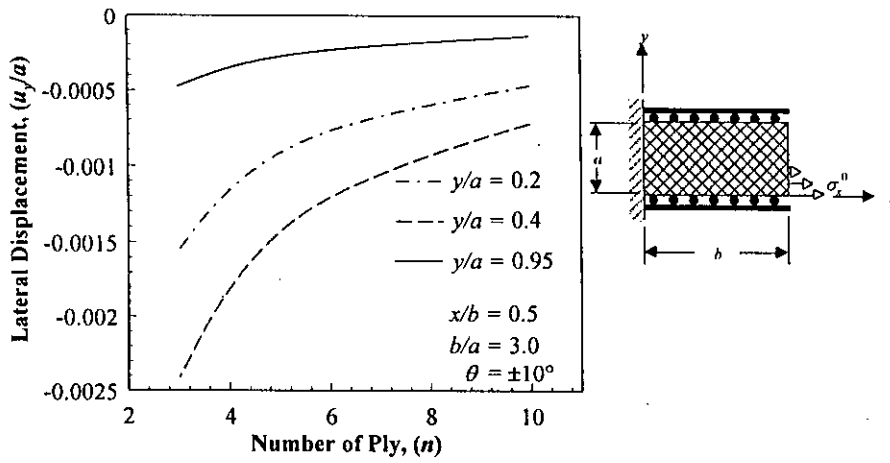


Fig. 4.149 Lateral displacement as a function of ply number.

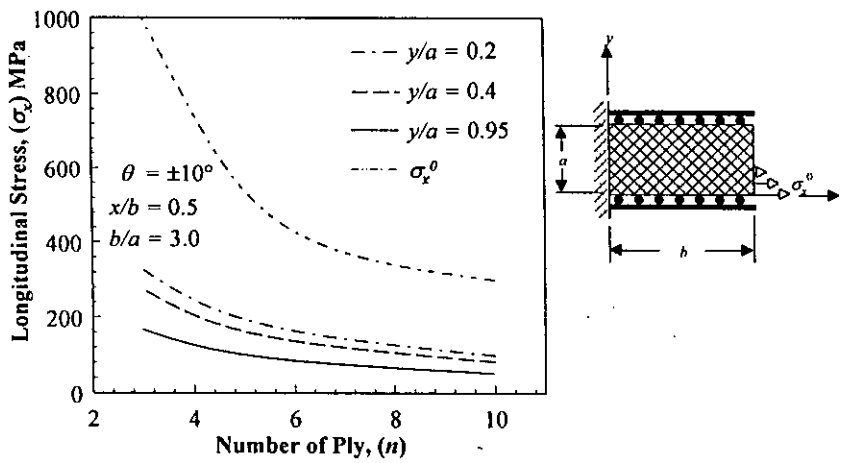


Fig. 4.150 Effect of ply number on the longitudinal stress component.

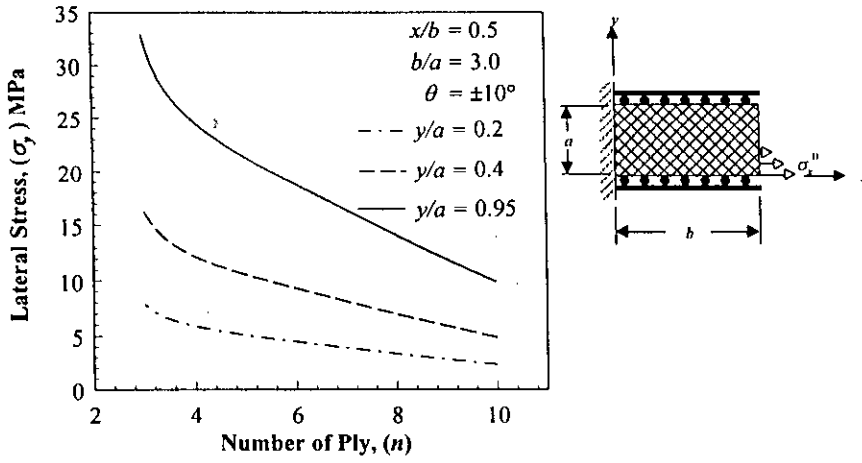


Fig. 4.151 Effect of ply number on the lateral stress component.

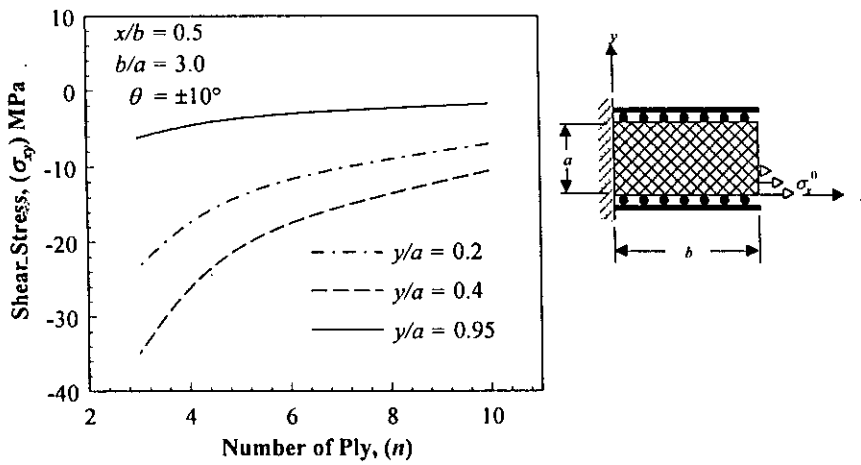


Fig. 4.152 Effect of ply number on the shear stress.

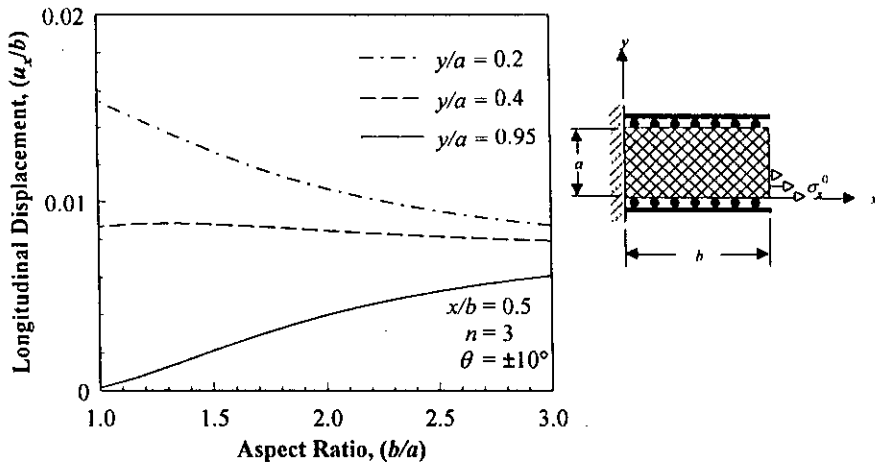


Fig. 4.153 Effect of aspect ratio on longitudinal displacement.

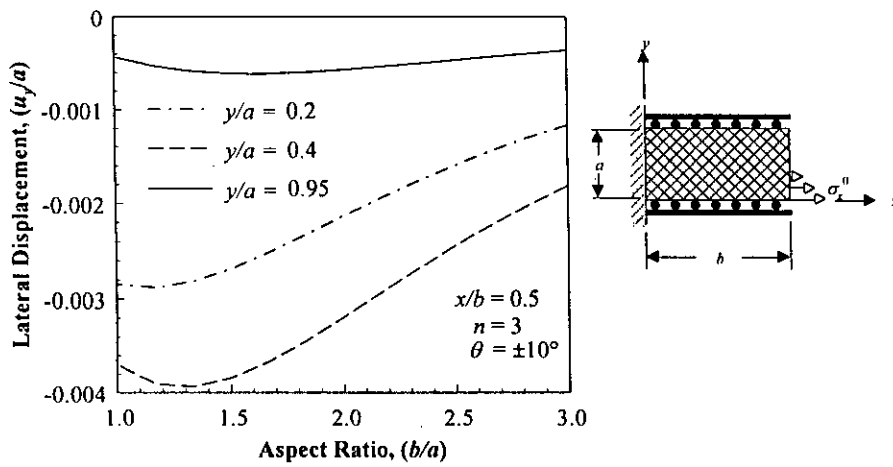


Fig. 4.154 Effect of aspect ratio on lateral displacement.

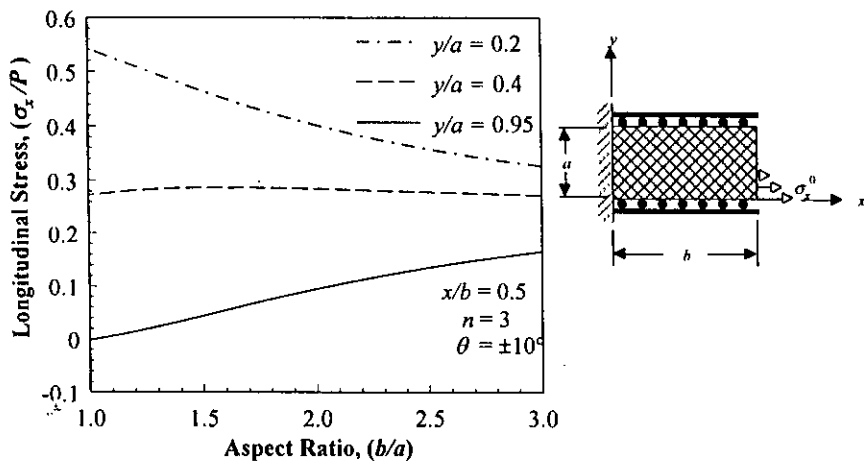


Fig. 4.155 Effect of aspect ratio on longitudinal stress component.

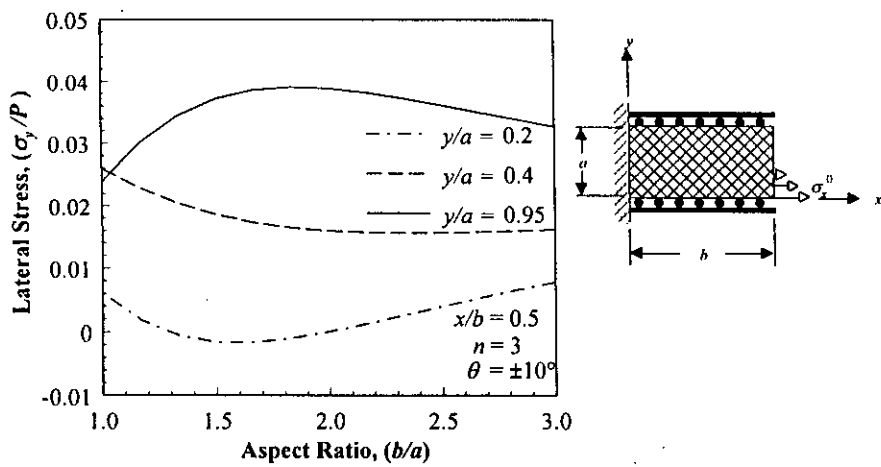


Fig. 4.156 Effect of aspect ratio on lateral stress component.

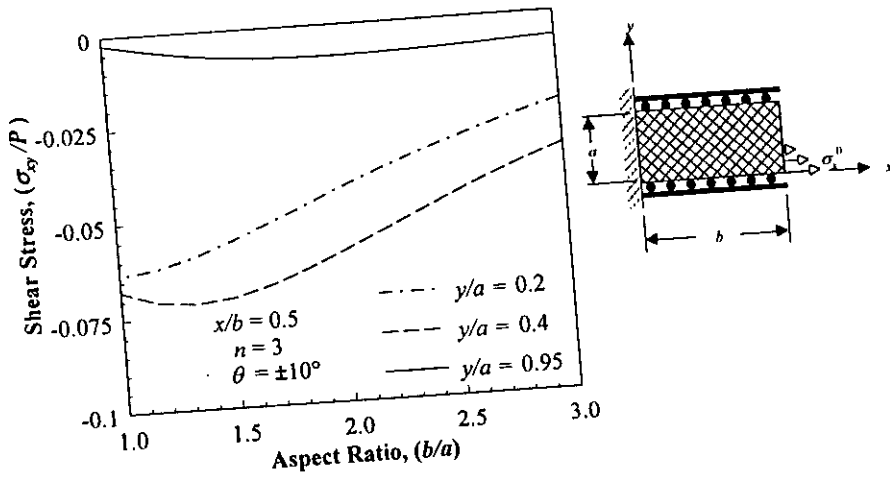


Fig. 4.157 Effect of aspect ratio on shear stress.

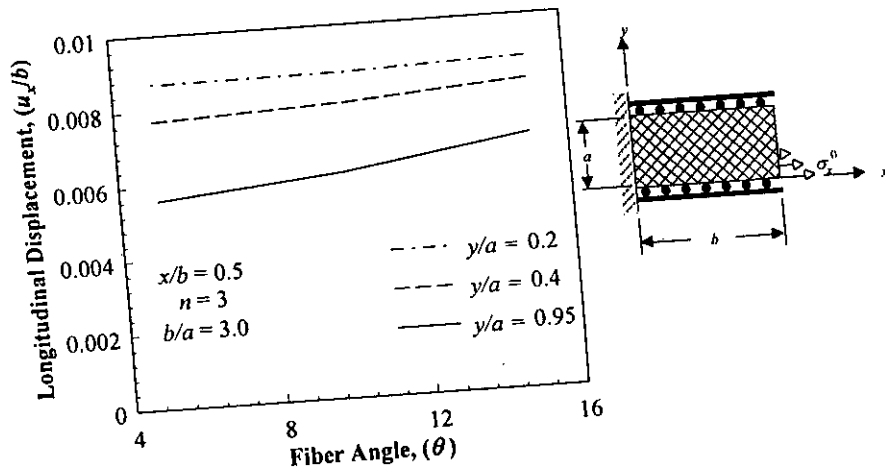


Fig. 4.158 Longitudinal displacement of laminated composite for various fiber angle.

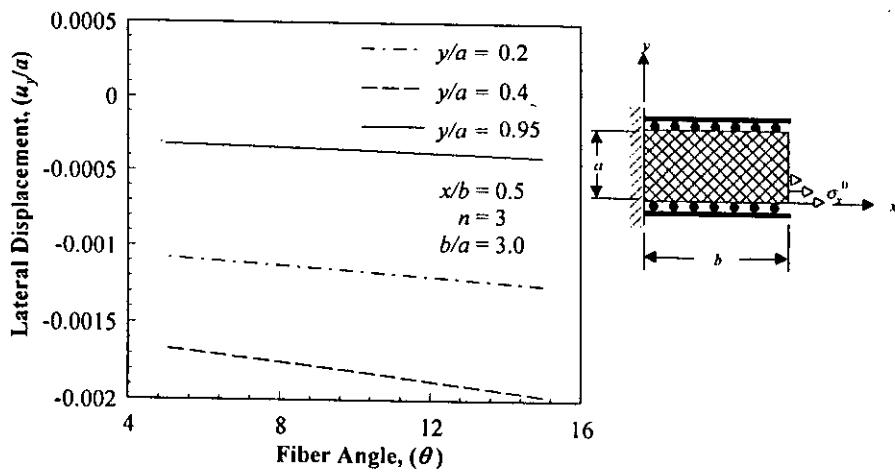


Fig. 4.159 Lateral displacement of laminated composite for various fiber angle.

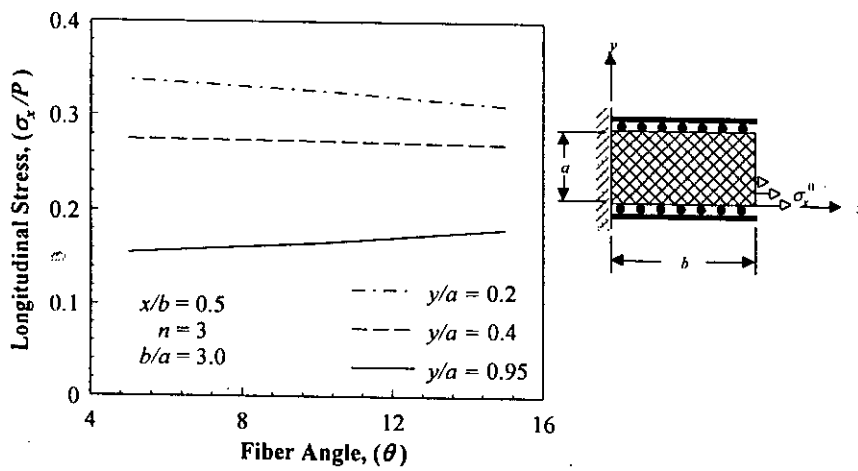


Fig. 4.160 Longitudinal stress of laminated composite for various fiber angle.

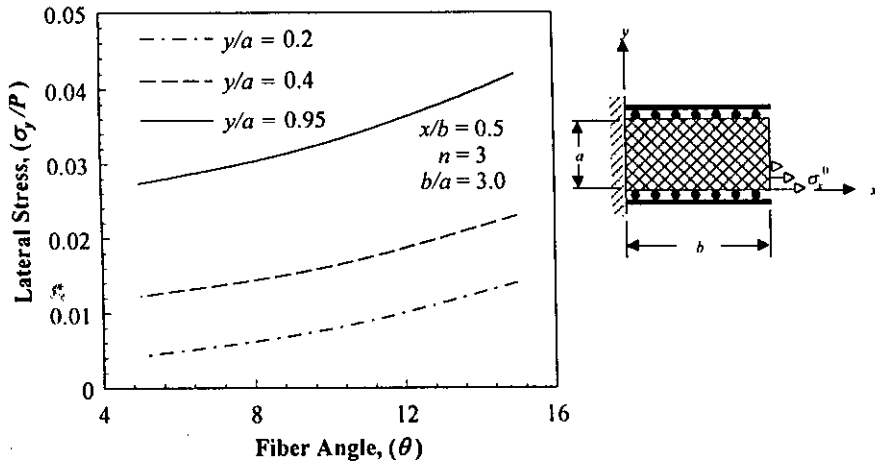


Fig. 4.161 Lateral stress of laminated composite for various fiber angle.

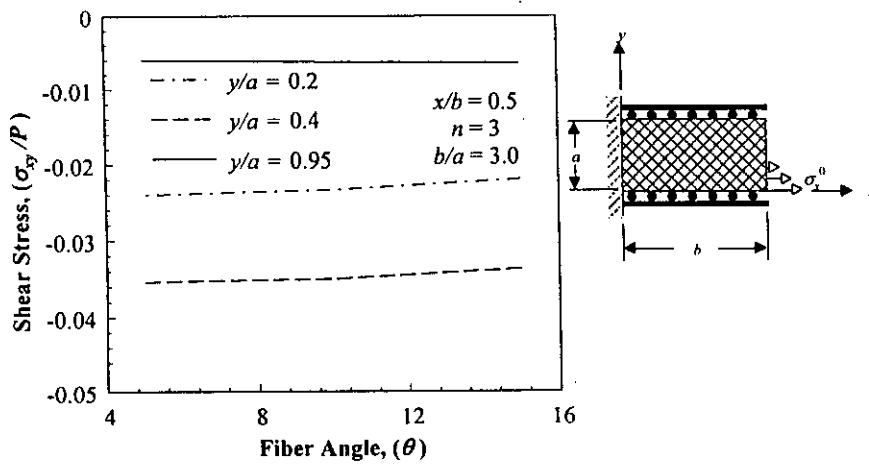


Fig. 4.162 Shear stress of laminated composite for various fiber angle.

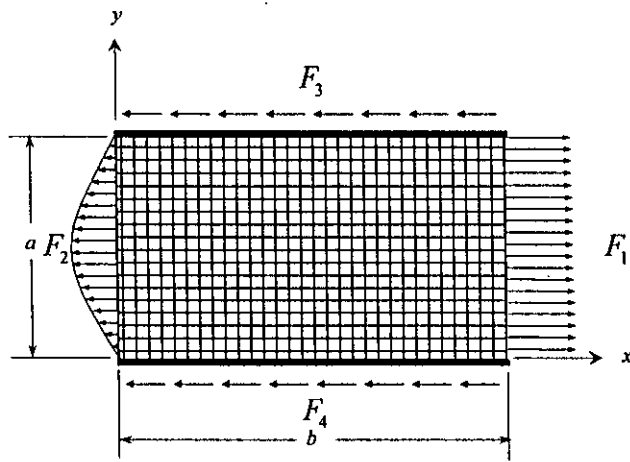


Fig. 4.163 Free body diagram of the problem of article 3.1.

P

References

- [1] Timoshenko, S.P. and Goodier, J. N., 1970, Theory of Elasticity, 3rd Ed., McGraw Hill Book Company, New York.
- [2] Airy, G.B., 1862, Brit.Assoc. Advanced Sci.Rept.
- [3] Mesnager, A., 1901, Compt. Rend., vol.132, pp.1475.
- [4] Timpe, A., Z. 1905, Math. Physic., vol.52, pp.348.
- [5] Rankine, 1895, Applied Mechanics, 14th ed., pp.344.
- [6] Grashof, 1878, Elastizitt Festigkeit, 2nd Ed.
- [7] Levy, M., 1898, Compt. Rend., vol.126, pp.1235.
- [8] Scewald, F., Abhandl., 1927, Aerodynam. Inst. Tech. Hochschule, Aachen, vol. 7, pp.11.
- [9] Mem. Savants Etrangers, 1855, vol.14.
- [10] Ribiere, M.C., 1889, Sur divers cas de la flexon des primses rectangles, thesis, Bordeaux.
- [11] Filon, L.N.G., 1903, Phil., Trans., Series A, vol.201, pp.63.
- [12] Bleich, F., 1923, Bauingenieur, vol.4, pp.255.
- [13] Beyer, K., 1934, Die Statik in Eisenbetonban, 2d Ed., pp.723.
- [14] Ribiere, 1901, Compt. Rend., vol. 132, p.315.
- [15] Sadowsky, M. Z. A., 1930, Math. Mech, vol.10, pp.77.
- [16] Flamant, 1892, Compt. Rend. Paris, vol.114, pp.1465.
- [17] Uddin, M. W., 1966, Finite Difference Solution of Two-dimensional Elastic Problems with Mixed Boundary Conditions, M. Sc. Thesis, Carleton University, Canada.
- [18] Stokes, G.G., 1935, Mathematical and Physical Papers, vol. 5, p.238.

- [19] Conway H. D., Chow L. and Morgan, G.W., 1951, Analysis of deep beams, Journal of Applied Mechanics, Trans ASME, vol. 18, No. 2, pp. 163-172.
- [20] Chow L., Conway H. D. and Winter G., 1952, Stresses in deep beams, Trans ASCE, Paper No. 2557.
- [21] Horgan C. O. and Knowels J. K., 1983, Recent developments concerning Saint-Venant's Principle, Advances in Applied Mechanics, vol. 23, pp.179-269.
- [22] Parker D. F. , 1979, The role of Saint-Venant's solutions in rod and beam theories, Journal of Applied Mechanics, Trans ASME, vol. 46, pp. 861-866.
- [23] Suzuki S., 1986, Stress analysis of short beams, AIAA Journal, vol. 24, pp.1396-1398.
- [24] Hardy S. J. and Pipelzadeh M. K., 1991, Static analysis of short beams, Journal of Strain Analysis, vol. 26, No. 1 , pp. 15-29.
- [25] Murty A.V. K., 1984, Towards a consistent beam theory, AIAA Journal, vol. 22, pp. 811-816.
- [26] Hetengi, M., J., 1943, Applied Mechanics (Trans ASME), vol.10, A-93.
- [27] John Wiley & Sons Inc., 1950, Handbook of Experimental Stress Analysis, New York.
- [28] Frocht, M.M., 1948, Photoelasticity, John Wiley & Sons, Inc., New York, vol.2.
- [29] Durelli A. J. and Ranganayakamma B., 1987, On the use of photoelasticity and some numerical methods, Photomechanics and Speckle Metrology, SPIE, vol.814 , pp.1-8.

- [30] Tabakov P.Y and Summers E.B., 2006, Lay-up optimization of multilayered anisotropic cylinders based on a 3-D elasticity solution, vol. 84, pp 374-384.
- [31] Conway H. D. and Ithaca N. Y., 1953, Some problems of orthotropic plane stress, Journal of Applied Mechanics, Trans ASME, Paper No. 52-A-4 , pp. 72-76.
- [32] Ahmed S. R., 1993, Numerical Solutions of Mixed Boundary Value Elastic Problems, M. Sc. Thesis, Bangladesh University of Engineering and Technology, Bangladesh.
- [33] Idris A. B. M., 1993, A New Approach to Solution of Mixed Boundary Value Elastic Problems, M. Sc. Thesis, Bangladesh University of Engineering and Technology, Bangladesh.
- [34] Ahmed S. R., Khan M. R., Islam K.M.S. and Uddin M.W., 1996, Analysis of stresses in deep beams using displacement potential function, Journal of Institution of Engineers (India), vol. 77, pp. 141-147.
- [35] Idris A. B. M., Ahmed S. R., and Uddin M. W., 1996, Analytical solution of a 2-D elastic problem with mixed boundary conditions, Journal of the Institution of Engineers (Singapore), vol. 36, No. 6, pp. 11-17.
- [36] Ahmed S. R., Idris A. B. M. and Uddin M. W., 1996, Numerical solution of both ends fixed deep beams, Computers & Structures, vol. 61, No.1, pp. 21-29.
- [37] Ahmed S. R., Khan M. R., Islam K. M. S. and Uddin M.W, 1998, Investigation of stresses at the fixed end of deep cantilever beams, Computers & Structures, vol. 69, pp. 329-338.

- [38] Ahmed S. R., Idris A. B. M. and Uddin M.W, 1999, An alternative method for numerical solution of mixed boundary-value elastic problems, *Journal of Wave-Material Interaction*, vol. 14, No. 1-2, pp. 12-25.
- [39] Akanda M. A. S, Ahmed S. R., Khan M. R. and Uddin M. W., 2000, A finite difference scheme for mixed boundary-value problems of arbitrary-shaped elastic bodies, *Advances in Engineering Software*, vol. 31, No.3, pp.173-184.
- [40] Akanda M. A. S., Ahmed S. R., and Uddin M. W, 2002, Stress analysis of gear teeth using displacement potential function and finite differences, *International Journal for Numerical methods in Engineering*, vol. 53, pp. 1629-1640.
- [41] Ahmed S. R., Hossain M. Z. and Uddin M. W, 2005, A general mathematical formulation for finite-difference solution of mixed-boundary-value problems of anisotropic materials, *Computers & Structures*, vol. 83, pp. 35-51.
- [42] Ahmed S.R., Deb Nath S. K and Uddin M.W, 2005, Optimum shapes of tire-treads for avoiding lateral slippage between tires and roads, *International Journal for Numerical methods in Engineering*, vol-64, pp. 729-750.
- [43] Deb Nath, S. K., 2002, A Study of Wear of Tire Treads, M.Sc. Thesis, Bangladesh University of Engineering and Technology, Bangladesh.
- [44] Hossain, M. Z., 2004, A New Approach to Numerical Solution of Three-Dimensional Mixed Boundary-Value Elastic Problems, M.Sc. Thesis, Bangladesh University of Engineering and Technology, Bangladesh.
- [45] Quddus, N. A. , 2003, Development of a Boundary Management Technique in Finite-Difference Method of Solution, M.Sc. Thesis, Bangladesh University of Engineering and Technology, Bangladesh.

- [46] Rahaman, M. A., 2004, A Finite Difference Scheme for Mixed Boundary Values of Two Dimensional Elastic Problems with Internal Hole, M.Sc. Thesis, Bangladesh University of Engineering and Technology, Bangladesh.
- [47] Mohiuddin, M., 2003, Stress Analysis of Screw Threads, M.Sc. Thesis, Bangladesh University of Engineering and Technology, Bangladesh.
- [48] Adams S.F., Maiti M., and Mark R.E., Three-Dimensional Elasticity Solution of a Composite Beam, *Journal of composite materials*, vol. 1, No. 2, pp.122-135 (1967)
- [49] Adams D.F., and Doner D.R., Transverse Normal Loading of a Unidirectional Composite, *Journal of composite materials*, vol. 1, No. 2, pp.152-164 (1967).
- [50] Whitney J.M., Elastic Moduli of Unidirectional Composites with Anisotropic Filaments, *Journal of composite materials*, vol. 1, No. 2, pp.188-193 (1967)
- [51] Pagano N.J., Analysis of the Flexure Test of Bi-directional Composites, *Journal of composite materials*, vol. 1, No. 4, pp.336-342 (1967)
- [52] Shu L.S., and Rosen B.W., *Journal of composite materials*, vol. 1, No. 4, pp.366-381 (1967).
- [53] Tsai S.W., and Wu E.M., A General Theory of Strength for Anisotropic Materials, *Journal of composite materials*, vol. 5, No. 1, pp.58-80 (1971).
- [54] Hwang Y. and Lacy T.E., *Journal of composite materials*, vol. 41, No. 3, pp.367-388 (2007).
- [55] Huq N.M.L., and Afsar A.M., Analysis of Elastic Field in Stiffened Bars of Composite Material by Displacement Potential Function, *Proceedings of the 3rd BSME-ASME international conference of thermal engineering (2006)*

- [56] Huq N.M.L., and Afsar A.M., Analysis of Elastic Field in Stiffened Bars of Laminated Composite by Displacement Potential Approach, Proceedings of the 11th IEB Annual Paper Meet (2006)
- [57] Deb Nath S.K., Displacement Potential Approach to Solution of Elasticity Problems of Orthotropic Composite Structure, M. Sc. thesis, Bangladesh University of Engineering and Technology, Bangladesh (2006)
- [58] Deb Nath S.K., Ahmed S.R., and Afser A.M., Displacement Potential Solution of Short Stiffened Flat Composite Bars Under Axial Loading, International journal of applied mechanics and engineering, voll. 11, No. 3, pp.557-575 (2006)
- [59] Deb Nath S.K., Afser A.M., and Ahmed S.R., Displacement Potential Approach to Solution of Stiffened Orthotropic Composite Panels Under Uniaxial Tensile Load, Accepted for IMechE, Journal of aerospace engineering, vol. 221, part G (2006)
- [60] Deb Nath S.K., Afser A.M., and Ahmed S.R., Displacement Potential Solution to a deep Stiffened Cantilever Beam of Orthotropic Composite Material, Journal of strain analysis, submitted
- [61] Kaw A.K., Mechanics of Composite Materials, CRC Press, United States of America (1997)

